

Radar Testbed Characterization for Evaluation of Modulated Scatterer Concepts

By

Matt Casper

Submitted to the graduate program in electrical engineering
and graduate faculty of the University of Kansas in partial fulfillment
of the requirements for the degree of Master's of Science.

Committee:

Chair

Defended: May 24, 2010

The Thesis Committee for Matt Casper certifies that this is the approved version of the following thesis:

Radar Testbed Characterization for Evaluation of Modulated Scatterer Concepts

Committee:

Chair

Date Approved: _____

Acknowledgements

I would like to thank Dr. Allen for the time he invested in helping me to understand the concepts inherent in radar research. I also appreciate the guidance offered when obstacles were faced and deadlines approached. Dr. Allen's efforts really made this a successful project and learning experience.

I would also like to thank my family, most notably, Heidi. She looked after our daughter during my late nights in lab, prepared excellent dinners to keep me going, and offered support when times were tough.

Table of Contents

Abstract	1
Chapter 1: Introduction	3
1.1 Why this Technique is Useful	3
1.2 Basic Operation	4
1.3 Scenario for Use	4
Chapter 2: Background	5
2.1 Past Research	5
2.2 Current Research	8
2.3 Example Application	8
2.4 Applied Theory	10
Chapter 3: Radar Specific Characteristics	12
3.1 Transmitter Characteristics	12
3.2 Receiver Characteristics	14
3.3 Antenna Specifics	19
3.4 Signal Processing	21
3.5 Cabled Loopback Testing	25
3.6 Receive Signal Assessment	28
Chapter 4: Modulated Scatterer Characterization	35
4.1 Modulated Scatterer Operation	35
4.2 Range Limitations	36
4.3 Data Processing	38

Chapter 5: Freespace Testing	40
5.1 Freespace Loopback	40
5.2 Indoor Testing	41
5.3 Outdoor Testing	45
Chapter 6: Conclusions	46
6.1 Summary of Results	46
6.2 Discrepancies and Shortcomings	47
6.3 Future Work	48
Bibliography	50
Appendices	52

List of Figures

Figure 1. Block Diagram of Transmitter Setup and General Receiver Layout	13
Figure 2. Detailed Block Diagram of 75-MHz Receiver	14
Figure 3. Detailed Block Diagram of 235-MHz Receiver	16
Figure 4. Correlation with Ideal Transmit Waveform	26
Figure 5. 10 m Loopback Autocorrelation (75 MHz)	29
Figure 6. Autocorrelation of 10 m Loopback Data with Complex Reference (75 MHz)	30
Figure 7. Correlation of Complex Reference with 15 m Cabled Loopback Data (75 MHz)	32
Figure 8. 10 m Loopback Autocorrelation with Complex Reference (235 MHz)	33
Figure 9. Correlation of Complex Reference with 15 m Cabled Loopback Data (235 MHz)	35
Figure 10. Processed Received Waveform from Modulated Scatterer (Frequencies of Interest)	39
Figure 11. Correlation of Direct Freespace Data with 10 m Cabled Loopback Data (235 MHz)	40
Figure 12. Nichols Hall Atrium Indoor Setup Geometry	42
Figure 13. Atrium Reflections Measurements	43
Figure 14. Atrium Reflection from Target	44

Abstract

The following research explores the concepts of communication-embedded radar with an emphasis on radar operation and modulated scatterer concepts. Once firmly established the concept of communication via radar backscatter could be used in a variety of fields including, mass data collection, SAR calibration, and military communication.

A radar testbed was developed and characterized to enable experimental evaluation of communication via modulated scatterer concepts. The radar operates with a 1.84-GHz center frequency and 75-MHz bandwidth (later upgraded to a 235-MHz bandwidth). A dual-channel arbitrary waveform generator is loaded with user-defined complex baseband signals for frequency upconversion for transmission via a 22 dBi parabolic reflector antenna. Backscattered signals are received and frequency downconverted on four identical channels, each fed by a dipole antenna. A 4-channel data acquisition system digitizes and records the output video signal at 1-GSa/s per channel for signal analysis.

The primary means of evaluating the radar testbed were loopback and freespace setups. The loopback setup consisted of a cable inserted between transmitter and receiver to provide a controlled propagation environment. In this setup results were shown to be desirable, and easily explained by theory. Linear FM (chirp) waveforms were used which enabled pulse compression to reduce the peak signal power while preserving range resolution. After pulse compression via matched filter routines, amplitude, phase, and resolution were characterized and found to agree with theory. In extending the tests to freespace, it was seen that near targets could be seen and resolved coherently across the 4 channels.

A prototype modulated scatterer constructed by a senior design group was further tested to evaluate the prototype's viability. This scatterer impresses a bit sequency on the radar

waveform by modulating the scatterer's termination impedance between an open and short circuit at a rate determined by the bit sequence to be communicated (similar to frequency-shift keying). Connected via a cabled-loopback configuration, the prototype was shown to impress a bit sequence onto the backscatter of the transmit chirp and, through processing, the bit stream associated with the modulated scatterer was decoded successfully. Followon testing will evaluate freespace operation and techniques for decoding information from multiple devices in the field of view.

This radar testbed will be used to experimentally evaluate various modulated scatterer concepts as well as other radar-related waveform and signal processing concepts in the future.

Chapter 1: Introduction

1.1 Why this technique is useful

In areas where radar is already being used, it would be favorable if the use of a system as simply, a radar, could be expanded. The typical operations of radar include transmitting some specific radio frequency (RF) signal, receiving a delayed version of that transmitted signal, and by the delay between transmit and receive, determine how far away a target it. This operation allows for the mapping of terrain in a quick, remote way.

When the waveform scatters off a target and propagates toward a receiver, it essentially opens up a “one-way communications channel” between the target and the radar receiver. In traditional radar the only information transmitted through this “channel” is the scatterer’s range, radial velocity, and radar cross section (RCS). Once a link is already established then it would be more efficient if more information were conveyed.

An advantage of communication via modulated backscatter is that the remote node could operate with minimal power requirements. This advantage could enable remote data collection from a passive sensor (e.g., temperature, pressure) or a sensor with minimal power requirements (e.g., acceleration). Furthermore if such data can be read from one low-power remote source, then it follows that collecting data from multiple sources should be feasible. By developing, the hardware, and processing necessary to decode bit sequences from multiple targets distributed over a scene, mass data collection could become faster, cheaper, and more reliable. In a hurricane specific application to be discussed later, this process is also much safer, further increasing the desirability of this application on all fronts.

1.2 Basic Operation

The concept of communication-embedded radar is not a new one. In fact it has been around since the 1940s [1]. Communication-embedded radar is the process of obtaining information from a specific scatterer in addition to the data contained in the backscattered waveform. This starts with any radar and a specialized scatterer. Normally the illuminating signal, transmitted by the radar, would scatter off objects in the scene, but in this case the signal is received by a modulated scatterer, manipulated within the scatterer, and then reradiated. The reradiated signal then propagates back to the receiver along with backscatter from the scene.

At this point the receiver processes the naturally occurring backscattered signal and derives some ranging and direction data for the scene. At the same time a different processing technique, one specific to the modulated scatterer, is used, and the information encoded in the reradiated signal is decoded. A bit sequence is then extracted and its meaning interpreted.

1.3 Scenario for Use

One potential area that this technology could be used is in meteorology. It has been found that prediction of storm characteristics, most notably hurricanes, from data taken from previous storms is insufficient to accurately predict current storm behavior.

By the use of many distributed scatterers, data could be taken for a longer time and across a larger area of any storm cell. On-board these scatterers would contain any number of desired sensors. The data from these sensors would be impressed on the backscatters of the waveform from the radar transmitter.

This would give meteorologists more and varied types of data from more areas within a storm. With this data, scientists would be more capable of modeling current storms, allowing for

better predictions of storm intensity preventing false alarms, and saving lives, especially in the case of hurricanes.

Chapter 2: Background

2.1 Past Research

The concept of communication by means of reflected power was introduced in the 1940s. At this point, it was established that communication was possible, and different techniques for embedding information on the backscatter were presented.

Many of these methods required some kind of mechanical device to produce the modulation. It was possible to vary the position of a metal sheet and therefore vary the phase of the reflected waveform would change with respect to the modulation rate of the sheet. This aperture could be modulated based on speech, to embed the information signal associated with that speech on the reflected wave. Overall, through mechanical manipulation, the reflection off a surface can be changed to convey information [1].

Since modulation by means of mechanical oscillation has limitations, electronic means to modulate backscatter were developed. To accomplish this, a modulated scatterer must receive in the illuminating waveform; once bound, the wave will be reflected based on an impedance mismatch within the target. This impedance can be varied as a sinusoid, square wave, or any other information signal necessary [2]. This reflection will then be reradiated with the backscatter.

As a number of papers point out [2, 4], the impedance modulation has some interesting effects. With the impedance changing with some frequency, that frequency is impressed on the return waveform. These frequency changes show up similar to that of Doppler frequencies

associated with moving targets. Because of this, processing methods used in Doppler radar apply in decoding the desired information signal [2].

Without any active devices onboard a modulated scatterer, the retransmitted power will naturally be very low. Because of this, it is necessary to reduce system losses. An on-off keying (OOK) modulation scheme can be applied, reflecting all the power in the “on” state, and absorbing all the power in the “off” state [2, 3] resulting in a signal loss of 50%. A variation on this is to apply a binary phase shift (changing between 0 and π radians), while maintaining that 100% of the power is reflected. This essentially provides double the impressed signal power, relative to the OOK method, at the radar receiver decreasing error in message decoding. Coherent detection is required to detect the applied phase modulation, and to collect as much return power as possible [4].

Another approach is seen by varying the radar cross section (RCS) by changing the target’s antenna pattern. If it is possible to use an antenna array at the target, then by turning certain elements on, off, or varying the phase that is reradiated, the antenna pattern can be varied [3]. This directly affects what RCS the transmit waveform sees. Due to this change in RCS, the reflection varies accordingly, and information is conveyed via RCS modulation.

The inherent level of covertness in this technique is mentioned a number of times in military applications. Since the reflected power is so low it is hard to identify, and also hard to process without an advanced receiver and prior system knowledge [9]. Applications have been shown where similar transmitters and modulators can operate with lasers, and other high frequency application in order to avoid bandwidth allocation restraints, and to make devices smaller and more mobile [7].

Since it has been established that this model for communication via radar backscatter is a viable option, it then leads to the question of how best to send data, as well as how much data can be sent. Bits can be encoded in a variety of ways to make the best use of the channel characteristics. Bits can be encoded using inter-pulse and intra-pulse modulation, polarization, and relative delay. The amount of information sent by these methods is affected by a number of quantities including target range, spatial resolution, and pulse repetition frequency (PRF) of the radar system used. Results have shown that with low PRFs clutter dominates the reflected response and therefore the larger the range the more efficient the data transfer is. This is because the clutter energy decreases as R^{-4} , which is a faster decay than the energy incident on a target. The converse is also true, as PRFs increase, above 2 kHz, the closer the target, the more efficient the communications become. However, as the PRF further increases, there is only a small change in efficiency. Another interesting result occurs in the form of resolution effects. It can be shown that with a relatively high PRF, the resolution of the radar system is independent of data transfer efficiency. This means that at a high PRF, resolution can be sacrificed for other desirable quantities while maintaining a high data rate. This is especially useful because many applications involve SAR processes, which inherently work at high PRFs [8].

It is further seen that by intra-pulse modulation higher data rates are achieved than simply with inter-pulse modulation. If a combination of these is used, the highest efficiency is achieved, albeit at the cost of complexity. In aforementioned military applications, this data rate can be sacrificed to increase data obscurity to unfriendly detectors [10].

With the prominence of synthetic aperture radar (SAR), there has been a need for accurate calibration of these systems to yield maximum performance. Active radar calibrators (ARCs) are a version of modulated scatterer that can project a larger radar cross section (RCS)

than is physically dictated [6, 12]. Since these scatterers are active, they can impart some gain on the reflected signal. Also by mimicking Doppler frequency characteristics of radar, an ARC can project its RCS into an area of low clutter [5]. This is especially useful in crowded and urban environments. Overall this increased performance by reducing clutter responses has given further accuracy and precision to SAR.

2.2 Current Research

To enable reliable application of this technology in a number of fields, the reception of data from a distributed source is being studied. It has been seen in early research, that a modulated scatterer can convey information to a radar receiver by embedding that information in the backscatter. The receiver, with prior knowledge of modulation scheme, can then decipher the encoded information. Along, with the knowledge itself, target position is acquired.

In the following chapters, a prototype radar test bed is characterized to determine necessary conditions to determine single target message and position. This test bed will then be used to verify data acquisition from a modulated scatterer in a controlled environment (cabled loopback). Once this is verified it follows that data can be retrieved from a remote modulated scatterer, and with the accuracy and fidelity shown, that this process is scalable to incorporating multiple scatters at multiple locations.

2.3 Example Application

In the recent past it has been made known by groups such as the American Meteorological Society (AMS), that the current techniques of obtaining data from hurricanes does not provide enough information to accurately predict vital hurricane characteristics.

With traditional radar techniques, only a few quantities can be measured. Measurements can be taken near the edges or the hurricane and within the eye of the storm, but even then, most measurements are simply that of rainfall. To get numbers for humidity, pressure, temperature, and therefore energy present in the hurricane, different techniques are necessary.

The communication-embedded radar concept gives the means for obtaining a significant amount of new data while minimizing human risk and cost. By developing a series of lightweight entities that can house any assortment of sensors, data can be gathered throughout the hurricane for a lengthy period of time.

Consider a recently proposed approach where the housing of instruments starts with the development of what is to be called a smart-chaff. This structure is a lightweight, aerodynamic vessel made of aluminized mylar. This assembly is made buoyant through a chemical reaction yielding a quantity of hydrogen, thus the base orientation of the smart-chaff is realized. One of the largest benefits of this technology surfaces in the form of cost. With respect to current techniques, costs can be decreased from around \$4000 to around \$25.

Inside this smart-chaff structure is where sensors will be held. To maintain minimal weight, a thermocouple and skin stress pressure sensor can be mounted, adding only 5 mg to the total weight. With electronics necessary to modulate the reflected waveform based on this data, the total added weight is less than 55 mg.

Since the smart-chaff structure is designed to flow with the wind currents, the orientation of the structure will vary with wind velocity. With the orientation changing, the polarization will change accordingly. The radar receiver can then strip off polarization data to determine wind direction and speed within the hurricane.

An unmanned aerial vehicle (UAV) capable of penetrating hurricanes would be used to deploy and disperse a large number of these smart-chaffs. This sets the stage for a distributed target gathering new, valuable data. By collecting data through radar backscatter, risk is lowered, cost is lowered, and necessary data is obtained.

2.4 Applied Theory

The experimental setup to evaluate these tests includes a radar testbed and a prototype modulated scatterer. The radar is expected to work like any regular radar. First and foremost, it can determine range data by measuring the time it takes for a transmitted signal to return to the receiver. The delay is then associated with the two way travel time between target and radar testbed. Since in freespace, waves travel at the speed of light, the equation that dictates this delay is, for this case,

$$\tau = \frac{2R}{c} \quad (1)$$

Where R is the range of the target, and c is the speed of light ($3 \cdot 10^8$ m/s).

In the event that two targets are very close together, multiple reflections will be superimposed on each other making it difficult for the receiver to discern how many targets are present, and the distance associated with those targets. This range resolution is based on how long the transmit pulse is.

$$\Delta R = \frac{\tau_p * c}{2} \quad (2)$$

Where ΔR is the unambiguous range, and τ_p is the pulse duration. As can be seen from equation 2, as τ_p increases, the range resolution is degraded. It would seem that the shorter the pulse length, the better, but the tradeoff is seen in terms of signal to noise ratio (SNR). If a target is illuminated, the received SNR is proportional to the time the target has been illuminated. The longer the pulse, the longer the illumination.

In equation 2, it is assumed that a simple rectangular pulse is the transmitted signal. For the specific radar testbed used in this experiment, a chirped waveform with a rectangular pulse envelope was used. The advantage of linearly increasing waveform frequency with time is seen in this range resolution/SNR tradeoff. Because the signal is not uniform throughout the pulse time, the receiver can determine the range of a target by seeing the low frequency components of the return chirp.

On the SNR side, a chirped waveform lends itself to a matched filter processing routine. A matched filter is a way to compress a received chirp signal into, ideally, a delta function. This is achieved by correlating the transmit chirp with the delayed receive signal. This would then give a delta function corresponding to an exact delay. In practice, a delta function is not achieved but a large peak is still seen. The exact matched filtering routine used for the following experiments will be discussed in the signal processing section of Chapter 3.

Since perfect resolution is not realistically achieved, it is useful to know what actual resolution to expect when using a chirped waveform. It is seen through simulation, that chirp waveforms that are matched filtered, exhibit a sinc-like shape. The half power width of the mainlobe is the theoretical resolution in time associated with that specific chirped waveform. This resolution in time is then directly related to resolution in distance. As the bandwidth of the

chirp increases, the mainlobe of the pulse compressed data shrinks giving better resolution. The exact relation is,

$$\Delta t = \frac{1}{f_1 - f_0} = \frac{1}{B} \Rightarrow \Delta R = c\Delta t = \frac{c}{2B} \quad (3)$$

Where f_0 and f_1 are the chirp's start and stop frequencies, respectively, giving the bandwidth (B).

It is seen then that a chirped waveform can provide fine range resolution with duration long pulses. In practice, if a radar is trying to view a moving target, a Doppler frequency shift is imparted on the received waveform making a target moving towards the receiver appear like a target that is stationary by closer to the receiver. For this experiment, targets will be stationary and Doppler frequency will be ignored.

Chapter 3: Radar Specific Characteristics

3.1 Transmitter Characteristics

Before even entering the transmitter hardware, a chirp waveform is generated in Matlab. This waveform is then uploaded to an arbitrary waveform generator (AWG). At this point the wave is physically realized.

The wave is designed to have an in-phase and quadrature components, and hence the AWG generates both. Both signals are then quadrature multiplexed and upconverted to the desired frequency range, around 1.8425 GHz in this case. According to Fourier theory, upon upconversion the positive and negative frequency content present at baseband will now be centered around the center frequency of the upconverter. With two signals that are 90° out of

phase, one of the sidebands can be eliminated, essentially halving the necessary transmission bandwidth. The architecture that performs this is shown in Figure 1.

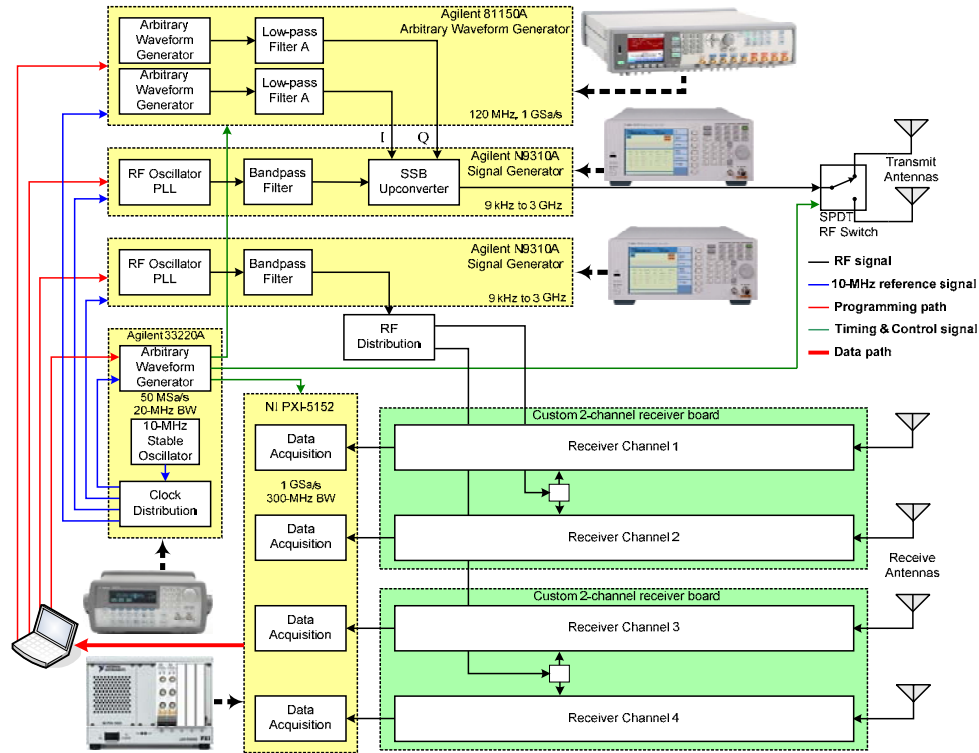


Figure 1: Block Diagram of Transmitter Setup and General Receiver Layout [14]

At this point the signal is sent to a parabolic reflector antenna and radiated. The signal specific to this project is a 1 μ s long linear chirp that either ramps from 10 MHz to 85 MHz, or 10 MHz to 245 MHz depending on what receiver setup is being utilized. The PRF of the radar is programmed into a signal generator and that tells the AWG when to repeat the transmission. For the majority of tests, the PRF was set to 100 kHz, giving a pulse repetition interval (PRI) of 10 μ s.

It is important to note that the AWG, signal generator, quadrature multiplexer, and data acquisition system, are all synchronized to a 10-MHz clock to provide signal coherence across instruments.

3.2 Receiver Characteristics

The radar receiver used in the radar test bed is a heterodyne architecture receiver that operates around 1.8425 GHz. The block diagram for the receive chain follows in Figure 2.

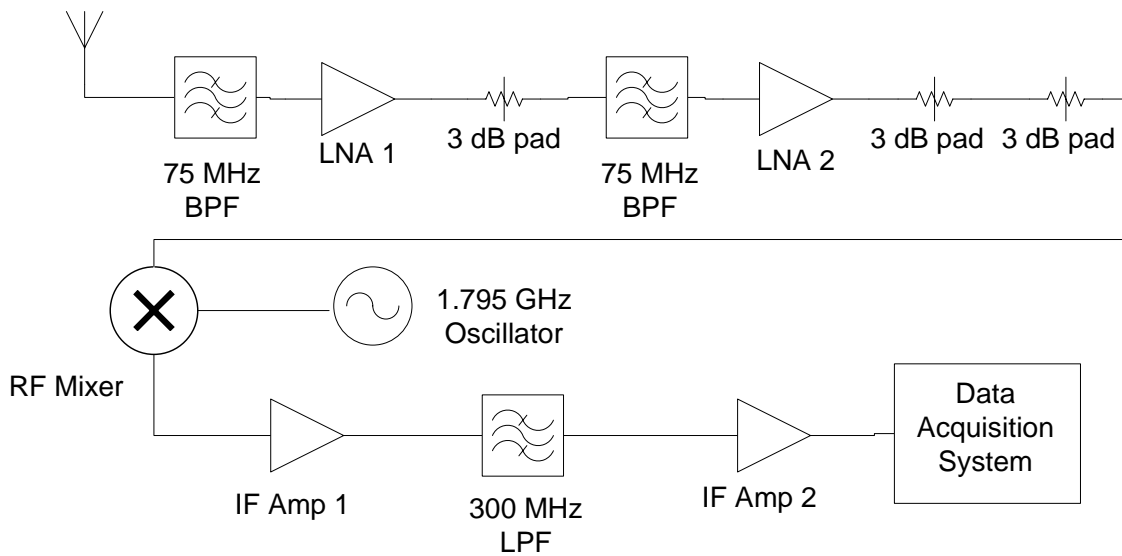


Figure 2: Detailed Block Diagram of 75-MHz Receiver

The important quantities associated with each component are shown in Table 1.

Table 1: Specific Component Data for Receiver Diagrams

Component	Manufacturer	Part Number	Gain (dB)	Loss (dB)	Noise Figure (dB)	Bandwidth (MHz)	Compression (dBm)
RF LNA	Minicircuits	ZX60-33LN	15		1.2	50-3000	17
RF Mixer	Minicircuits	ZX05-30W		7 (Conv)		300-4000	12
IF Amplifier 1	Minicircuits	ZFL-500LN	28		2.9	0.1-500	8
IF Amplifier 2	Analog Devices	ADL5530	16.5		3	0.1-1000	22
IF LPF	Minicircuits	BLP-300		1 (ins)		0-297	
<u>RF Filters</u>							
75 MHz BPF	Abracon Corp.	AFS1842.5S4		3.7 (ins)		1.805-1.88	
235 MHz BPF	Minicircuits	ZX75BP-1842		1.5 (ins)		1725-1960	
Custom BPF	K&L Microwave	CAV-02851		0.5 (ins)		1686-2013	

This specific receiver works very similar to any other heterodyne receiver. First, the incoming signal is filtered to reject any out of band noise. Since the signal is very low power, it is then amplified by the first low noise amplifier (LNA). Since the output impedance of the LNA and the input impedance of the second bandpass filter (BPF) generally aren't a great match, a 3 dB attenuator is inserted to attenuate reflected waves and minimize ringing in the system. The signal is again filtered and amplified for the same reasons. Then, because of a poor impedance match between the second LNA and the mixer, 6 dB of attenuation is inserted to greatly diminish ringing. At the mixer the received signal is downconverted to baseband where the signal is further conditioned by adding significant gain and low-pass filtering before being digitized. Once the signal is run through the analog to digital converter (ADC) in the data acquisition system, it is stored into a text file through a National Instruments Labview interface.

There were two different setups that were tested, both giving similar, but inherently different receiver characteristics. The alternate setup replaces the RF surface acoustic wave (SAW) 75 MHz bandwidth filters with a custom 300 MHz bandwidth K&L Microwave BPF at the front end of the receiver, and a 235 MHz bandwidth Minicircuits BPF further down in the RF section of the receiver. The block diagram for the wider bandwidth case is provided below.

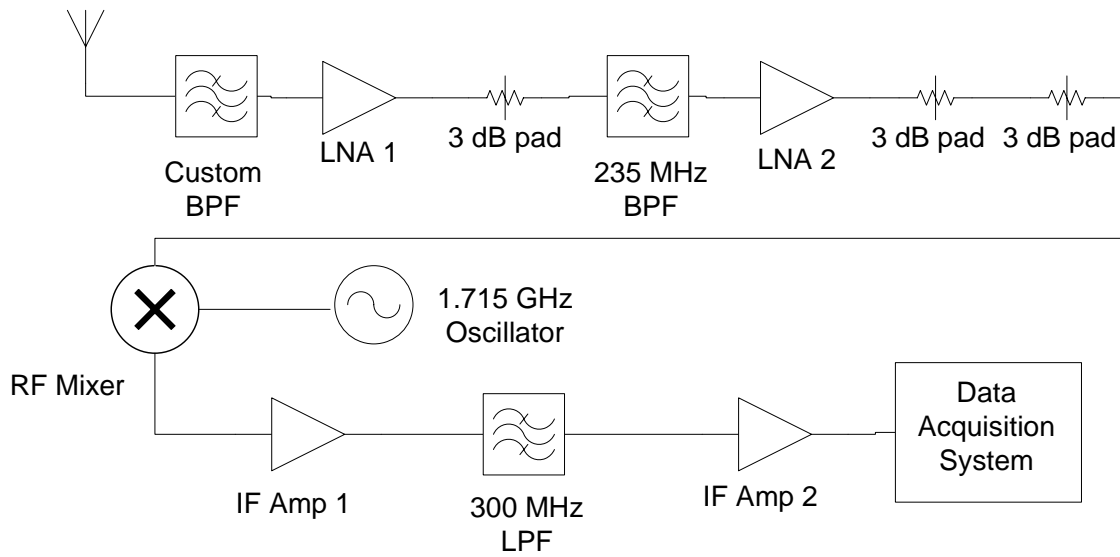


Figure 3: Detailed Block Diagram of 235-MHz Receiver

From the component specific values overall receiver characteristics can be determined. First it is useful to know the receiver gain. This is the amount of amplification the signal (and in-band noise) experience. This gain raises the signal power to the level required by the digitizer. For the 75-MHz bandwidth case, the overall receiver gain is,

$$G(dB) = -3.7dB + 15dB - 3dB - 3.7dB + 15dB - 6dB - 7dB + 28dB - 1dB + 16.5dB \quad (4)$$

$$G(dB) = 50.1dB$$

With the gain of each device known, the overall system noise figure can be calculated. The noise figure is a value that tells how much noise is generated from within the receiver.

Typically, amplifiers generate their own additive noise before amplifying a signal. As can be seen in the following calculation, components at the front end of the receiver contribute most to the overall noise figure. By having high gain and low individual noise figure at the front end of the receiver, the noise figure can be driven down.

$$\begin{aligned}
 F = & \frac{1}{0.43} + \frac{1.32-1}{0.43} + \frac{2-1}{0.43*31} + \frac{2.344-1}{0.43*31*0.5} + \frac{1.32-1}{0.43*31*0.5*0.43} \\
 & + \frac{4-1}{0.43*31*0.5*0.43*31} + \frac{5-1}{0.43*31*0.5*0.43*31*0.25} + \\
 & \frac{1.95-1}{0.43*31*0.5*0.43*31*0.25*0.2} + \frac{1.26-1}{0.43*31*0.5*0.43*31*0.25*0.2*631} \\
 & + \frac{2-1}{0.43*31*0.5*0.43*31*0.25*0.2*631*0.79} = 3.67 = 5.65dB \tag{5}
 \end{aligned}$$

At some point, each of the individual components will receive a certain input power, and not be able to perform their function with perfect efficiency. When this occurs, a component is said to be saturated. By tracking the received signal back to the antenna, the input power that saturates a device further down the receive channel can be determined. There will be a receiver input power associated with each device; the lowest input power is said to be the saturation point for the receiver as a whole. In this case the first IF amplifier saturates first, giving a receiver saturation point of,

$$P_{1dB} = 8dBm - 28dB + 7dB + 6dB - 15dB + 3.7dB + 3dB - 15dB + 3.7dB = -26.6dBm \tag{6}$$

It is also useful to know what range of signal powers the receiver can accurately process. These calculations start with the range of the digitizer, known as the instantaneous dynamic range (IDR). According to its data sheet, the data acquisition system can handle signal between -41 dBm and 7 dBm for an IDR of 48 dB.

Since there is a significant gain in the receiver, the IDR can be translated into a range based on power received at the antenna. This range is called the total dynamic range (TDR). TDR is based on the gain of the receiver as well as the minimum discernible signal (MDS) of the radar. The MDS is determined by the bandwidth and noise figure of the receiver. Effectively, the MDS is the power level at which a reflection can be detected without being lost in the noise. The calculation for MDS follows.

$$MDS = k_B T B F = 1.38 * 10^{-23} \frac{J}{K} * 290K * 75MHz * 3.67 * 10^3 \frac{mW}{W} = 1.1 * 10^{-9} mW \quad (7)$$

$$MDS(dBm) = 10 \log_{10}(MDS) = -89.58 dBm$$

Where k_B is Boltzman's constant, T is the antenna temperature in Kelvin (assumed to be 290K), B is the system bandwidth and F is the linear noise figure. Since the MDS is higher than the lower bound of the IDR minus the receiver gain, this value becomes the lower bound of the TDR. The upper bound of the TDR is then figured as the upper limit of the IDR with the receiver gain subtracted from it.

These calculations were then repeated by replacing the filter attenuation values with the respective values from the K&L Microwave and Minicircuits wider bandwidth filters. The procedure for the calculations is the same. A summary of the calculated results for both cases is presented in Table 2.

Table 2: Overall Receiver Characteristics for 75-MHz and 235-MHz Receivers

Receiver Specifics	75 MHz Bandwidth	235 MHz Bandwidth
Gain (dB)	50.1	55.5
Noise Figure (dB)	5.65	2.49
Saturation (dBm)	-26.6	-32
Bandwidth (MHz)	75	235
MDS (dBm)	-89.58	-87.78
IDR (dBm)	48 (-41 to 7)	48 (-41 to 7)
TDR (dBm)	46 (-89.58 to -43.1)	39 (-87.78 to -48.5)

3.3 Antenna Specifics

The antenna used for transmitting the radar waveform is a parabolic reflector with 22 dBi of gain. This allows for a relatively narrow beam, and therefore minimal illuminated area, reducing clutter.

The receiving antenna is actually an array of 4 dipoles all spaced at $d=\lambda/2$ (~8 cm). By having multiple elements not only is a more directive pattern achieved (when their signals are combined), but the signal's angle of arrival can be deciphered. The array was positioned in front of a metal plane, to eliminate backlobes and further increase the gain of the receive array. The back plane was placed $\lambda/4$ (~4 cm) from the array to make the image antennas appear $\lambda/2$ m away. In appearing $\lambda/2$ m away, the phase is also reversed; this causes the phases of the dipole pair to add coherently. Each dipole was fed into a separate, identical channel of the radar receiver.

It is important to understand both antenna characteristics to obtain the best estimates for maximum range of the radar test bed. From the data sheet, it is known that the parabolic transmit antenna, has a gain of 22 dBi, assuming that the horizontal and vertical beamwidths are roughly equal this gives the beamwidth to be:

$$22dBi = 10^{2.2} = 158.49 = \frac{25000}{HP_E HP_H}$$

$$Assume : HP_E = HP_H \quad (7)$$

$$HP_E^2 = \frac{25000}{158.49} \Rightarrow HP_E = 12.56^\circ$$

This provides the knowledge of what exactly is illuminated. It can be seen from the data presented that the half power beamwidth of 12.56° is in between the 10° and 14° horizontal and vertical beamwidths specified in the data sheet. A summary of the transmit and receive antenna specifications follows in Table 3.

Table 3: Antenna Specifications

	Transmit	Receive
Type	Parabolic Reflector	λ/4 Dipole
Model Number	TDJ-1800SP10	ANT-DB1-HDP-RPS
Bandwidth (MHz)	1710-1880	1770-1880
Gain (dBi)	22	
Impedance (Ω)	50	50
VSWR	≤1.5	≤1.5
Vertical Beamwidth	14°	
Horizontal Beamwidth	10°	

The receive array is somewhat more complicated. With four elements, the receive data from each can be adjusted according to each channels relative phase, and added coherently to form a more directive pattern broadside to the array. Higher directivity leads to higher gain. In the following tests, the array data is not compounded, but in the future the extra gain could be useful.

Upon reception, each antenna receives a relative signal phase that is different than its counterparts. This data is then used to determine what direction the reflected data came from.

It is seen that the bandwidth of the antennas does not take full advantage of the full receiver bandwidth in the 235-MHz setup. This manifests itself in the resolution of the system, as will be seen later in the analysis. Some signal outside of the antenna bandwidth is still radiated and received making the 235 MHz BPF valuable for out of band noise rejection.

3.4 Signal Processing

As discussed in the theory section of chapter 2, a matched filtering routine allows for an increase in SNR and resolution when processing a chirp waveform. The quintessential matched filter is the ideal transmit chirp reversed in time. During convolution of the received data and the matched filter, the matched filter is reversed in time (now forward) and multiplied across the received waveform. At some point, the two data line up exactly giving rise to a large peak associated with the target distance.

This idea of a matched filter was not robust enough to handle all of the test data that needed to be processed. Because of this, the ideal reference matched filter was only used in system delay approximations.

In the following sections, problems associated with the ideal reference are seen. Because of system imperfections, matched filtering yielded an asymmetric sidelobe structure in the pulse compressed data.

To fix this a new filter was derived. Since the received waveform, generated in loopback setup, had the similar chirp structure but already had the imperfections of the system imparted on it, it was used as the new reference waveform. Specifically this reference was the receive data from a loopback setup with 10 m of cabling between the transmitter and receiver. Details of this setup will be discussed in the next section. The received waveform was then time gated between 450 ns and 1550 ns. The majority of the receive data lay between 500 ns and 1500 ns, but a 50 ns buffer was inserted to ensure that all signal data were retained. All four channels had distinct receive data and therefore these were saved as separate references to account for the nuances in each channel.

As will be seen, when this reference waveform was used, the asymmetric sidelobe structure was eliminated. The imperfections in the received signals were cancelled because of the imperfections were accounted for in the reference waveform.

It should be noted that two different matched filter routines were examined as well, one being a complex, reversed chirp, and the other being a simply real, reversed chirp. The complex reference was generated by applying the Hilbert command in Matlab to the real reference. The Hilbert command applies a 90° phase shift to the real reference and adds it as an imaginary part to the original real waveform. This produces the complex filter. It was seen that the main lobe width for the real filter is much narrower than that of the complex term. This is because the complex term essentially forms an envelope lobe that is phase independent. The purely real filter may appear to have better resolution but its accuracy, being somewhat phase dependent, is

widely suspect. Hence, the complex matched filter is used for more consistent results. It is also seen that the complex matched filter's output corresponds well with theory, in terms of main lobe width and sidelobe levels.

For the 235-MHz bandwidth receiver configuration, the transmit chirp was modified to chirp from 10 MHz to 245 MHz in the same 1 μ s. After running this waveform through the system, it was seen that the higher frequency components were being attenuated somewhat and leading to undesirable pulse compressed waveforms. This attenuation is most likely due to the roll-off of the bandwidth of the data-acquisition system.

To account for the early bandwidth roll-off, the transmit chirp was predistorted by quadratically increasing the amplitude throughout the chirp, giving the higher frequency components a higher starting amplitude. The exact amplitude function is in appendix 1, and was shown to give a mostly even amplitude distribution upon reception.

With this amplitude weighting in effect more undesirable effects occurred. At the end of the waveform, the signal was abruptly going from a higher amplitude 245 MHz signal to no signal at all. This sharp transition created some undesirable harmonics that caused a sinusoidal offset to the received waveform. To prevent this, an amplitude ramp was applied at the beginning and end of the transmit waveform. This was executed by linearly increasing the amplitude with a constant frequency of 10 MHz for 50 ns prior to "time zero" of the transmit waveform. At the end, the same linear taper was applied with a constant frequency of 245 MHz, for 50 ns. Having this in place, countered the harmonic generation and gave a clean receive waveform.

The complex reference was then used in assessing the operation of the system for the freespace loopback setups discussed in chapter 5. When these results were deemed reliable, the receive data from the freespace loopback setup could be used as a new reference.

With this freespace loopback data there will inevitably be a problem with multipath (reflections off the floor, etc). In the time domain this will be somewhat difficult to see due to power loss upon reflection and because it will essentially be embedded within the direct path signal. In order to obtain a pure waveform this unwanted response will need to be filtered out. To do this, the matched filter routine is applied to the freespace loopback data. This will give two peaks, one corresponding to the direct path delay, and one smaller peak corresponding to the floor reflection. By windowing this pulse-compressed data, the peak due to the unwanted floor reflection can be eliminated. Since the matched filter routine is a linear process, an inverse matched filter can be applied to obtain the time-domain waveform containing only the direct path response. This signal can then be used as the reference signal for a new matched filter routine. This routine takes into effect, transmitter, receiver and antenna effects and allows for the most accurate processing of other freespace data.

An alternate processing method was also used to add further certainty to the delay measurements. This method is a form of stretch processing. The received signal is multiplied by the ideal transmit waveform, in a process called “dechirping.” The result of this product in the frequency domain three distinct spectra: a chirp band, a chirp-squared band, and a beat frequency. This beat frequency is directly related to the delay through the system as follows

$$f_b = kT \quad (8)$$

Where T is the delay through the system, f_b is the beat frequency, and k is the chirp rate, defined as

$$k = \frac{f_1 - f_0}{\tau_p} \quad (9)$$

Where f_1 is the stop frequency (85 MHz), f_0 is the start frequency (10 MHz), and τ_p is the pulse duration (1 μ s). Therefore by knowing the chirp rate, and observing the beat frequency generated by the signal processing, a delay estimate can be found.

3.5 Cabled Loopback Testing

With a theoretical knowledge of the radar testbed operation, a loopback setup was constructed so that experimental data could be fitted to theory and imperfections could be determined. This was done by splitting the delayed and attenuated transmitted signal into four parts and feeding each to their respective receiver ports. This allowed for a controlled environment with no interference, or clutter, and minimal noise.

Early in the testing phase, it was desired to determine an approximate system delay to use in later tests. With a delay figure, the cabled or freespace travel time could be inferred, and the validity of tests results could be determined at a glance. The received waveform was processed using the matched filter routine that convolved each channel's receive data with a complex, time-reversed version of the original transmit waveform. This pulse compressed data have a large peak at a time value associated with the delay of the system with a specific cable length inserted between the transmitter and receiver. The time associated with this peak can then be said to be

the system delay with that specific cabling attached. After calculating delay for the cabling, the cable-independent system delay can be calculated.

This setup was first tested with approximately 10 m of cabling between the transmitter and the receiver. This length was chosen because this is the cable length present in the setup with antennas, which will be discussed later.

After processing, the data for all four channels appeared as shown in Figure 4. It can be seen that the delay in all four channels is roughly the same. The marker shows that this delay is 488 ns. This value was then verified using the stretch processing technique. Therefore, this is the system delay with 10 m of cabling.

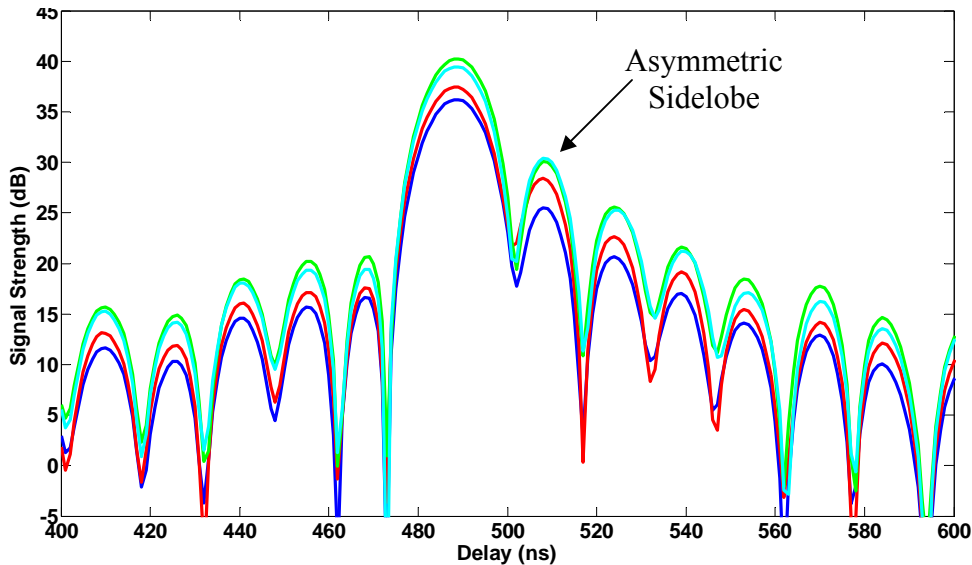


Figure 4: Correlation with Ideal Transmit Waveform

It can also be seen from Figure 4, that the sidelobes are not symmetric about the main lobe. This was unexpected. There are a number of potential causes for this inconsistency. First, there may be amplitude and phase differences between the received signal and the reference

chirp used in the matched filter routine. However in independently changing both the amplitude and phase of the reference waveform, the pronounced sidelobe neither decreased in amplitude nor moved in time.

This leads to a second possible cause: multiple reflections. It is possible that due to either an impedance mismatch, a bad connection, or a variety of other reasons, the signal could reflect off an interface and propagate back towards the transmitter. At another juncture the signal is then reflected back towards the receiver. This, now delayed signal, propagates through the proper receiver path and is sampled by the digitizer. This delay is then associated with what is being called the asymmetric sidelobe.

Since perfect impedance matches are never realized throughout a radar receiver, this is rather common. However, this delayed signal experiences additional cable loss, reducing received power. Also the receiver is designed to attenuated signals due to multiple reflections more than direct signals. Between the mixer and RF amplifier, there tends to be a notorious impedance mismatch causing rather large reflections. By inserting 6 dB worth of attenuation in the signal path, the incident wave is attenuated 6 dB, while a wave reflected off the mixer and reflected off the amplifier would see 18 dB of attenuation (passing through the 6 dB attenuators 3 times).

To determine whether or not multiple reflections are a concern, the delay between the two peaks is determined and converted to a distance. As seen in Figure 1, the time difference between peaks is roughly 20 ns. With this knowledge, a cable length is back calculated by estimating signal travel speed through a cable. The equation for doing this is shown below.

$$\tau_d = \frac{\text{cable length [m]} * \sqrt{\epsilon_r}}{c} = \frac{\text{cable length [m]}}{0.7c} \quad (10)$$

For the coaxial cable that was used, the dielectric was polytetrafluoroethylene (PTFE). The relative permittivity of PTFE is about 2.2, giving rise to the 0.7 factor in the denominator.

The equivalent cable length is found to be 4.2 m, meaning that a signal would have to travel through a 2.1 m cable twice to exhibit this excess delay.

It turned out that there were two such 2.1 m cables in the system. Those cables were replaced with longer cables to see if the asymmetric sidelobe moved. When it did not, it was determined that multiple reflections in the loopback setup was not the cause of the inconsistency.

This leaves the option that there are multiple reflections inherent in the transmitter and the devices associated with that. This is not testable, but can be assumed without any degradation in output. If the multiple reflections are in the transmitter, then it will be present in all receive waveforms, and with that knowledge, the unwanted sidelobe can be eliminated in future tests.

To verify consistency an additional 5 m of cabling was added between the transmitter and the receiver and the delay was found again. After pulse compression it appeared that the main lobe shifted approximately 25 ns in time. Using the above equation, it is seen that 25 ns is an expected additional delay for a 5 m cable. This adds further certainty to the system delay estimate.

3.6 Receive Signal Assessment

As discussed in the signal processing section, the use of the received signal in the loopback setup as the reference function in the matched filter routine, eliminates the asymmetric

sidelobe. The results for a 10 m loopback test correlated with the purely real reference function are seen in Figure 5.

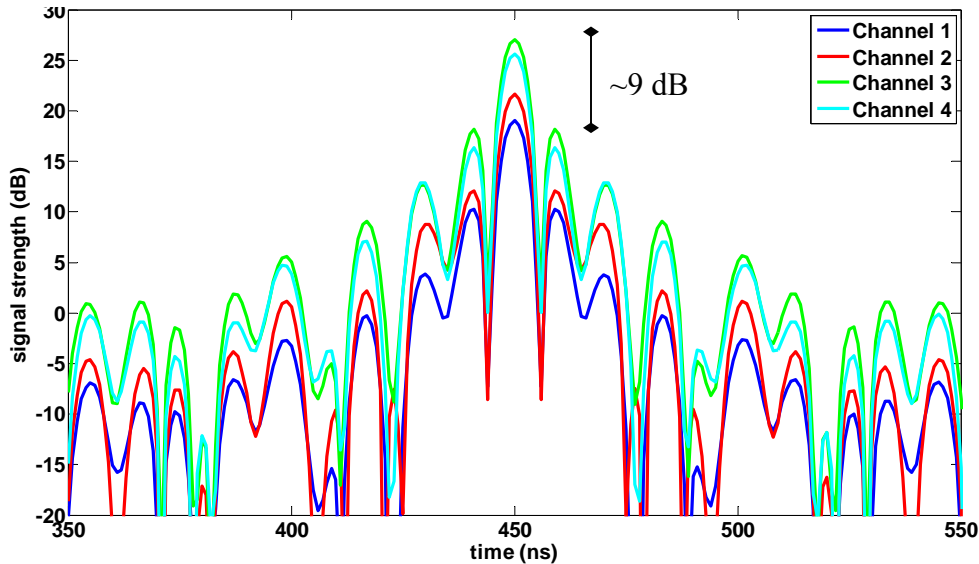


Figure 5: 10 m Loopback Autocorrelation (75 MHz)

As expected the signal is symmetric about 450 ns. This is because 450 ns was the start of the reference waveform in the pretruncated receive data. The symmetry is expected since this operation is essentially an autocorrelation, and one property of an autocorrelation is that it is always symmetric. This then accounts for the multiple reflections in the transmitter as seen by the absence of the asymmetric sidelobe.

Also seen in Figure 5, is that the amplitude characteristics across all four channels are very similar. This is desirable because it allows for one processing routine to be run for a data set. If there were large differences in channel data, then a specific routine would need to be run for each channel, to account for amplitude variations.

At this point it was noticed that the sidelobe levels for the correlation in Figure 2 were only about 9 dB below the main lobe. This was troubling because by only applying a rectangular window to the reference function, the sidelobes should be down around 13 dB relative to the mainlobe. To fix this the reference function was changed again.

In MATLAB the hilbert command was used to make the reference waveform complex by breaking it up into in-phase and quadrature components (For specifics, see Section 3.4). When this reference function was used, the cross-correlation result changed to that of Figure 6.

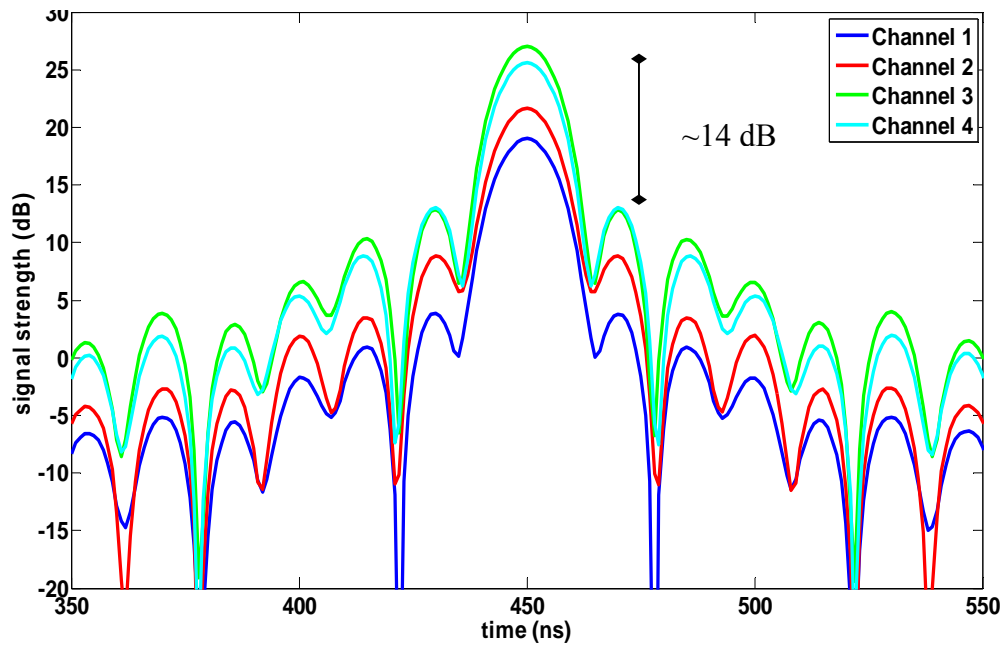


Figure 6: Autocorrelation of 10 m Loopback Data with Complex Reference (75 MHz)

In this figure, the sidelobe levels are 14 dB below the mainlobe level, much closer to the theoretical. Also the mainlobe width can be measured through interpolation at 12.6 ns. For a 75 MHz bandwidth signal, the theoretical range resolution is,

$$\Delta t = \frac{1}{B} = \frac{1}{75\text{MHz}} = 13.3\text{ns} \quad (11)$$

It is seen that the experimental findings agree closely with theory further backing the results. In Figure 5 the mainlobe is narrower as expected with a purely real reference function. This however does not match theory and the peak is highly variable, being dependent on signal phase.

Another byproduct of this complex reference function is that the pulse compressed data are complex. This allows for the determination of absolute phase of each channel. By using the angle function in MATLAB, the phase at the pulse compressed peak was found, and is presented in Table 5.

Table 5: Absolute Phase of Receive Data Across All Channels (75 MHz)

Channel	Absolute Phase (rad)
1	0.2815
2	0.2785
3	0.2814
4	0.2785

As seen in Table 5 the phases of all four channels are in close agreement. This is to be expected since the travel distance is the same for all four channels.

To further verify, the complex reference function was cross-correlated with the data from the 15 m loopback setup. In Figure 7 it is seen that the extra cable length compared to the 10 m setup is about 5 m. This matches the 15 m of cabling placed between the transmitter and receiver.

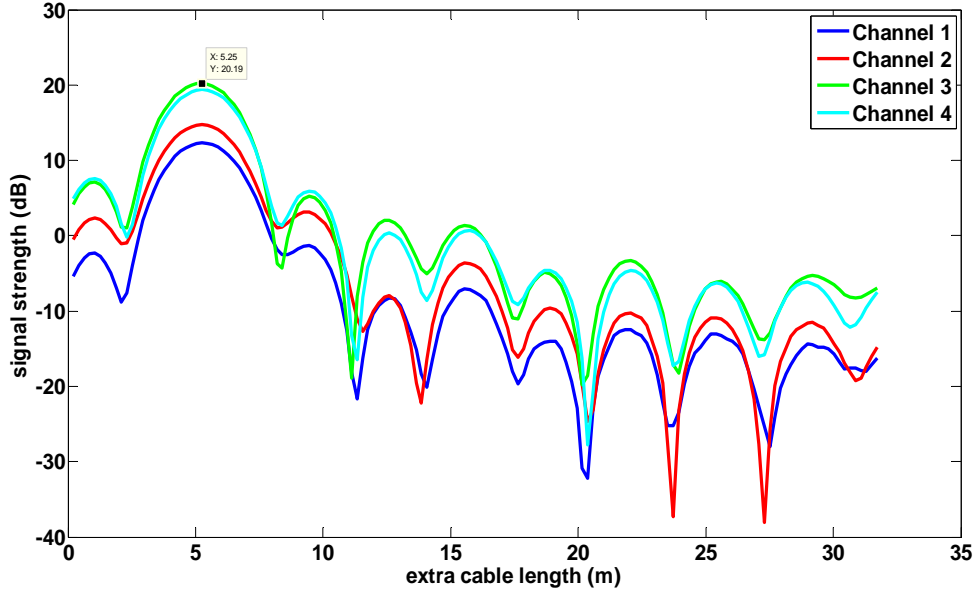


Figure 7: Correlation of Complex Reference with 15 m Cabled Loopback Data (75 MHz)

As noted earlier, a second wider bandwidth signal was necessary for freespace data collection. The same process was used to obtain a complex reference waveform specific to each receive channel.

After the wider bandwidth signal was conditioned as described in Section 3.4, the received data were pulse compressed to verify channel characteristics. The reference waveform generated from the 10 m cabled loopback setup was correlated against its pretruncated self.

Figure 8 shows the results.

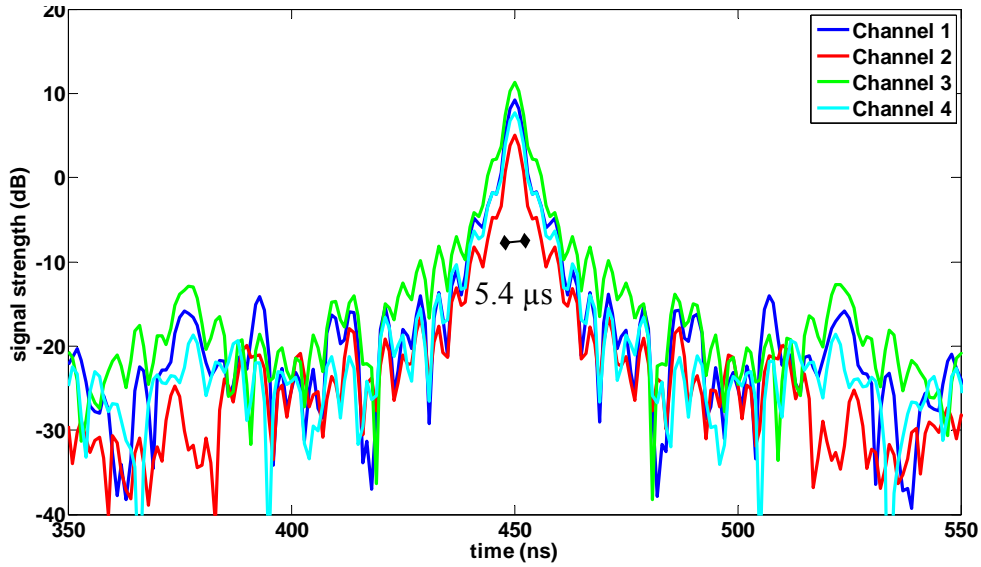


Figure 8: 10 m Loopback Autocorrelation with Complex Reference (235 MHz)

The symmetry is again evident, as well as the relative sidelobe level agreeing with theory. All amplitude peaks line up as expected, and all phases are nearly equal across channels. For reference, the phases are presented in Table 6.

Table 6: Absolute Phase of Receive Data Across All Channels (235 MHz)

Channel	Absolute Phase (rad)
1	0.6822
2	0.6613
3	0.6359
4	0.653

One noticeable difference seen in Figure 8, is that the main lobe is much narrower. This is expected because the mainlobe width determines resolution, and resolution is inversely

proportional to bandwidth, as described earlier. The half power width of the pulse compressed peak is 5.4 ns. This is the system resolution with a 235 MHz bandwidth. For comparison, the theoretical resolution is,

$$\Delta t = \frac{1}{B} = \frac{1}{235MHz} = 4.25ns \quad (12)$$

It can be seen that the numbers are very similar further verifying the data collection and processing. One reason that the numbers don't exactly match is because the full 235 MHz of bandwidth is not being utilized due to the lack of bandwidth in the transmit and receive antennas. Even though the antennas are not designed for some of the frequencies in use, most are still transmitted; hence the greater improvement in resolution.

For completeness, the 15 m cabled loopback setup was reproduced for the wider bandwidth case. Figure 6 depicts the pulse compressed data associated with those receive data. Again, an extra 5 m is expected.

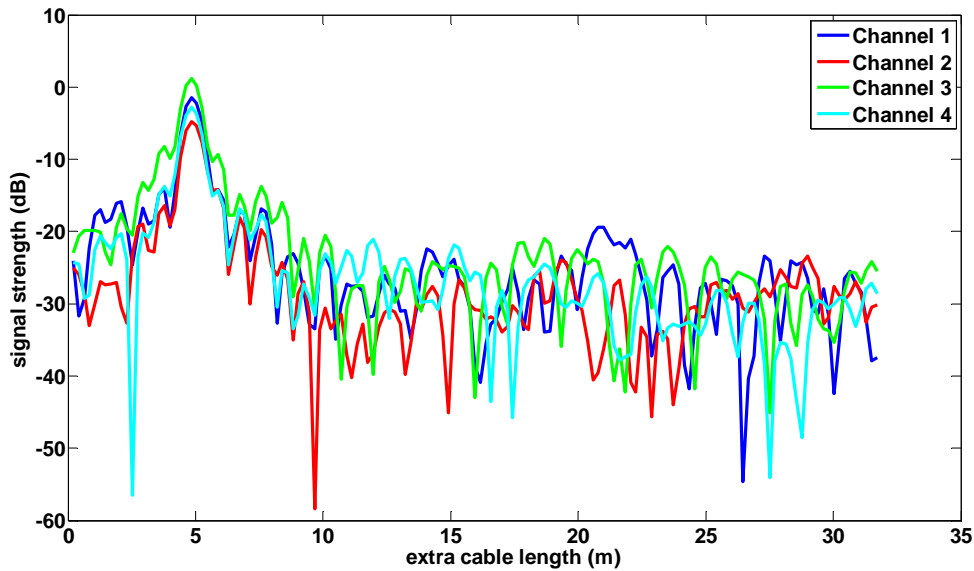


Figure 9: Correlation of Complex Reference with 15 m Cabled Loopback Data (235 MHz)

Chapter 4: Modulated Scatterer Characterization

4.1 Modulated Scatterer Operation

A group of students in the senior design lab, Michael Cribbs, Esnath Ochweri, Jackie Paschang, and Satyan Telikepalli, built a modulated scatterer that embeds 28 bits of information in the “backscatter.” This is done by way of frequency shift keying (FSK). Each bit is paired with another bit and depending on the bit values is assigned one of 4 frequencies. These two-bit control words are fed to a variable frequency oscillator that toggles an RF switch. The RF switch is connected to an antenna so that the antenna is alternately terminated in an open or short circuit. Thus the termination is toggled at a rate controlled by the bit pair. After an interval inversely related to frequency step size ($3 \mu\text{s}$), the toggling frequency changes to that associated with the next bit pair. Because 14 bit pairs were assigned $3 \mu\text{s}$ intervals, the transmit waveform needed to be lengthened from $1 \mu\text{s}$ to $100 \mu\text{s}$ in order to ensure that all the impressed data would be recorded upon reception [13].

This approach allows for a minimum delay between signal reception and retransmission since the signal is only being coupled in and reflected. This is important because if too much delay is added then the radar receiver may determine an incorrect target position.

4.2 Range limitations

For the radar test bed to be able to discern a modulated scatterer, the scatterer needs to have a detectable RCS. Since the insertion loss of the current modulated scatterer was found to be around 18 dB, these antennas placed on the modulated scatterer have some rather high minimum requirements. The gain of these antennas directly affects the scatterer's RCS. The RCS of a target goes as:

$$\begin{aligned}
 RCS &= G_T(dB) + I.L.(dB) + G_R(dB) + 10 \log_{10} \left(\frac{\lambda^2}{4\pi} \right) \\
 &= 2G_T(dB) - 18dB + 10 \log_{10} \left(\frac{(0.1628)^2}{4\pi} \right) = 2G_T(dB) - 44.76dB
 \end{aligned} \tag{13}$$

Where I.L. is the insertion loss of the modulated scatterer. Since many quantities of the radar test bed have been established, the necessary gain of the scatterer antennas can be determined through use of the radar equation:

$$P_R = \frac{P_T G_T G_R \lambda^2 \sigma}{(4\pi)^3 R^4} \tag{14}$$

From analysis, it is known that the test bed can detect signals around -87 dBm. It is also known that 13dBm is near the highest calibrated transmit power. With a frequency of 1.8425GHz, and antenna gains associated with the radar test bed, the RCS (σ) can be determined. The dipoles in the receive array are assumed to be ideal dipole to simplify calculation.

$$\begin{aligned}
 f = 1.8425 \text{ GHz} &\Rightarrow \lambda = \frac{c}{f} = \frac{3 * 10^8}{1.8425 * 10^9} = 0.1628 \text{ m} \\
 P_T (\text{dB}) = 13 \text{ dBm} &= 10 \log_{10} \left(\frac{P_T}{1 \text{ mW}} \right) = 10^{1.3} = 20 \text{ mW} \\
 P_R (\text{dB}) = -87 \text{ dBm} &= 10^{-8.7} \text{ mW} \\
 G_T = 22 \text{ dBi} &= 10^{2.2} = 158.49 \\
 G_R = 1.5 & \text{ (ideal)} \\
 RCS = \sigma &= \frac{10^{-8.7} (4\pi)^3 R^4}{20 * 158.49 * 1.5 * (0.1628)^2} = 3.14 * 10^{-8} * R^4
 \end{aligned} \tag{15}$$

From here, the RCS based on antenna requirements is substituted to give modulated scatterer antenna requirements, based on distance.

$$G_T (\text{dB}) = \frac{10 \log_{10} (4.97 * 10^{-8} * R^4) + 44.76 \text{ dB}}{2} \tag{16}$$

Based on the above equation, for a target at 100 m, the antenna associated with the modulated scatterer would need a gain of 25.86 dB. This case assumes that the transmit and receive antennas on the modulated scatterer are either one in the same, or identical. As can be seen, as the target distance increases, the antenna gain will also need to increase. A practical limitation on antenna gain would then put a limitation on communication range.

4.3 Data Processing

To decipher the data encoded on the backscatter, a process similar to the stretch processing technique is used. The received waveform is multiplied by the ideal transmit waveform. At this stage, the chirp spectrum, chirp-squared spectrum, the beat frequency, and the frequency content associated with the FSK modulation are all present. Then data are bandpass filtered with bounds of 400 kHz and 4.5 MHz [13]. This preserves the frequencies associated with each dibit. Those frequencies are shown in Table 7.

Table 7: Frequencies Associated with Bit Pairs

Dibit	Frequency
00	500 kHz
01	1 MHz
10	2 MHz
11	4 MHz

The 14 bit pairs are arranged so that they alternate between the 00 and 11 states to give the largest frequency differential. The large frequency differential is easiest to see with the eye allowing for a quick assessment on whether or not the results are correct.

The start of the encoded bit sequence is signaled by a framing pulse. This framing pulse is a 6 μ s, 32 kHz pulse. In bandpass filtering, this frequency content is filtered out, so a 6 μ s

period of very low signal power is determined to be the start bit. This start bit, and the frequencies associated with each bit pair are seen in Figure 10.

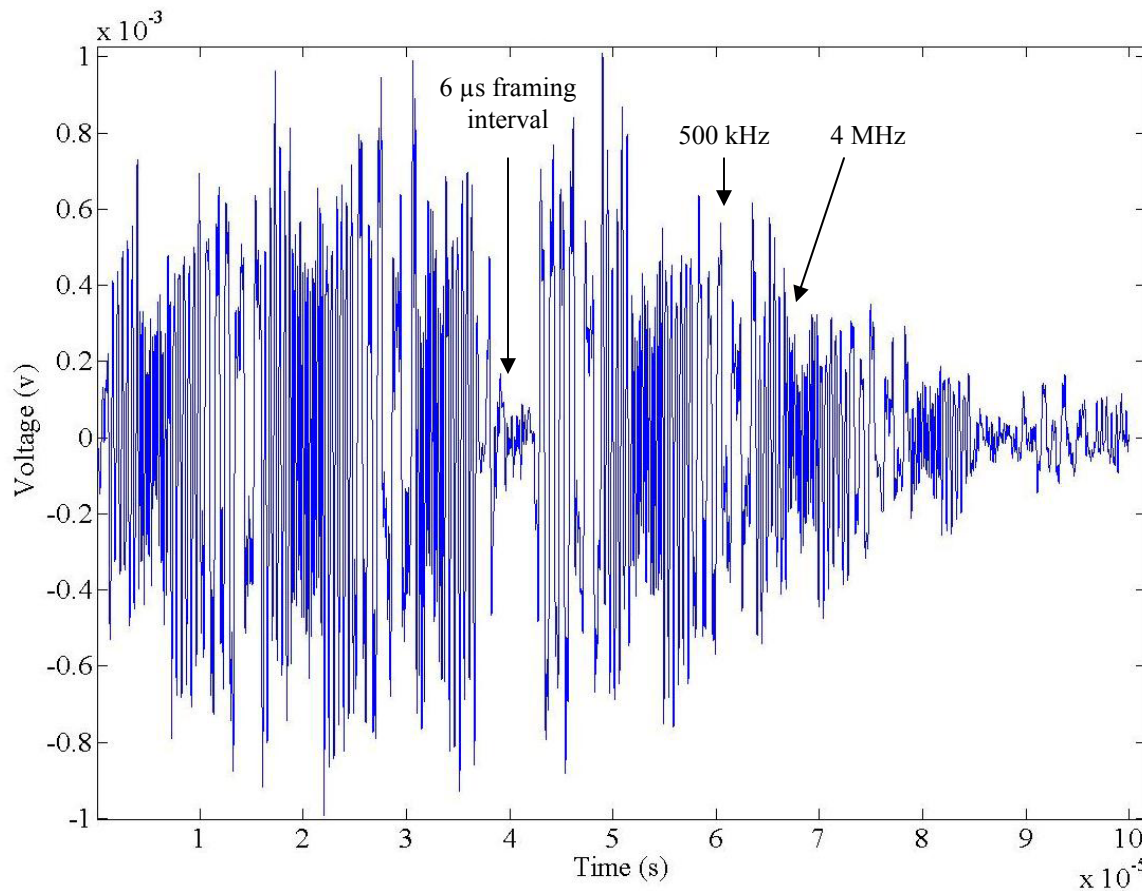


Figure 10: Processed Received Waveform from Modulated Scatterer (Frequencies of Interest) [13]

Although the different frequencies can be seen above, it is necessary to determine the exact frequencies. Two approaches can be taken. One approach is to estimate where the specific bit's frequency starts, and take a fast Fourier transform (FFT) of the proceeding $3 \mu\text{s}$. Another way is to do a correlation of the waveform with ideal sinusoids, $3 \mu\text{s}$ in length, with frequencies of 500 kHz, 1 MHz, 2 MHz, and 4 MHz. After the correlation there will be peaks at where those frequencies occurred allowing the sequencing bits, effectively extracting the binary message.

Chapter 5: Freespace Testing

5.1 Freespace Loopback

After the preliminary loopback characterization, antennas take the place of the loopback cable and freespace data are collected. A freespace loopback setup is implemented where the transmit antenna is pointed directly at the receive array. The separation is roughly 3 m. This setup allows for a characterization of the system that includes the antennas. With the antennas pointed directly at each other, the first response can be attributed to the direct freespace path between transmit and receive antennas. Since this distance is known we can calculate the delay, add on the now known system delay and verify that it matches the experimental delay.

The received data was correlated with the complex filter associated with the 10 m loopback setup. The results of this freespace loopback test and related signal processing are shown in Figure 11.

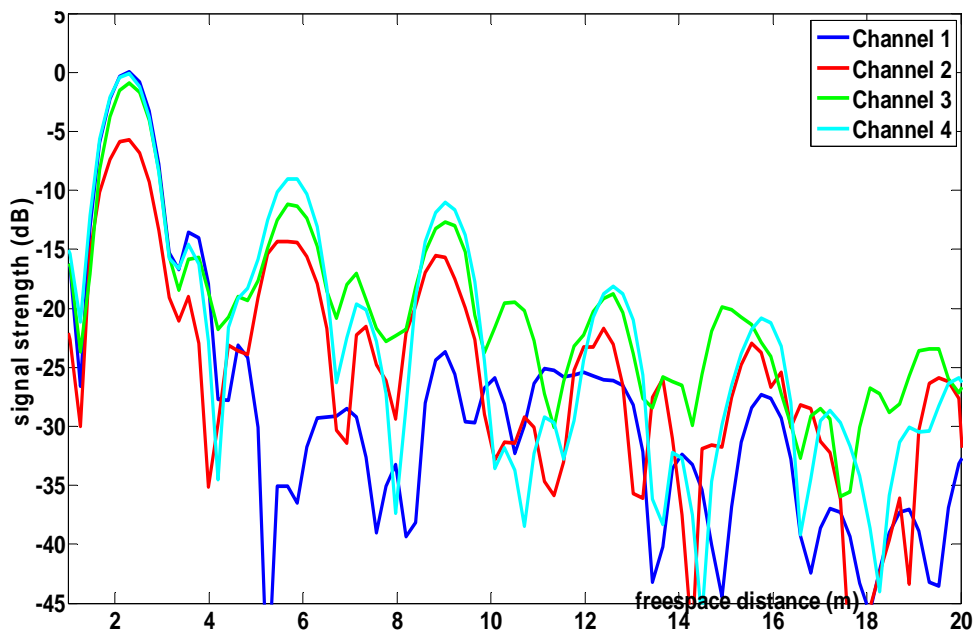


Figure 11: Correlation of Direct Freespace Data with 10 m Cabled Loopback Data (235 MHz)

Since this setup's goal is to generate a new filter for use in freespace data processing, the 235-MHz receiver is used. This wider bandwidth gives the needed resolution to resolve targets and clutter in the following tests. In Figure 11, the mainlobe width is nearly identical to that seen in the cabled loopback setups with the wider bandwidth signal.

It is interesting to see periodic peaks decaying with distance. This can be attributed to the transmit waveform being reflected off the backplane on the receive array, propagating back to the transmitter, reflecting off the parabolic reflector, and being received again at the receiver.

In seeing this data, it can be said that the radar is performing in a desirable fashion. Amplitude traces are similar across the channels, and the incident phases are roughly equal across the channels for broadside incidence.

5.2 Indoor Testing

With indoor tests, the most successful test was that done in the Nichols Hall atrium. The setup is shown in the figure below:

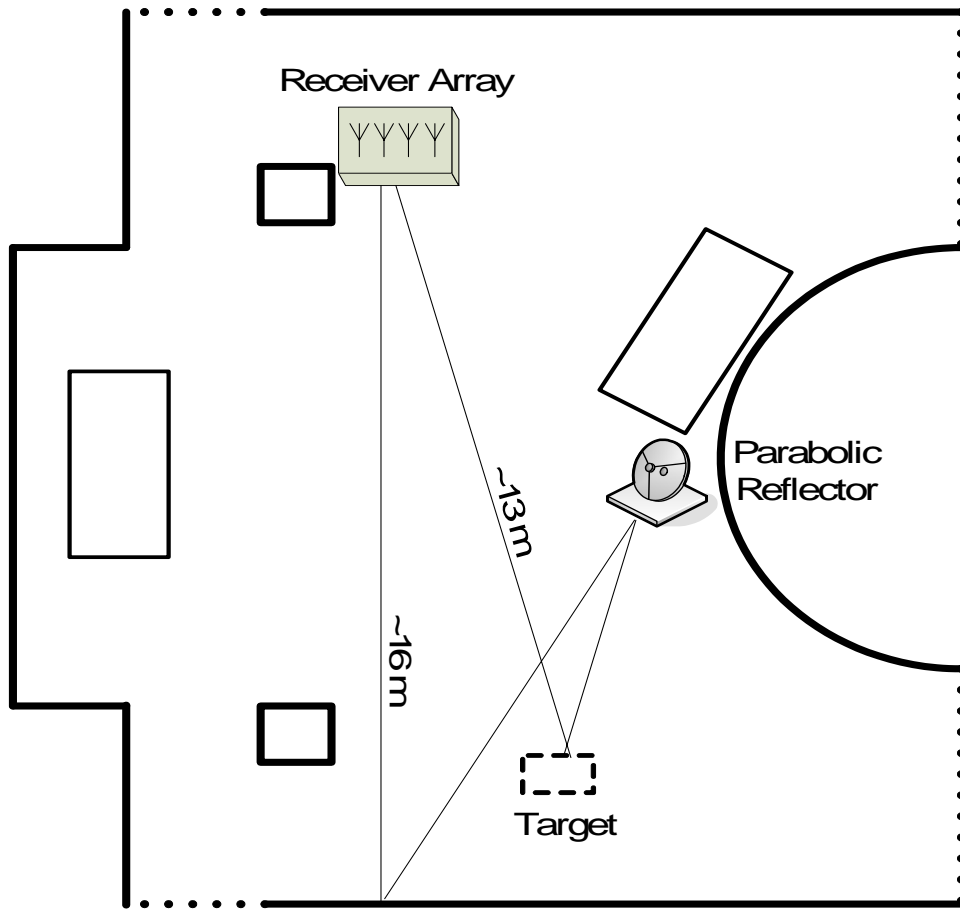


Figure 12: Nichols Hall Atrium Indoor Setup Geometry

The transmit antenna is far enough away to prevent any significant direct coupling. The expected direct path was to reflect off of the far wall and return to the receiver (as shown in Figure 12). The results of this test are shown in Figure 13.

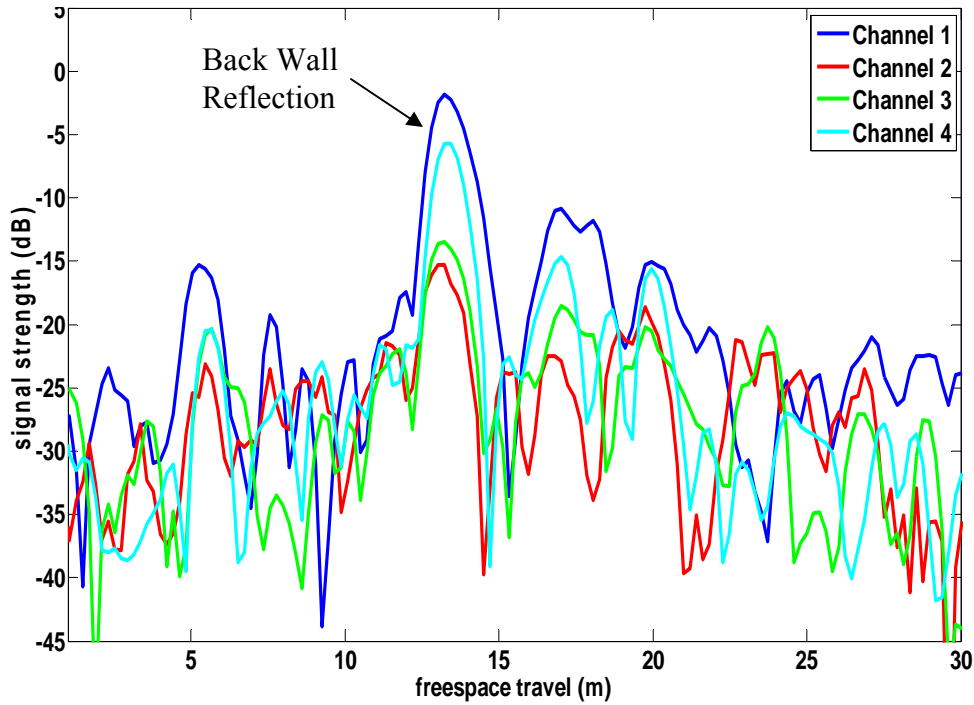


Figure 13: Atrium Reflections Measurements

The pulse compressed data show a coherent response on all four channels at about 14 m. The measured distance from the transmitter to the wall, and the wall to the receiver, is around 16 m. The calculated distance is about 2 m shorter than the estimated distance. Causes for the difference can be explained by error in estimating the travel distance or slight calibration offsets in the receiver. Since 2 m is approximately 7 ns of delay difference, any slight error in delay calibration could lead to a significant distance offset.

With the background scene data collected, a scatterer (trash can) was inserted into the scene. With the 75-MHz setup, the target was absorbed into the reflection associated with the back wall. However, when the 235-MHz setup was used, Figure 14 resulted.

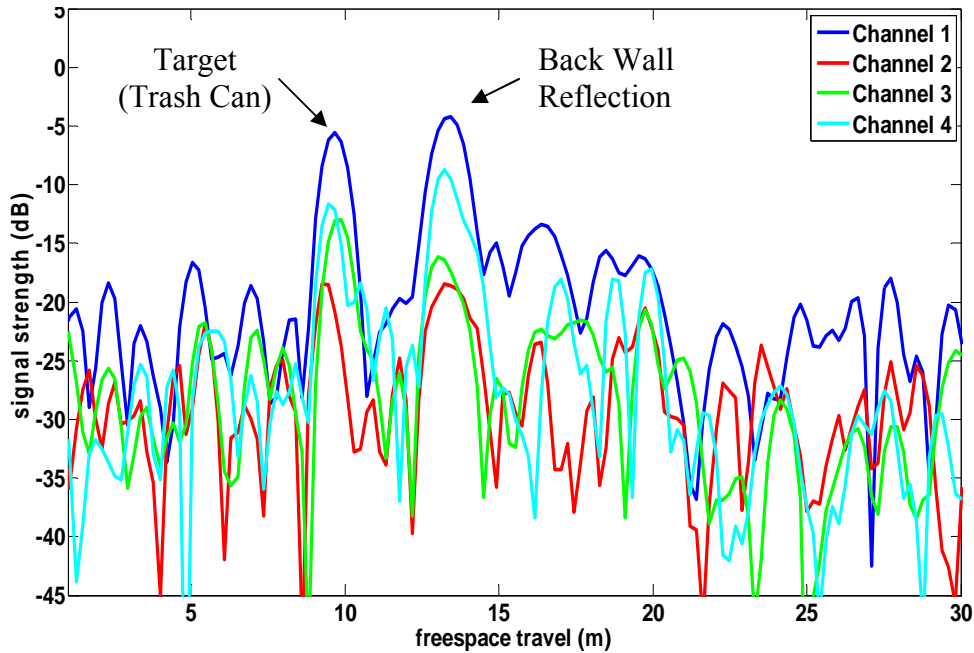


Figure 14: Atrium Reflection from Target

Figure 14, shows a large coherent response at 10 m in addition to the wall reflection at 14 m. Again this is closer than the estimated distance. However, since the difference between measured and estimated is similar, the error can be attributed to the same causes, and the results are determined to be reasonable.

It is interesting to note that the received signal power from the target and the wall are very close. Even though the signal from the target travels less distance, therefore experiencing less spherical spreading loss, its RCS is smaller causing less reflected signal power. These effects roughly cancel giving rise to equal received signal powers.

Since these tests were indoors, freespace multipath is a definite concern. From the diagram of the setup, it appears that the column nearest the far wall could provide an extra reflection and cause some of the peaks seen after the wall reflection. After that it is seen that

multiple reflections decrease signal power enough that there are no more coherent responses after 20 m. This can also be attributed to the low transmit power (~10 dBm).

When the phases of each channel were examined, channels 1, 3, and 4 had their phases change linearly. Since it is very plausible that the angle of incidence of the reflected wave is not normal to the receive array, this is acceptable. When calculating the angle of incidence, it was seen that the angle was slightly larger than expected, but still within reason. An error in distance estimation could be one cause.

The phase for channel 2 did not line up with the other channels. This is most likely due to the structure of the back wall. Since the surface is not a perfectly flat reflector, certain phase data may be skewed due to partial oblique incidence.

5.3 Outdoor Testing

After running some preliminary outdoor tests with the radar test bed, it was seen that the direct path, transmitted through a side lobe of the transmit antenna, was the major response. It also appears that there is a considerable reflection off the building behind the scene. Any targets that were too close were masked by those responses. In contrast, with low transmit power, and small RCS, distant targets were difficult to detect.

In some instances it proved useful to sample over a number of pulse repetition intervals (PRIs). With multiple responses, the responses can all be added to each other for a cumulative response. Since noise is a zero-mean signal, the addition of the other echoes will bring the noise level closer to its mean, while the target response will add in phase. This causes the average signal level to be mostly constant, while the noise level will decrease. Overall this increases the

signal to noise ratio (SNR), and gives a better chance of detecting targets that are either far away, or have a low RCS.

Chapter 6: Conclusions

6.1 Summary of Results

At this point, it can be said that the radar test bed is characterized. All channels show similar amplitude traces for loopback data, cabled and freespace. Also the phases across the channels are nearly the same as expected. Pulse compressed data show mainlobes with a half power width in time close to that calculated from theory.

In processing indoor data, the major reflector, the far wall, is seen without absorbing the response from a target placed nearer to the receiver. The phases of the receive traces gave an angle of incidence in line with what was expected despite one channel having errant phase data due to the wall being a non-uniform surface.

Outdoor testing was inconclusive, but opened up possibilities for further testing. Since indoors range was limited, outdoors would be the only way to test the range limitations of both the radar test bed and modulated scatterer.

It was seen that in a controlled loopback setup that a modulated scatterer could impress data on a chirped waveform. Through some simple signal processing, that data could then be deciphered with high fidelity. It follows that with such good performance in loopback, that even with the noisy, clutter filled environment of freespace testing, that data could be retrieved remotely.

6.2 Discrepancies and Shortcomings

The loopback testing went relatively smoothly, and hence most of the difficulties to be discussed involve freespace testing. For some time indoor testing was all that was practical. In this setup clutter and multipath were major concerns. Responses from both appeared in a number of traces either drowning out targets, or causing doubt in estimated distances. With an uneven surface for a planar reflector, phase data was somewhat unreliable, and even scattering characteristics were drawn into question. By manipulating the angle of incidence, relatively sound data was collected.

Another issue that was encountered was that on occasion the data received from the antenna assigned to channel 1 would cause that channel to saturate. The exact reason for this is not entirely known, it could simply be a faulty components. An explanation that could've caused the receiver saturation as well as degradation in results is that a GSM cell phone frequency band lay within the bandwidth of the wider bandwidth receiver. These signals would then be coupled in and processed exactly the same as the desired signal would be.

In outdoor tests, with the building providing a large response, a target needed to be a significant distance away from the transmitter. However with such a low calibrated transmit power, the signal power being received at the test bed was minimal. It was difficult to get any definitive results.

For the modulated scatterer, it was easy enough to determine the bit pattern in loopback, but in a less ideal environment, decoding could prove to be difficult. It would seem to be useful if the frequencies assigned to each dibit were not harmonics of each other. When being processed in the receiver, these harmonics may be generated naturally, and therefore cause an error in bit assignment.

Also with so many bits to encode, a very long transmit pulse was necessary. For precise processing, a lengthy receive trace was necessary. Processing of those lengthy receive traces proved to be time consuming and inefficient.

6.3 Future Work

In the future it would be desirable to verify the scalability of this setup. If data can be retrieved from one remote source, can it reliably be retrieved from multiple sources simultaneously? A freespace test would need to be conducted in which not only the scene could be depicted accurately, but in which the location of each modulated scatterer and the data they're impressing could be deciphered.

This could be done with an antenna with a wider beamwidth in order to illuminate more targets at one time instance. This would allow for faster scene scanning. This would come at the cost of some antenna gain, which as seen earlier is vital in detecting a target at a large distance with a relatively small RCS.

For the current setup, this is very difficult due to the low transmit power and high insertion loss of the modulated scatterer. If the transmit power could be increased then it directly follows that the radar has a larger range associated with it, and also sees closer targets more clearly. It, in turn, follows that a redesign of the modulated scatterer may be necessary. An insertion loss of 18 dB is rather high and leaves much to be desired. A decrease in that could increase the practical range of the system by relaxing some of the rather strict antenna requirements on the target.

With a higher transmit power, the beamwidth of the transmit antenna could be widened, illuminating a larger scene. In that scene, multiple modulated scatterers could be placed, and data could be processed from multiple scatterers simultaneously, verifying the scalability claim.

If there are a number of targets, it is necessary to assume that some modulated scatterers may lay much closer to the transmitter/receiver than others. With a higher transmit power, it is possible that some targets could be close enough, that their response could exceed the upper limit of the radar TDR. It is seen that the upper bound of the radar test bed's TDR (-48.5 dBm for the 235-MHz receiver setup) is well below the receiver saturation point (-32 dBm, for the same setup). The addition of an automatic gain control (AGC) stage in the receiver to attenuate strong responses and amplify weak responses could maximize the TDR of the receiver. This increased dynamic range then allows the radar test bed to sample an even larger area.

Bibliography

- [1] Stockman, H; “Communication by means of reflected power,” *Proc. of the IRE*, pp. 1196-1204, 1948.
- [2] Bracht R; Miller EK; Kuckertz T; “Using an impedance-modulated reflector for passive communication,” *1997 Digest IEEE Antennas and Propagation Society International Symposium*, v. 2, pp.1070-1073, 1997.
- [3] Thornton J; Edwards DJ; “Modulating retro-reflector as a passive radar transponder,” *Electronics Letters*, 34(19), pp. 1880-1881, 1998.
- [4] Bracht R; Miller EK; Kuckertz T; “An impedance-modulated reflector system,” *IEEE Potentials*, 18(4), pp. 29-33, 1999.
- [5] Shimada M; Oaku H; Nakai M; “SAR calibration using frequency-tunable active radar calibrators,” *IEEE Transactions on Geoscience and Remote Sensing*, 37(1), pp. 564-573, 1999.
- [6] Waegel K; Hounam D; Bauer R; Bloetscher H; Zink M; Schwerdt M; Mayr B; “An encoding SAR-transponder for target identification,” *IEEE International Geoscience and Remote Sensing Symposium, IGARSS '99*, v.1, pp. 20-22, 1999.
- [7] Gilbreath GC; Rabinovich WS; Meehan TJ; Vilcheck MJ; Mahon R; Burris R; Ferraro M; Solkolsky I; Vasquez JA; Bovais CS; Cochrell K; Goins KC; Barbehenn R; Katzer DS; Ikossi-Anastasiou K; Montes MJ; “Large-aperture multiple quantum well modulating retroreflector for free-space optical data transfer on unmanned aerial vehicles,” *Optical Engineering*, 40(7), pp. 1348-1356, 2001.

- [8] Bidigare P; “The Shannon channel capacity of a radar system,” *Conference Record of the Thirty-Sixth Asilomar Conference on Signals, Systems and Computers*, v.1, pp. 113-117, 2002.
- [9] Bidigare P; Stevens T; Correll B; Beauvais M; “Minimum radar cross section bounds for passive radar responsive tags,” *Conference Record of the Thirty-Eighth Asilomar Conference on Signals, Systems and Computers*, v.2, pp. 1441-1445, 2004.
- [10] Blunt SD; Yantham P; “Waveform design for radar-embedded communications,” *International Waveform Diversity and Design Conference*, pp. 214-218, June 4-8, 2007.
- [11] Farokhi S; Allen C; Barret R; Blunt SD; Tucker D; “PIRE: Hurricane Endoscopic Latent Instrumented Observation System,” NSF 06-589, Feb 28, 2007.
- [12] Brunfeldt DR; Ulaby FT; “Active reflector for radar calibration,” *IEEE Transactions on Geoscience and Remote Sensing*, 22(2), pp. 165-169, 1984.
- [13] Cribbs M; Ochweri E; Paschang J; Telikepalli S; “Radar Embedded Communication,” Final Project Report – EECS 502, 2009.
- [14] Allen C; Blunt SD; “Testbed Evaluation of Radar-Embedded Communication Concepts,”

Appendices

Appendix I - Datasheets

Quick Fact Sheet

Agilent 81150A Pulse Function Arbitrary Noise Generator

Triple versatility, optimum signal fidelity—from anywhere at any time

Standard, complete connectivity!
LXI Class C compliant



A 3-in-1 device for accelerated and accurate insight into your device

- Create pulse, sine, square, ramp, noise and arbitrary waveforms to test your device — not the source
- A 2 Channel version can be used either as 2 independent generators or as time synchronized coupled or added
- Integrated in one instrument, which increases signal performance, minimizes cabling, space and test time
- Glitch free change of timing parameters (delay, frequency, transition time, width, delay cycle).
- Programming language compatible with Agilent 81101A, 81104A and 81110A

1. Coupler/uncouple channels/channel add

2. USB 2.0A
3. Channel 2:
Trigger out; Strobe out; Differential output
4. Channel 1:
Trigger out; Strobe out; Differential output
5. Trigger mode
6. Waveform mode
7. Advanced mode: Modulation/Sweep/Burst
8. Keypad

Choose your hardware

Code	Description
#001	81150A with 1 channel
#002	81150A with 2 channels
#DOC	Printed documentation
#TCP	Rack mount kit
#1A6	Z-540 calibration documents
#1A7	ISO 17025 calibration documents
#PAT	Pattern generator license

Key specifications

Bandwidth	1 µHz - 120 MHz (250 sine)
Waveforms	Noise, adjustable crest factor, sine, pulse, square, ramp, arbitrary waveform
Channels	1 or 2, differential outputs
Output Amplitude Amplifier	
High voltage:	50 mV to +10 V
High bandwidth:	50 mV to +5 V
Modulation types:	AM, FM, PM, FSK, PWM external and internal
Transition Times	>2.5 ns
Output impedance	50 Ω / 5 Ω selectable
Sample rate	14-bit, 2 G/s arbitrary waveform
Memory	Arbitrary: 512 k points per channel Pattern: 16 Mbit per channel
Noise repetition rate	26 days
Display	Color, bright
Programming interfaces	LAN, SCPI 1992, IEEE 488.2 (GPIB), USB
Supported drivers	Agilent VEE, VI-COM, NI Labview, Matlab®



Agilent Technologies

Quick Fact Sheet

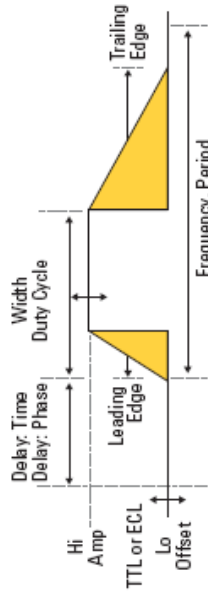
Pulse Pattern Generator Selection Guide

Model	Bandwidth	Channels	Voltage
8114A	15 MHz	1-ch	100 V / 2 A
81101A	50 MHz	1-ch	100 mV - 10 V
81104A + 81105A	80 MHz	1 or 2 ch	100 mV - 10 V
81110A + 81111A	165 MHz	1 or 2 ch	100 mV - 10 V
81110A + 81112A	330 MHz	1 or 2 ch	100 mV - 3.8 V
81130A + 81131A	400 MHz	1 or 2 ch	100 mV - 3.8 V
81130A + 81132A	680 MHz	1 or 2 ch	100 mV - 2.5 V

Complementary products

Model	Description
DSO/MSO 6000, 7000	InfiniVision 7000 Series oscilloscopes up to 1 GHz bandwidth
DSO/MSO 8604A	Infiniium DSO/MSO oscilloscope with 800 MHz bandwidth
DSO/MSO 5000	InfiniVision 5000 Series oscilloscopes up to 500 MHz bandwidth
DSO 3000	Economy DSO 3000 Series up to 200 MHz bandwidth
33210A, 33220A, 33250A	Function generators with 10, 20 and 80 MHz, 1 channel

Characteristics on a Pulse Pattern Shape



All parameters can be selected and edited with the Agilent Pulse Pattern Generators

MX11A18 is a U.S. registered trademark of the MathWorks, Inc. PCI Express is a registered trademark of PCI SIG.

Recommended service options

Additional two years of Return-to-Agilent warranty
 Additional two years of Return-to-Agilent calibrations
 For more information go to www.agilent.com/find/removefault

Product specifications and descriptions in this document subject to change without notice.
 © Agilent Technologies, Inc. 2009. Printed in USA, August 21, 2009
 5990-4565EN

Typical Applications

FlexRay/CAN physical layer receiver test (Flyer: 5660-31 60EN)
Sensor simulation
Clock signal generation
Radar distance testing
Disc drive tests
Noise and jitter source with selectable crest factor
Signal source with modulation
Pulsed IV measurements
System trigger source
Capture and reproduce live signals

Related Literature

Pub Number	Name
5989-6433EN	81150A Pulse Function Arbitrary Noise Generator Data Sheet
5989-0489E	Pulse Pattern and Data Generators For Digital and Analog Testing
5989-7860EN	Agilent 81150A Pulse Function Arbitrary Noise Generator Applications
5990-3233EN	PCI Express® Revision 2.0 Receiver Testing with J-BERT N4903A and 81150A Pulse Function Arbitrary Noise Generator
5989-9826EN	Agilent 15431A Filter Set for 81150A
5989-9364EN	Agilent 81150A Precision Digital Noise

LXI is the LAN-based successor to GPIB, providing faster, more efficient connectivity. Agilent is a founding member of the LXI consortium.

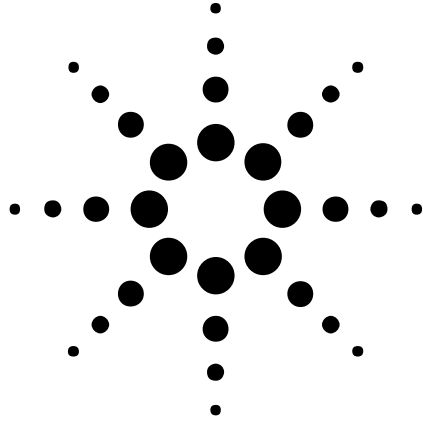
www.lxistandard.org



Agilent Technologies

Agilent N9310A RF Signal Generator

Technical Overview



All the capability
and reliability of an
Agilent instrument
you need — at a price
you've always wanted



N9310A RF Signal Generator



Agilent Technologies

Specifications

Supplemental Information

Frequency

Range:	9 kHz to 3.0 GHz	
Resolution:	0.1 Hz	
Switching speed:	< 10 ms	within 0.1 ppm of final frequency

Internal Reference Oscillator

Stability:	< ±1ppm/year < ±1ppm	Aging Temperature over 0 to 45 °C
-------------------	-------------------------	--------------------------------------

Timebase Reference Output

Frequency:	10 MHz
Amplitude:	> 0.35 Vrms level into 50 Ω
Connector:	BNC female

External Reference Input

Range:	2 MHz, 5 MHz, 10 MHz
Amplitude:	0.5 ~ 2 Vrms
Connector and impedance:	50 Ω; BNC female

Output

Power:	-127 to +13 dBm	+20 dBm settable
Resolution:	0.1 dB	
Accuracy:	< ±1dB	$F_c \geq 100 \text{ kHz}$, $-120 \leq \text{Level} \leq +13\text{dBm}$, 20 to 30 °C
Switching speed:	< 10 ms	< 0.3 dB deviation
VSWR (typical) :	< 1.6 < 1.8	1.5 MHz ≤ F_c < 2.5 GHz 2.5 GHz ≤ F_c ≤ 3 GHz
Output connector and impedance:	N-type; 50 Ω nominal	

Reversal Power Protection

DC voltage:	30 V	
RF power:	+36 dBm	1 minute; the warning for reversed power protection is nominally at +25 dBm

Spectral Purity

SSB Phase Noise:	< -95 dBc/Hz	Typical, Fc = 1 GHz; at 20 kHz offset
Residual FM:	< 30 Hz rms; < 90 Hz peak < 20 Hz rms	CW mode, Fc = 1 GHz; BW = 0.3 to 3 KHz ResFM optimized mode
Harmonics:	< -30 dBc	Level ≤ 0 dBm, Fc ≥ 1 MHz
Non-harmonics:	< -50 dBc	Level ≤ 0 dBm, >10 kHz from carrier

Sweep Modes

RF and LF:	
LF Sweep range:	20 Hz to 80 kHz
RF Sweep range:	9 kHz to 3 GHz
Sweep points:	2 to 1001
Dwell time:	10 ms to 1s
Amplitude:	
Sweep range:	-127 to +13 dBm
Sweep points:	2 to 1001
Dwell time:	10 ms to 1s

Simultaneous Modulation *

		AM		I/Q	FM		ΦM	Pulse	
		Internal	External		Internal	External		Internal	External
AM	Internal	-	•	-	•	•	•	-	-
	External	•	-	-	•	•	•	-	-
I/Q		-	-	-	•	•	•	•	•
FM	Internal	•	•	•	-	•	-	•	•
	External	•	•	•	-	-	-	•	•
ΦM		•	•	•	-	-	-	•	•
Pulse	Internal	-	-	•	•	•	•	-	-
	External	-	-	•	•	•	•	-	-

Amplitude Modulation (Fc > 100 kHz)

Operating modes:	Internal, external AC/DC	Envelope peak < maximum specified power
Range:	0 to 100%	
Resolution:	0.1%	
Rates:	DC/20 Hz to 20 kHz	
Accuracy:	< ± (5 % of setting +0.2%)	1 kHz, 0 dBm and 80% modulation
Distortion:	< 2%	1 kHz, 0 dBm and 80% modulation, THD
External input:	MOD IN connector	
Sensitivity:	0.5 Vpeak	Input voltage for 100% modulation depth
Input impedance:	BNC; > 100 k Ω	Nominal

* N9310A only has one external modulation input connector. The simultaneous external modulations are applied to the same input signal.

Frequency Modulation

Operating modes:	Internal, external AC/DC	
Frequency deviation:	20 Hz to 100 kHz	
Resolution:	< 1%	Minimum 1Hz
Rates:	AC/20 Hz to 80 kHz	
Distortion:	< 1%	1 kHz rate, THD, Deviation = 50 kHz
Deviation accuracy:	< \pm (5 % of FM deviation +300 Hz)	1 kHz, 0 dBm and 50 kHz deviation
Carrier frequency		
Deviation:	< 200 Hz	Relative to carrier; external mode
External input:	MOD IN connector	
Sensitivity:	1 Vpeak	Input voltage for 100 kHz modulation deviation
Input impedance:	BNC; > 100 k Ω	Nominal

Phase Modulation

Operating modes:	Internal	
Phase deviation:	0 to 10 rad 0 to 5 rad	Rate \leq 10 kHz 10 kHz < Rate \leq 20 kHz
Resolution:	< 1%	
Rates:	300 Hz to 20 kHz	
Deviation accuracy:	< \pm (5% of FM deviation +0.2 rad)	1 kHz rate
Distortion:	< 1.5%	1 kHz rate, THD, Deviation = 5 rad
External input:	MOD IN connector	
Sensitivity:	1 Vpeak	Input voltage for 10 rad modulation deviation
Input impedance:	BNC; > 100 k Ω	Nominal

Pulse Modulation

Operating modes:	Internal, external, AC/DC	
On/Off ratio:	\geq 40 dB	
Rise/fall time:	< 3 μ s	
Pulse width:	100 μ s to 1s	Internal, external
Pulse period:	200 μ s to 2s	Internal
Time resolution:	1 μ s	
Input connector and voltage level:	BNC female; TTL	

Internal Modulation Source

Waveform:	Sine	
Frequency range:	20 Hz to 80 kHz	
Resolution:	0.1 Hz	
Accuracy:	0.005%	Typical

LF Out
(Internal
Modulation Source)

Amplitude:	0 to 3 Vpeak	Level to high impedance
Output voltage		
Resolution:	< 1%	1 mV minimum resolution
Frequency response:	< ± 0.2 dB	20 Hz to 20 kHz
Total Harmonic		
Distortion:	< 0.1%	20 Hz to 20 kHz
Connector		
and impedance:	BNC female; < 1 Ω	Front panel

I/Q Modulation
(Option 001 only)

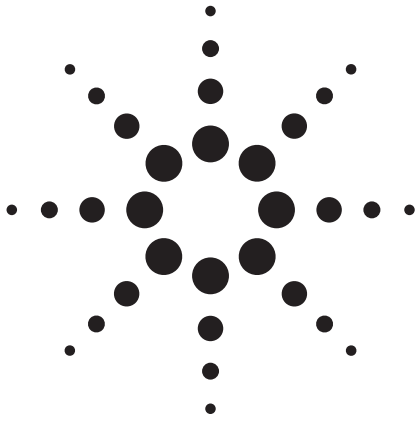
Operating mode:	External I/Q inputs	
VSWR:	< 1.5	
Full scale input:	$\sqrt{I^2 + Q^2} = 0.5V_{rms}$	
Modulation frequency		
range:	DC to 40 MHz	At 3 dB points
Carrier suppression:	40 dBc	Typical; Modulation frequency = 10 kHz
QPSK EVM:	3%	Typical; 1Msps. 0.22 RRC Filter
GMSK Phase error:	1.2° rms	Typical; 1Msps. BT= 0.5
Connector		
and impedance:	BNC female; 50 Ω	Rear panel

USB Connector

USB Host interface:	3 x A Plug	V 1.1 protocol
USB Device interface:	1 x B Plug	V 1.1 protocol

General

Power requirement:	100~240 Vac; 50~60 Hz	Auto-ranging
Power consumption:	65 W	
Temperature range:	5 ~ 45 °C	Operating
	-20 to 70 °C	Storage
Weight:	9.2 kg	Approximately
Dimensions:	132.5x320x400 mm	H x W x D



Agilent 33220A 20 MHz Function/Arbitrary Waveform Generator

Data Sheet



- Fully compliant to LXI Class C specification 
- 20 MHz Sine and Square waveforms
- Pulse, Ramp, Triangle, Noise, and DC waveforms
- 14-bit, 50 MSa/s, 64 k-point Arbitrary waveforms
- AM, FM, PM, FSK, and PWM modulation types
- Linear & logarithmic sweeps and burst operation
- 10 mV_{pp} to 10 V_{pp} amplitude range
- Graph mode for visual verification of signal settings
- Connect via USB, GPIB and LAN

Uncompromising performance for functions and waveforms

The Agilent Technologies 33220A Function/Arbitrary Waveform Generator uses direct digital synthesis (DDS) techniques to create a stable, accurate output signal for clean, low distortion sine waves. It also gives you square waves with fast rise and fall times up to 20 MHz and linear ramp waves up to 200 kHz.

Pulse generation

The 33220A can generate variable-edge-time pulses up to 5 MHz. With variable period, pulse width, and amplitude the 33220A is ideally suited to a wide variety of applications requiring a flexible pulse signal.

Custom waveform generation

Use the 33220A to generate complex custom waveforms. With 14-bit resolution, and a sampling rate of 50 MSa/s, the 33220A gives you the flexibility to create the waveforms you need. It also lets you store up to four waveforms in nonvolatile memory.

The Agilent IntuiLink Arbitrary Waveform software allows you to easily create, edit, and download complex waveforms using the waveform editor. Or you can capture a waveform using IntuiLink for Oscilloscope and send it to the 33220A for output. To find out more about IntuiLink, visit www.agilent.com/find/intuilink.



Agilent Technologies

Measurement Characteristics

Easy-to-use functionality

Front-panel operation of the 33220A is straight-forward and user friendly. You can access all major functions with a single key or two. The knob or numeric keypad can be used to adjust frequency, amplitude, offset, and other parameters. You can even enter voltage values directly in V_{pp} , V_{rms} , dBm, or as high and low levels. Timing parameters can be entered in Hertz (Hz) or seconds.

Internal AM, FM, PM, FSK, and PWM modulation make it easy to modulate waveforms without the need for a separate modulation source. Linear and logarithmic sweeps are also built in, with sweep rates selectable from 1 ms to 500 s. Burst mode operation allows for a user-selected number of cycles per period of time. GPIB, LAN, and USB interfaces are all standard, plus you get full programmability using SCPI commands.

External frequency reference (Option 001)

The 33220A external frequency reference lets you synchronize to an external 10 MHz clock, to another 33220A, or to an Agilent 33250A. Phase adjustments can be made from the front panel or via a computer interface, allowing precise phase calibration and adjustment.

Waveforms	
Standard	Sine, Square, Ramp, Triangle, Pulse, Noise, DC
Built-in arbitrary	Exponential rise, Exponential fall, Negative ramp, Sin(x)/x, Cardiac
Waveforms Characteristics	
Sine	
Frequency Range	1 μ Hz to 20 MHz
Amplitude Flatness ^{(1),(2)} (relative to 1 kHz)	< 100 kHz 0.1 dB 100 kHz to 5 MHz 0.15 dB 5 MHz to 20 MHz 0.3 dB
Harmonic distortion ^{(2),(3)}	< 1 V_{pp} \geq 1 V_{pp}
DC to 20 kHz	-70 dBc -70 dBc
20 kHz to 100 kHz	-65 dBc -60 dBc
100 kHz to 1 MHz	-50 dBc -45 dBc
1 MHz to 20 MHz	-40 dBc -35 dBc
Total harmonic distortion ^{(2),(3)}	DC to 20 kHz 0.04%
Spurious (non-harmonic) ^{(2),(4)}	DC to 1 MHz -70 dBc 1 MHz to 20 MHz -70 dBc + 6 dB/octave
Phase noise (10 kHz offset)	-115 dBc / Hz, typical
Square	
Frequency range	1 μ Hz to 20 MHz
Rise/Fall time	< 13 ns
Overshoot	< 2%
Variable duty cycle	20% to 80% (to 10 MHz) 40% to 60% (to 20 MHz)
Asymmetry (@ 50% duty)	1% of period + 5 ns
Jitter (RMS)	1 ns + 100 ppm of period
Ramp, Triangle	
Frequency range	1 μ Hz to 200 kHz
Linearity	< 0.1% of peak output
Variable Symmetry	0.0% to 100.0%
Pulse	
Frequency range	500 μ Hz to 5 MHz
Pulse width (period \leq 10s)	20 ns minimum, 10 ns resolution
Variable edge time	< 13 ns to 100 ns
Overshoot	< 2%
Jitter (RMS)	300 ps + 0.1 ppm of period

Noise	
Bandwidth	9 MHz typical
Arbitrary	
Frequency range	1 μ Hz to 6 MHz
Waveform length	2 to 64 k points
Amplitude resolution	14 bits (including sign)
Sample rate	50 MSa/s
Min. Rise/Fall Time	35 ns typical
Linearity	< 0.1% of peak output
Settling Time	< 250 ns to 0.5% of final value
Jitter (RMS)	6 ns + 30 ppm
Non-volatile memory	four waveforms

Common Characteristics

Frequency	
Accuracy ⁽⁵⁾	\pm (10 ppm + 3 pHz) in 90 days \pm (20 ppm + 3 pHz) in 1 year
Resolution	1 μ Hz
Amplitude	
Range	10 mV _{pp} to 10 V _{pp} into 50 Ω 20 mV _{pp} to 20 V _{pp} into open circuit
Accuracy ^{(1),(2)} (at 1 kHz)	\pm 1% of setting \pm 1 mV _{pp}
Units	V_{pp} , V_{rms} , dBm
Resolution	4 digits
DC Offset	
Range (peak AC + DC)	\pm 5 V into 50 Ω \pm 10 V into open circuit
Accuracy ^{(1),(2)}	\pm 2% of offset setting \pm 0.5% of amplitude \pm 2 mV
Resolution	4 digits
Main Output	
Impedance	50 Ω typical
Isolation	42 Vpk maximum to earth
Protection	Short-circuit protected, overload automatically disables main output
External Frequency Reference (Option 001)	
Rear Panel Input	
Lock Range	10 MHz \pm 500 Hz
Level	100 mV _{pp} to 5 V _{pp}
Impedance	1 k Ω typical, AC coupled
Lock Time	< 2 seconds
Rear Panel Output	
Frequency	10 MHz
Level	632 mV _{pp} (0 dBm), typical
Impedance	50 Ω typical, AC coupled

Measurement Characteristics (Continued)

Phase Offset

Range	+ 360° to - 360°
Resolution	0.001°
Accuracy	20 ns

Modulation

AM

Carrier waveforms	Sine, Square, Ramp, Arb
Source	Internal/External
Internal modulation	Sine, Square, Ramp, Triangle, Noise, Arb (2 mHz to 20 kHz)
Depth	0.0% to 120.0%

FM

Carrier waveforms	Sine, Square, Ramp, Arb
Source	Internal/External
Internal modulation	Sine, Square, Ramp, Triangle, Noise, Arb (2 mHz to 20 kHz)
Deviation	DC to 10 MHz

PM

Carrier waveforms	Sine, Square, Ramp, Arb
Source	Internal/External
Internal modulation	Sine, Square, Ramp, Triangle, Noise, Arb (2 mHz to 20 kHz)
Deviation	0.0 to 360.0 degrees

PWM

Carrier waveform	Pulse
Source	Internal/External
Internal modulation	Sine, Square, Ramp, Triangle, Noise, Arb (2 mHz to 20 kHz)
Deviation	0% to 100% of pulse width

FSK

Carrier waveforms	Sine, Square, Ramp, Arb
Source	Internal/External
Internal modulation	50% duty cycle square (2 mHz to 100 kHz)

External Modulation Input^[6] (for AM, FM, PM, PWM)

Voltage range	± 5 V full scale
Input impedance	5 kΩ typical
Bandwidth	DC to 20 kHz

Sweep

Waveforms	Sine, Square, Ramp, Arb
Type	Linear or Logarithmic
Direction	Up or Down
Sweep time	1 ms to 500 s
Trigger	Single, External, or Internal
Marker	falling edge of sync signal (programmable frequency)

Burst^[7]

Waveforms	Sine, Square, Ramp, Triangle, Pulse, Noise, Arb
Type	Counted (1 to 50,000 cycles), Infinite, Gated
Start/Stop Phase	-360° to +360°
Internal Period	1 μs to 500 s
Gate Source	External trigger
Trigger source	Single, External or Internal

Trigger Characteristics

Trigger input	
Input level	TTL compatible
Slope	Rising or Falling, selectable
Pulse width	> 100 ns
Input impedance	>10 kΩ, DC coupled
Latency	< 500 ns
Jitter (rms)	6 ns (3.5 ns for pulse)
Trigger output	
Level	TTL compatible into ≥ 1 kΩ
Pulse width	> 400 ns
Output Impedance	50 Ω, typical
Maximum rate	1 MHz
Fanout	≤ 4 Agilent 33220As

Programming Times (typical)

Configuration times	USB	LAN	GPIOB
Function Change	111 ms	111 ms	111 ms
Frequency Change	1.5 ms	2.7 ms	1.2 ms
Amplitude Change	30 ms	30 ms	30 ms
Select User Arb	124 ms	124 ms	123 ms
Arb Download Times (binary transfer)			
64 k points	96.9 ms	191.7 ms	336.5 ms
16 k points	24.5 ms	48.4 ms	80.7 ms
4 k points	7.3 ms	14.6 ms	19.8 ms

General

Power Supply	CAT II 100 - 240 V @ 50/60 Hz (-5%, +10%) 100 - 120 V @ 400 Hz (±10%)
Power Consumption	50 VA max
Operating Environment	IEC 61010 Pollution Degree 2 Indoor Location
Operating Temperature	0°C to 55°C
Operating Humidity	5% to 80% RH, non-condensing
Operating Altitude	Up to 3000 meters
Storage Temperature	-30°C to 70°C
State Storage Memory	Power off state automatically saved. Four user-configurable stored states
Interface	USB, GPIB, and LAN standard
Language	SCPI - 1993, IEEE-488.2
Dimensions (W x H x D)	
Bench top	261.1 mm x 103.8 mm x 303.2mm
Rack mount	212.8mm x 88.3mm x 272.3mm
Weight	3.4 kg (7.5 lbs)
Safety Designed to	UL-1244, CSA 1010, EN61010
EMC Tested to	MIL-461C, EN55011, EN50082-1
Vibration and Shock	MIL-T-28800, Type III, Class 5
Acoustic Noise	30 dBa
Warm-up Time	1 hour
Warranty	1 year standard

Footnotes

^[1] add 1/10th of output amplitude and offset spec per °C for operation outside the range of 18°C to 28°C

^[2] Autorange enabled

^[3] DC offset set to 0 V

^[4] spurious output at low amplitude is -75 dBm typical

^[5] add 1 ppm/°C average for operation outside the range of 18°C to 28°C

^[6] FSK uses trigger input (1 MHz maximum)

^[7] Sine and square waveforms above 6 MHz are allowed only with an "infinite" burst count

Ordering Information

Agilent 33220A

20 MHz Function/Arbitrary
Waveform Generator

Accessories included

Operating manual, service manual,
quick reference guide, IntuiLink waveform
editor software, test data, USB cable,
and power cord (see language option).

Options

- Opt. 001** External timebase reference
- Opt. 0B0** Delete manual
- Opt. 1CM** Rackmount kit
(also sold as Agilent 34190A)
- Opt. A6J** ANSI Z540 calibration
- Opt. AB0** Taiwan: Chinese manual
- Opt. AB1** Korea: Korean manual
- Opt. AB2** China: Chinese manual
- Opt. ABA** English: English manual
- Opt. ABD** Germany: German manual
- Opt. ABF** France: French manual
- Opt. ABJ** Japan: Japanese manual

Other Accessories

- 34131A** Carrying case
- 34161A** Accessory pouch
- 34190A** Rackmount kit

Agilent Technologies' Test and Measurement Support, Services, and Assistance

Agilent Technologies aims to maximize the value you receive, while minimizing your risk and problems. We strive to ensure that you get the test and measurement capabilities you paid for and obtain the support you need. Our extensive support resources and services can help you choose the right Agilent products for your applications and apply them successfully. Every instrument and system we sell has a global warranty. Two concepts underlie Agilent's overall support policy: "Our Promise" and "Your Advantage."

Our Promise

Our Promise means your Agilent test and measurement equipment will meet its advertised performance and functionality. When you are choosing new equipment, we will help you with product information, including realistic performance specifications and practical recommendations from experienced test engineers. When you receive your new Agilent equipment, we can help verify that it works properly and help with initial product operation.

Your Advantage

Your Advantage means that Agilent offers a wide range of additional expert test and measurement services, which you can purchase according to your unique technical and business needs. Solve problems efficiently and gain a competitive edge by contracting with us for calibration, extra-cost upgrades, out-of-warranty repairs, and on-site education and training, as well as design, system integration, project management, and other professional engineering services. Experienced Agilent engineers and technicians worldwide can help you maximize your productivity, optimize the return on investment of your Agilent instruments and systems, and obtain dependable measurement accuracy for the life of those products.



Agilent Email Updates

www.agilent.com/find/emailupdates

Get the latest information on the products and applications you select.



Agilent Direct

www.agilent.com/find/agilentdirect

Quickly choose and use your test equipment solutions with confidence.



Agilent Open

www.agilent.com/find/open

Agilent Open simplifies the process of connecting and programming test systems to help engineers design, validate and manufacture electronic products. Agilent offers open connectivity for a broad range of system-ready instruments, open industry software, PC-standard I/O and global support, which are combined to more easily integrate test system development.

www.agilent.com

For more information on Agilent Technologies' products, applications or services, please contact your local Agilent office. The complete list is available at:

www.agilent.com/find/contactus

Phone or Fax

United States:

(tel) 800 829 4444
(fax) 800 829 4433

Canada:

(tel) 877 894 4414
(fax) 800 746 4866

China:

(tel) 800 810 0189
(fax) 800 820 2816

Europe:

(tel) 31 20 547 2111

Japan:

(tel) (81) 426 56 7832
(fax) (81) 426 56 7840

Korea:

(tel) (080) 769 0800
(fax) (080) 769 0900

Latin America:

(tel) (305) 269 7500

Taiwan:

(tel) 0800 047 866
(fax) 0800 286 331

Other Asia Pacific Countries:

(tel) (65) 6375 8100
(fax) (65) 6755 0042

Email: tm_ap@agilent.com

Contacts revised: 09/26/05

Product specifications and descriptions in this document subject to change without notice.

© Agilent Technologies, Inc. 2006
Printed in the USA, April 19, 2006
5988-8544EN



Agilent Technologies

SMD 1842.5MHz SAW FILTER

AFS1842.5S4

APPLICATION: Cellular Phone



3 x 3 x 1.5mm

STANDARD SPECIFICATIONS:

CHARACTERISTICS	UNIT	MIN.	TYP.	MAX.
Center Frequency Fc	MHz	-	1842.5	-
Bandwidth	MHz	-	$F_c \pm 37.5$	-
Insertion Loss @ Passband				
1805 ~ 1815 MHz @ (15°C ~ +70°C)	dB	-	-	3.3
1805 ~ 1815 MHz @ (-20°C ~ 15°C)	dB	-	-	3.7
1815 ~ 1870 MHz	dB	-	-	3
1870 ~ 1880 MHz	dB	-	-	3.6
Ripple @ Passband	dB	-	-	N/A
Relative Attenuation				
0 ~ 1720 MHz	dB	20	-	-
1720 ~ 1765 MHz	dB	25	-	-
1765 ~ 1785 MHz	dB	8	-	-
1920 ~ 1980 MHz	dB	15	-	-
1980 ~ 2410 MHz	dB	17	-	-
2410 ~ 3120 MHz	dB	20	-	-
3120 ~ 4000 MHz	dB	17	-	-
DC Voltage	V	10		
Source Power	dBm	15		
Operating Temperature	°C	-20°C to +70°C		
Storage Temperature	°C	-40°C to +85°C		
Return Loss @ 1805 ~ 1880	MHz	6		

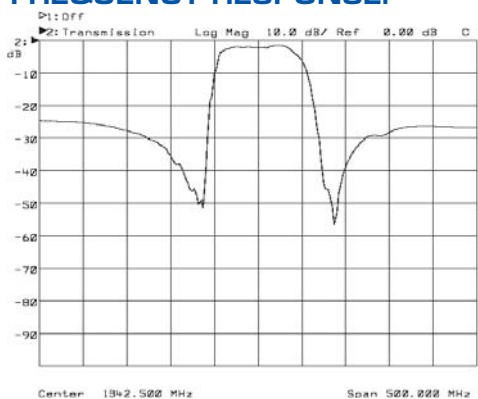
Electrostatic Sensitive Device. Handle with precaution.

MARKING:

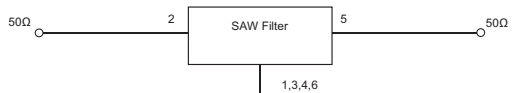
- 1575.42 (1575.42 Frequency in MHz)
- AF ZYX (ZY: Date code Z for month from A to L; Y for year, i.e. 4 for 2004; X: Traceability code)

PIN NO.	CONNECTIONS
2	Input
5	Output
1,3,4,6	Ground

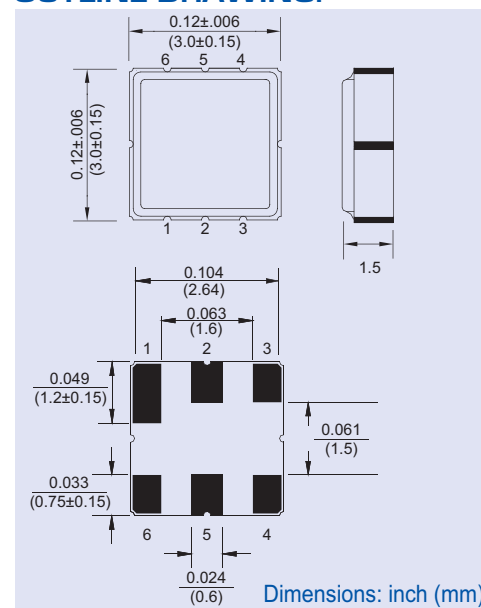
FREQUENCY RESPONSE:



TEST CIRCUIT:



OUTLINE DRAWING:



Bandpass Filter

ZX75BP-1842+

50Ω 1725 to 1960 MHz

The Big Deal

- Low Insertion Loss, 1.4 dB
- Excellent Rejection
 - 1450 MHz, 2350 MHz, 30 dB
 - 1350 MHz, 2560 MHz, 49 dB
- Rejection band extends to 7 GHz



CASE STYLE: HY1238

Product Overview

The Mini-Circuits ZX75BP-1842+ ceramic coaxial resonator based filter offers outstanding close-in rejection in the PCS/DCS communication band. Built using Mini-Circuits proven unibody construction which integrates the RF connectors with the case body, the ZX75BP-1842+ takes very little space, and includes a multi-section low pass filter to prevent second harmonic re-entry that is characteristic of typical ceramic resonator filters.

Key Features

Feature	Advantages
Outstanding close-in rejection	Using high Q ceramic resonators enables this filter to support applications where tight rejection performance is required.
Rejection band extended to 7 GHz	Integrated "clean up" low pass filter enables excellent rejection up to 7 GHz eliminates the need for additional external filters.
High Power Handling, 6W	Ability to withstand high power signals allows operation in many lab and integrated assembly applications, or for use in field applications as a quick-fix filter solution.
Excellent Temperature Stability	±0.35 dB insertion loss over the full temperature range.
Compact Versatile Case	Case Body: 1.2"x0.75"x0.46" With connectors and flanges: 2.05"x1.18"x0.46" Connectors: SMA Female (1), SMA Male (1)

Bandpass Filter

50Ω 1725 to 1960 MHz

ZX75BP-1842+



CASE STYLE: HY1238

SMA Connectors	Model	Price	Qty.
IN MALE OUT FEM	ZX75BP-1842-S+	\$59.95 ea.	(1-9)

+ RoHS compliant in accordance with EU Directive (2002/95/EC)

The +Suffix has been added in order to identify RoHS Compliance. See our web site for RoHS Compliance methodologies and qualifications.

Maximum Ratings

Operating Temperature	-55°C to 100°C
Storage Temperature	-55°C to 100°C
RF Power Input*	6W max. at 25°C

* Derate linearly to 3W at 100°C ambient. Permanent damage may occur if any of these limits are exceeded.

Features

- Low Insertion loss, 1.4 dB typ.
- Minimal Insertion loss variation over temperature, ±0.35 dB
- Sharp stop band rejection
- Protected by US Patent 6,790,049

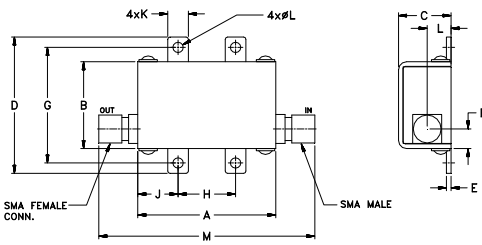
Applications

- Harmonic & Sub-harmonic filtering
- Image rejection
- PCS/DCS

Electrical Specifications at 25°C

Parameter	F#	Frequency (MHz)	Min.	Typ.	Max.	Unit	
Pass Band	Center Frequency		—	1842	—	MHz	
	Insertion Loss	F1-F2	1725-1960	—	1.4	3.0	dB
	VSWR	F1-F2	1725-1960	—	—	2.0	:1
Stop Band, Lower	Insertion Loss	DC-F5	0.3-1350	40	—	dB	
		F5-F3	1350-1450	20	—	dB	
	VSWR	DC-F3	0.3-1450	—	30	—	:1
Stop Band, Upper	Insertion Loss	F4-F6	2350-2560	20	—	dB	
		F6-F7	2560-2600	40	—	dB	
		F7-F8	2600-7000	—	20	—	dB
	VSWR	F4-F8	2350-7000	—	10	—	:1

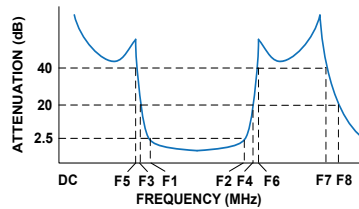
Outline Drawing



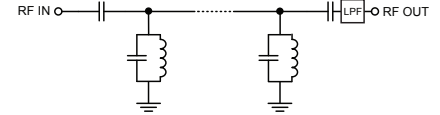
Outline Dimensions (inch/mm)

A	B	C	D	E	F	G
1.20	.75	.46	1.18	.04	.17	1.00
30.48	19.05	11.68	29.97	1.02	4.32	25.40
H	J	K	L	M	wt	
.50	.35	.18	.106	2.05	grams	
12.70	8.89	4.57	2.69	52.07	35.00	

Typical Frequency Response

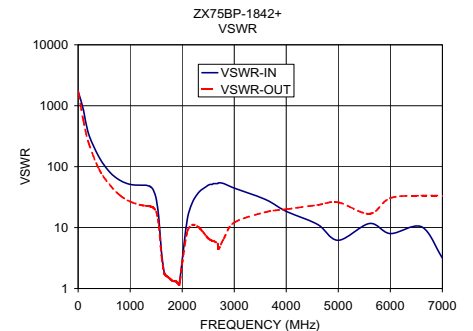
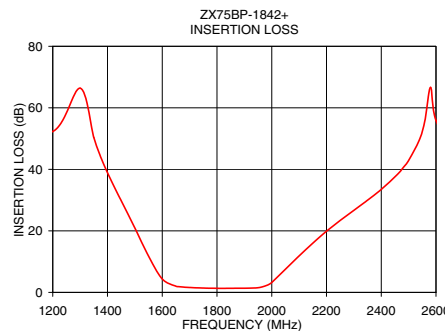
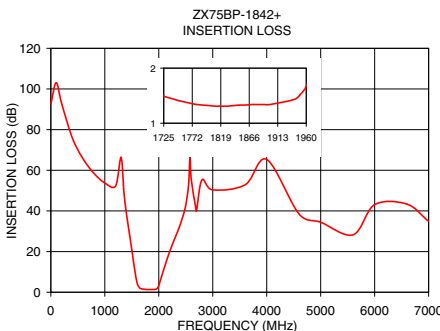


Functional Schematic



Typical Performance Data at 25°C

Frequency (MHz)	Insertion Loss (dB)	VSWR-IN (:1)	VSWR-OUT (:1)
0.30	92.61	1737.18	1737.18
500.00	70.30	102.19	66.82
1000.00	53.74	51.10	26.74
1350.00	50.38	48.26	22.58
1415.00	36.07	44.55	21.73
1450.00	29.80	40.41	20.95
1600.00	4.36	4.09	3.49
1725.00	1.49	1.54	1.55
1730.00	1.47	1.53	1.54
1842.00	1.32	1.31	1.34
1842.50	1.32	1.31	1.34
1960.00	1.67	1.49	1.37
1975.00	2.05	1.86	1.70
2015.00	4.24	3.94	3.34
2350.00	29.96	40.41	9.48
2480.00	40.52	48.26	6.94
2580.00	66.63	51.10	6.09
2600.00	55.89	52.65	6.05
4000.00	65.32	18.50	19.98
7000.00	34.84	3.18	33.42



Mini-Circuits
 ISO 9001 ISO 14001 AS 9100 CERTIFIED
 IF/RF MICROWAVE COMPONENTS

P.O. Box 350166, Brooklyn, New York 11235-0003 (718) 934-4500 Fax (718) 332-4661 The Design Engineers Search Engine Provides ACTUAL Data Instantly at minicircuits.com

Notes: 1. Performance and quality attributes and conditions not expressly stated in this specification sheet are intended to be excluded and do not form a part of this specification sheet. 2. Electrical specifications and performance data contained herein are based on Mini-Circuit's applicable established test performance criteria and measurement instructions. 3. The parts covered by this specification sheet are subject to Mini-Circuits standard limited warranty and terms and conditions (collectively, "Standard Terms"); Purchasers of this part are entitled to the rights and benefits contained therein. For a full statement of the Standard Terms and the exclusive rights and remedies thereunder, please visit Mini-Circuits' website at www.minicircuits.com/MCLStore/terms.jsp.

REV. OR
 M125420
 ZX75BP-1842+
 EDU-1374
 URJ/NY
 100112
 Page 2

Coaxial Low Noise Amplifier

ZX60-33LN+

50Ω 50 to 3000 MHz

Features

- wide bandwidth, 50 to 3000 MHz
- low noise figure 1.1 dB typ.
- output power, up to 17.5 dBm typ.
- protected by US patent 6,790,049

Applications

- front-end amplifier
- cellular
- GPS
- bluetooth
- lab
- instrumentation
- test equipment



Connectors	Model	Price	Qty.
SMA	ZX60-33LN-S+	\$79.95 ea.	(1-9)

Case Style: GC957

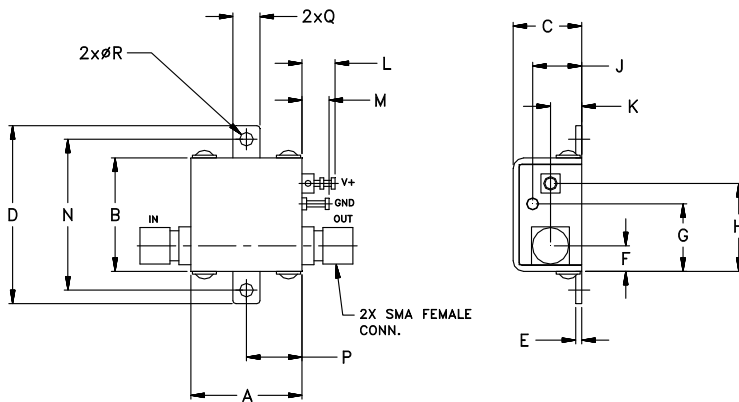
+ RoHS compliant in accordance with EU Directive (2002/95/EC)

The +Suffix has been added in order to identify RoHS Compliance. See our web site for RoHS Compliance methodologies and qualifications.

Electrical Specifications at 25°C

Parameter	Condition	Min	Typ.	Max.	Units
Frequency		50		3000	MHz
Noise Figure			1.1	1.9	dB
Gain	100 MHz 1000 MHz 2000 MHz 3000 MHz	13	21.9 18.8 14.5 11.9		dB
Gain Flatness			—		dB
Output Power at 1dB compression		14.5	16.5		dBm
Output third order intercept point			+32		dBm
Input VSWR			2.0		:1
Output VSWR			1.6		:1
Active Directivity			—		dB
DC Supply Voltage			5	5.5	V
Supply Current			70	80	mA

Outline Drawing



Maximum Ratings

Parameter	Ratings
Operating Temperature	-40°C to 85°C Case
Storage Temperature	-55°C to 100°C
Input RF Power (no damage)	+13 dBm
Power Dissipation	0.44W

Permanent damage may occur if any of these limits are exceeded.

Outline Dimensions (inch/mm)

A	B	C	D	E	F	G	H	J	K	L	M	N	P	Q	R	wt
.74	.75	.46	1.18	.04	.17	.45	.59	.33	.21	.22	.18	1.00	.37	.18	.106	grams
18.80	19.05	11.68	29.97	1.02	4.32	11.43	14.99	8.38	5.33	5.59	4.57	25.40	9.40	4.57	2.69	23.0



P.O. Box 350166, Brooklyn, New York 11235-0003 (718) 934-4500 Fax (718) 332-4661 The Design Engineers Search Engine Provides ACTUAL Data Instantly at minicircuits.com

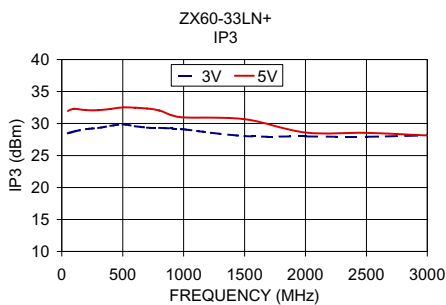
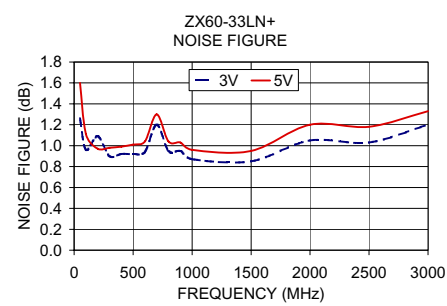
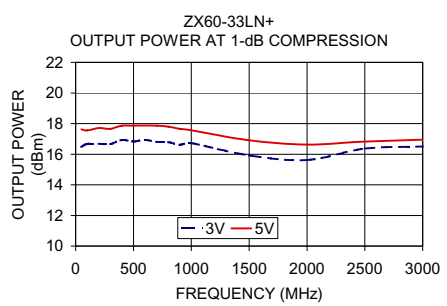
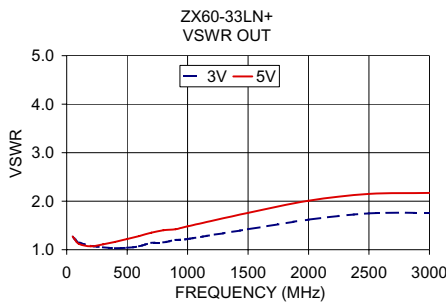
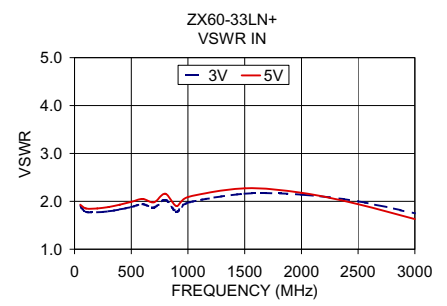
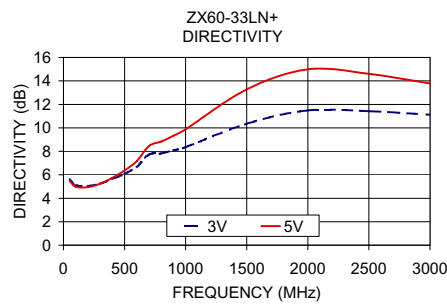
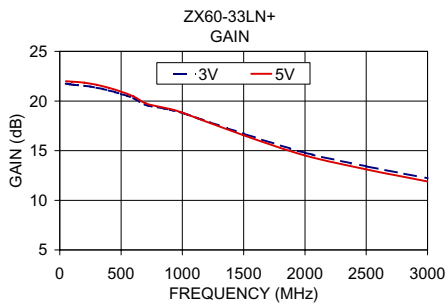
IFIRF MICROWAVE COMPONENTS

For detailed performance specs & shopping online see web site

Notes: 1. Performance and quality attributes and conditions not expressly stated in this specification sheet are intended to be excluded and do not form a part of this specification sheet. 2. Electrical specifications and performance data contained herein are based on Mini-Circuit's applicable established test performance criteria and measurement instructions. 3. The parts covered by this specification sheet are subject to Mini-Circuits standard limited warranty and terms and conditions (collectively, "Standard Terms"); Purchasers of this part are entitled to the rights and benefits contained therein. For a full statement of the Standard Terms and the exclusive rights and remedies thereunder, please visit Mini-Circuits' website at www.minicircuits.com/MCLStore/terms.jsp.

REV. A
M116867
ZX60-33LN+
ED-12875/2
MM/CP/AM
090819
Page 1 of 2

FREQUENCY (MHz)	GAIN (dB)		DIRECTIVITY (dB)		VSWR IN (:1)		VSWR OUT (:1)		NOISE FIGURE (dB)		POUT at 1dB COMPR. (dBm)		IP3 (dBm)	
	3V	5V	3V	5V	3V	5V	3V	5V	3V	5V	3V	5V	3V	5V
50.00	21.75	21.99	5.60	5.48	1.89	1.93	1.26	1.27	1.26	1.60	16.47	17.63	28.47	31.95
100.00	21.65	21.94	5.12	4.98	1.78	1.85	1.15	1.12	0.96	1.11	16.67	17.55	28.75	32.29
200.00	21.54	21.84	5.05	4.95	1.77	1.85	1.08	1.07	1.09	0.97	16.68	17.71	29.11	32.08
300.00	21.34	21.63	5.24	5.24	1.79	1.88	1.05	1.11	0.90	0.98	16.66	17.66	29.31	32.09
400.00	21.06	21.32	5.64	5.74	1.83	1.93	1.03	1.16	0.92	0.99	16.93	17.86	29.63	32.27
500.00	20.71	20.94	6.09	6.37	1.88	1.99	1.04	1.22	0.92	1.01	16.83	17.87	29.86	32.51
600.00	20.28	20.47	6.67	7.17	1.94	2.05	1.07	1.28	0.94	1.04	16.94	17.88	29.59	32.48
700.00	19.61	19.76	7.73	8.45	1.87	1.98	1.14	1.35	1.20	1.30	16.80	17.87	29.35	32.33
800.00	19.37	19.46	7.82	8.83	2.03	2.16	1.15	1.40	0.95	1.04	16.79	17.80	29.32	32.03
900.00	19.11	19.19	8.08	9.32	1.78	1.90	1.20	1.42	0.95	1.03	16.61	17.66	29.23	31.29
1000.00	18.80	18.82	8.35	9.88	1.97	2.09	1.22	1.48	0.87	0.96	16.72	17.56	29.10	30.95
1500.00	16.71	16.54	10.35	13.28	2.16	2.27	1.42	1.76	0.85	0.95	15.92	16.91	28.04	30.66
2000.00	14.79	14.51	11.49	14.99	2.14	2.18	1.62	2.01	1.05	1.20	15.62	16.63	27.99	28.58
2500.00	13.42	13.11	11.42	14.60	2.00	1.94	1.75	2.15	1.03	1.18	16.37	16.83	27.92	28.55
3000.00	12.22	11.90	11.12	13.78	1.75	1.63	1.76	2.17	1.20	1.33	16.50	16.95	28.16	28.14



Coaxial Frequency Mixer

ZX05-30W+ ZX05-30W

Level 7 (LO Power +7 dBm) 300 to 4000



CASE STYLE: FL905

Maximum Ratings

Operating Temperature	-40°C to 85°C
Storage Temperature	-55°C to 100°C
RF Power	50mW
IF Current	40mA

Coaxial Connections

LO	1
RF	2
IF	3

Features

- rugged construction
- small size
- low conversion loss
- high L-R isolation
- protected by US Patents 6,133,525 & 6,790,049

Applications

- cellular
- PCS
- instrumentation
- satellite communication

Connectors	Model	Price	Qty.
SMA	ZX05-30W-S(+)	\$37.95 ea.	(1-24)

+ RoHS compliant in accordance with EU Directive (2002/95/EC)

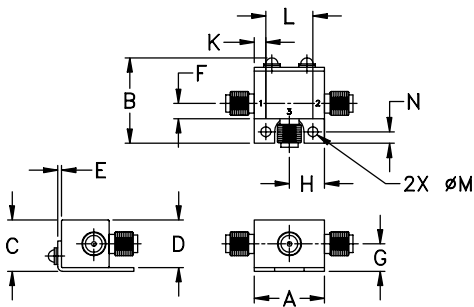
The + suffix identifies RoHS Compliance. See our web site for RoHS Compliance methodologies and qualifications.

Electrical Specifications (T_{AMB}=25°C)

FREQUENCY (MHz)	CONVERSION LOSS (dB)	LO-RF ISOLATION (dB)		LO-IF ISOLATION (dB)		IP3 at center band (dBm)				
		Typ.	Min.	Typ.	Min.					
300-4000	DC-950	6.8	0.2	9.0	9.8	35	17	16	7	12

1 dB COMP.: +1 dBm typ.
m= mid band [2f_L to f_U/2]

Outline Drawing



Outline Dimensions (inch/mm)

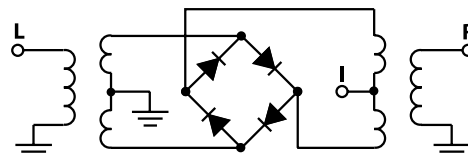
A	B	C	D	E	F	G
.74	.90	.54	.50	.04	.16	.29
18.80	22.86	13.72	12.70	1.02	4.06	7.37

H	J	K	L	M	N	wt
.37	--	.122	.496	.106	.122	grams
9.40	--	3.10	12.60	2.69	3.10	20.0

Typical Performance Data

Frequency (MHz)		Conversion Loss (dB)	Isolation L-R (dB)	Isolation L-I (dB)	VSWR RF Port (:1)	VSWR LO Port (:1)
RF	LO	LO +7dBm	LO +7dBm	LO +7dBm	LO +7dBm	LO +7dBm
300.10	330.10	5.34	45.30	34.86	2.04	5.44
450.10	480.10	4.98	41.41	32.02	1.54	3.61
600.10	630.10	5.02	39.35	28.89	1.73	3.17
781.35	751.35	5.11	37.95	28.09	2.81	2.51
943.85	913.85	6.22	37.02	28.05	3.48	1.97
1106.35	1076.35	6.36	39.38	23.65	2.77	1.70
1268.85	1238.85	6.45	42.76	20.82	2.59	1.80
1431.35	1401.35	5.84	40.76	18.75	3.06	2.17
1675.10	1645.10	7.37	37.69	16.07	1.89	2.72
1837.60	1807.60	7.03	37.60	14.80	2.87	3.10
2000.10	1970.10	7.54	37.84	13.54	3.39	3.13
2211.87	2181.87	7.80	37.90	12.47	3.19	3.29
2435.39	2405.39	7.94	38.15	11.59	3.90	3.27
2658.92	2628.92	7.71	39.90	10.55	4.70	3.21
2882.45	2852.45	7.49	44.86	9.56	4.72	2.76
3105.98	3075.98	6.88	38.93	10.01	4.06	1.96
3329.51	3299.51	6.50	39.01	11.39	2.83	1.89
3553.04	3523.04	6.26	41.76	14.66	2.41	2.39
3776.57	3746.57	6.25	38.02	19.20	1.48	3.74
4000.10	3970.10	6.55	34.99	25.24	1.19	5.27

Electrical Schematic



Mini-Circuits®
ISO 9001 ISO 14001 CERTIFIED

ALL NEW
minicircuits.com

P.O. Box 350166, Brooklyn, New York 11235-0003 (718) 934-4500 Fax (718) 332-4661 For detailed performance specs & shopping online see Mini-Circuits web site

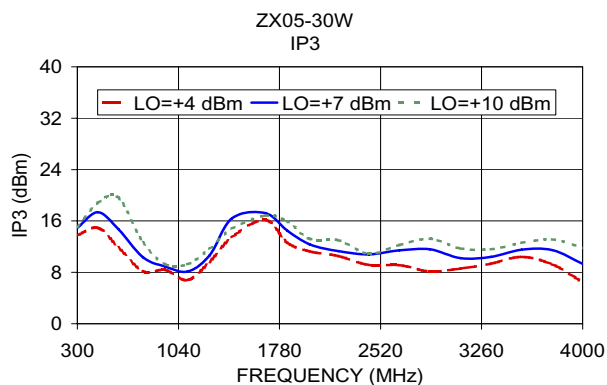
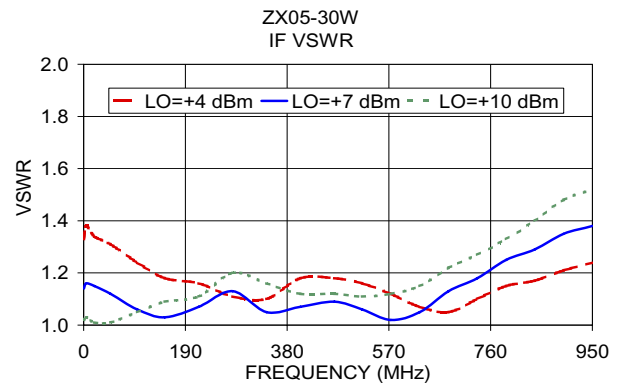
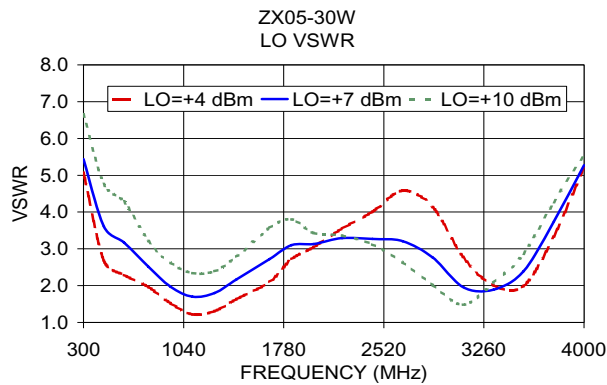
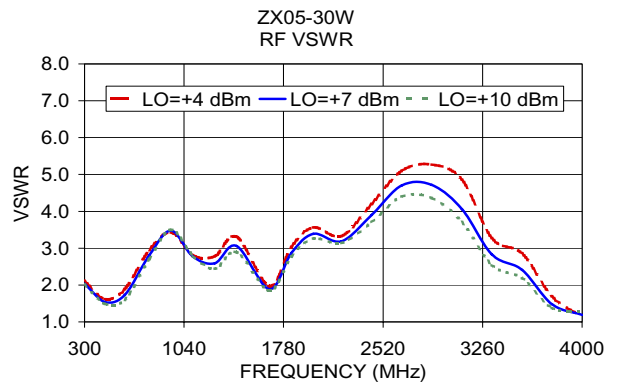
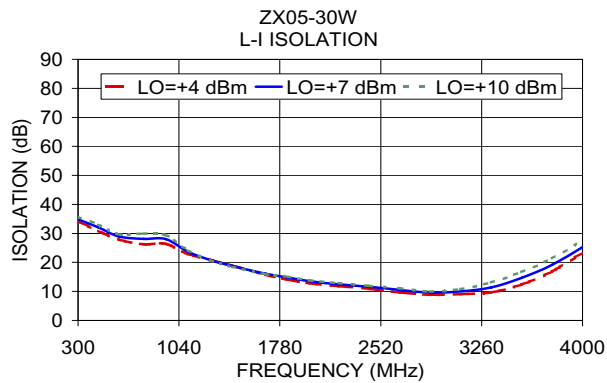
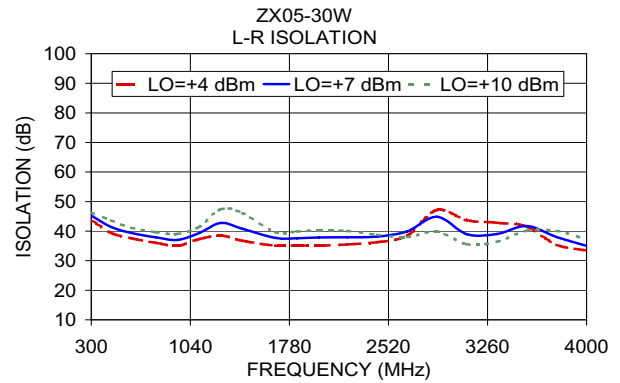
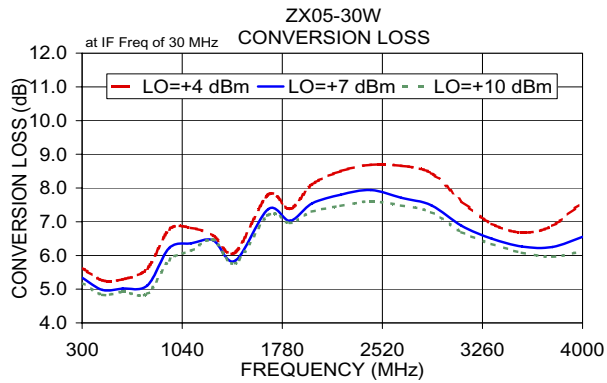


The Design Engineers Search Engine Provides ACTUAL Data Instantly From MINI-CIRCUITS At: www.minicircuits.com

RF/IF MICROWAVE COMPONENTS

REV. C
M98898
ZX05-30W
RAV/TD/CP
070117
Page 1 of 2

Performance Charts



Coaxial Low Noise Amplifier

ZFL-500LN+ ZFL-500LN

50Ω 0.1 to 500 MHz

Features

- very low noise, 2.9 dB typ.
- good VSWR, 1.5 :1 typ.
- protected by US Patent, 6,943,629

Applications

- VHF/UHF
- small signal amplifier
- communications system



CASE STYLE: Y460

Connectors	Model	Price	Qty.
SMA	ZFL-500LN+	\$79.95	(1-9)
BNC	ZFL-500LN-BNC(+)	\$84.95	(1-9)
BRACKET (OPTION "B")		\$2.50	(1+)

+ RoHS compliant in accordance with EU Directive (2002/95/EC)

The +Suffix identifies RoHS Compliance. See our web site for RoHS Compliance methodologies and qualifications.

Low Noise Amplifier Electrical Specifications

MODEL NO.	FREQUENCY (MHz)		NOISE FIGURE (dB)	GAIN (dB)		MAXIMUM POWER (dBm)		INTERCEPT POINT (dBm)	VSWR (:1) Typ.		DC POWER	
	f_L	f_U		Typ.	Min.	Total Range	Output (1 dB Compr.)		Input (no damage)	IP3 Typ.	In	Out
ZFL-500LN(+)	0.1	500	2.9	24	±0.5	+5	+5	+14	1.5*	1.6	15	60

m = mid range [2 fL to fU/2]

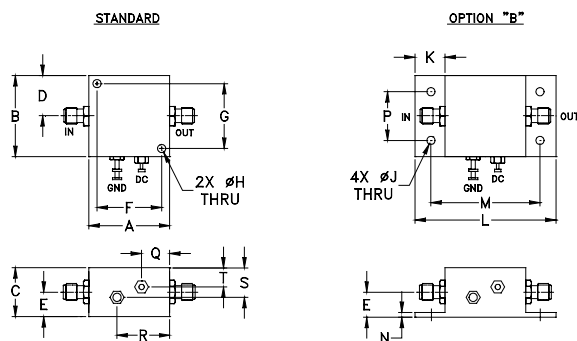
*VSWR 1.6:1 max. from 0.1 to 0.2 MHz.

Open load is not recommended, potentially can cause damage.
With no load derate max input power by 20 dB

Maximum Ratings

Operating Temperature	-20°C to 71°C
Storage Temperature	-55°C to 100°C
DC Voltage	+17V Max.

Outline Drawing



Outline Dimensions (inch/mm)

A	B	C	D	E	F	G	H	J	K	L	M	N	P	Q	R	S	T	wt.
1.25	1.25	.75	.63	.36	1.000	1.000	.125	.125	.46	2.18	1.688	.06	.750	.50	.80	.45	.29	grams
31.75	31.75	19.05	16.00	9.14	25.40	25.40	3.18	3.18	11.68	55.37	42.88	1.52	19.05	12.70	20.32	11.43	7.37	38

Mini-Circuits®
ISO 9001 ISO 14001 AS9100 CERTIFIED

minicircuits.com

P.O. Box 350166, Brooklyn, New York 11235-0003 (718) 934-4500 Fax (718) 332-4661 For detailed performance specs & shopping online see Mini-Circuits web site



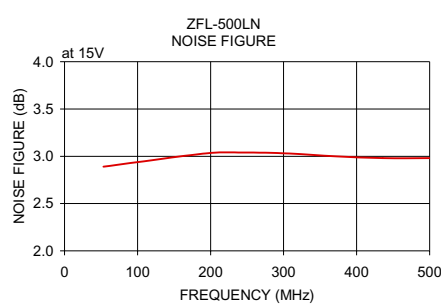
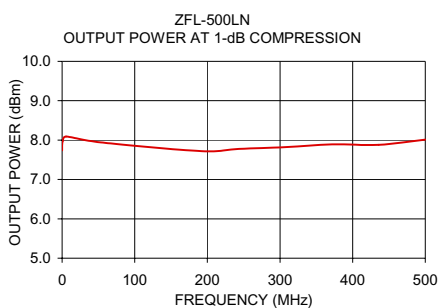
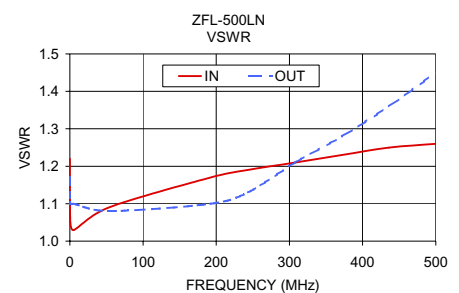
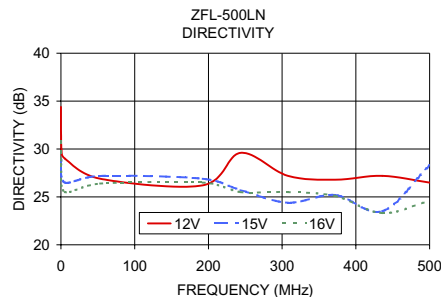
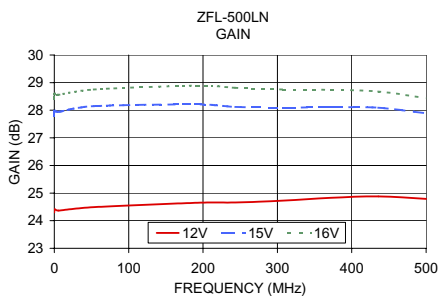
The Design Engineers Search Engine Provides ACTUAL Data Instantly From MINI-CIRCUITS At: www.minicircuits.com

RF/IF MICROWAVE COMPONENTS

Typical Performance Data/Curves

ZFL-500LN+ ZFL-500LN

FREQUENCY (MHz)	GAIN (dB)			DIRECTIVITY (dB)			VSWR (:1)		NOISE FIGURE (dB)	POUT at 1 dB COMPR. (dBm)
	12V	15V	16V	12V	15V	16V	IN	OUT		
0.10	24.30	27.80	28.40	34.40	27.80	30.80	1.22	1.17	—	7.74
0.60	24.41	27.98	28.60	30.00	28.80	28.40	1.05	1.10	—	7.97
5.40	24.37	27.94	28.56	29.00	26.50	25.50	1.03	1.10	—	8.09
53.30	24.49	28.15	28.75	26.90	27.20	26.40	1.09	1.08	2.89	7.94
192.40	24.65	28.21	28.89	26.20	26.90	26.50	1.17	1.10	3.03	7.72
243.60	24.66	28.12	28.81	29.60	25.70	25.50	1.19	1.13	3.04	7.78
307.70	24.73	28.10	28.75	27.20	24.40	25.50	1.21	1.21	3.03	7.82
371.80	24.83	28.11	28.74	26.80	25.20	25.10	1.23	1.28	3.00	7.89
435.90	24.88	28.09	28.68	27.20	23.50	23.30	1.25	1.36	2.98	7.88
500.00	24.79	27.89	28.44	26.50	28.30	24.60	1.26	1.45	2.98	8.01



Coaxial Low Pass Filter

BLP-300+ BLP-300

50Ω DC to 270 MHz

Maximum Ratings

Operating Temperature	-55°C to 100°C
Storage Temperature	-55°C to 100°C
RF Power Input	0.5W max.

Features

- rugged shielded case
- other standard and custom BLP models available with wide selection of fco

Applications

- test equipment
- lab use
- video equipment



CASE STYLE: FF55

Connectors	Model	Price	Qty.
BNC	BLP-300(+)	\$32.95 ea.	(1-9)

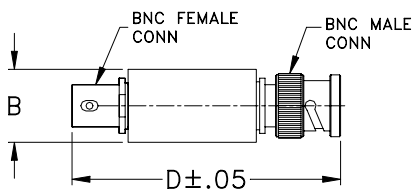
+ RoHS compliant in accordance with EU Directive (2002/95/EC)

The +Suffix identifies RoHS Compliance. See our web site for RoHS Compliance methodologies and qualifications.

Low Pass Filter Electrical Specifications

PASSBAND (MHz)	fco (MHz) Nom.	STOPBAND (MHz)		VSWR (:1)	
		(loss > 20 dB)	(loss > 40 dB)	Passband Typ.	Stopband Typ.
DC-270	297	410-550	550-1200	1.7	18

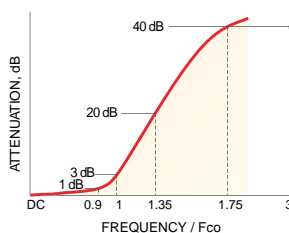
Outline Drawing



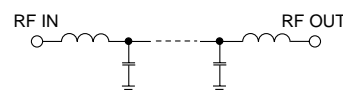
Outline Dimensions (inch/mm)

B	D	wt
.54	2.59	grams
13.72	65.79	40.0

typical frequency response

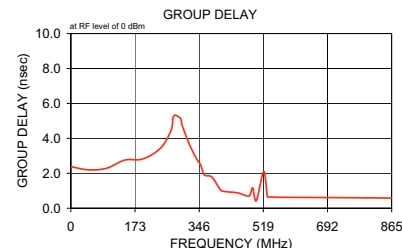
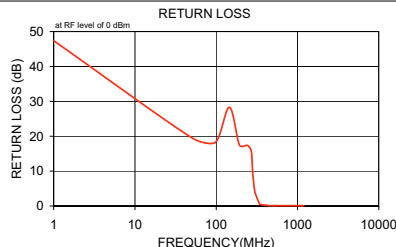
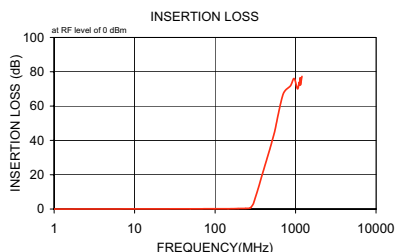


electrical schematic



Typical Performance Data

Frequency (MHz)	Insertion Loss (dB)		Return Loss (dB)	Frequency (MHz)	Group Delay (nsec)
	\bar{x}	σ			
1.00	0.02	0.1	47.4	1.00	2.37
49.00	0.13	0.1	19.7	49.00	2.20
97.00	0.17	0.1	18.2	97.00	2.29
145.00	0.15	0.1	28.3	145.00	2.76
193.00	0.28	0.1	17.5	193.00	2.82
241.00	0.36	0.1	17.4	241.00	3.42
270.00	0.53	0.1	15.6	270.00	4.45
280.00	1.00	0.1	9.8	275.00	5.14
297.00	2.83	0.2	4.3	280.00	5.33
300.00	3.29	0.2	3.8	290.00	5.24
340.00	11.27	0.3	0.7	297.00	5.08
360.00	15.31	0.3	0.4	300.00	4.75
380.00	19.09	0.4	0.3	320.00	3.64
400.00	22.62	0.4	0.2	340.00	2.79
410.00	24.31	0.4	0.2	350.00	2.49
450.00	30.64	0.6	0.1	360.00	1.91
490.00	36.51	0.9	0.1	380.00	1.79
520.00	40.88	1.2	0.1	400.00	1.15
530.00	42.34	1.3	0.1	410.00	0.98
540.00	43.72	1.3	0.1	450.00	0.88
550.00	45.07	1.5	0.1	480.00	0.70
700.00	66.82	5.7	0.1	490.00	1.16
864.00	71.78	6.6	0.1	500.00	0.43
960.00	76.06	6.9	0.1	520.00	2.11
1056.00	70.05	3.2	0.1	530.00	0.67
1110.00	73.87	7.7	0.1	540.00	0.65
1120.00	72.31	5.1	0.1	550.00	0.63
1140.00	76.33	5.1	0.1	700.00	0.61
1150.00	72.33	3.5	0.1	800.00	0.59
1200.00	77.29	5.8	0.1	864.00	0.58



Mini-Circuits®
ISO 9001 ISO 14001 CERTIFIED

ALL NEW
minicircuits.com

P.O. Box 350166, Brooklyn, New York 11235-0003 (718) 934-4500 Fax (718) 934-4661 For detailed performance specs & shopping online see Mini-Circuits web site



The Design Engineers Search Engine Provides ACTUAL Data Instantly From MINI-CIRCUITS At: www.minicircuits.com

RF/IF MICROWAVE COMPONENTS

REV. A
M98898
BLP-300
070305

FEATURES

Fixed gain of 16.5 dB
Operation up to 1000 MHz
37 dBm Output Third-Order Intercept (OIP3)
3 dB noise figure
Input/output internally matched to 50 Ω
Stable temperature and power supply
3 V or 5 V power supply
110 mA power supply current

APPLICATIONS

VCO buffers
General purpose Tx/Rx amplification

GENERAL DESCRIPTION

The ADL5530 is a broadband, fixed-gain, linear amplifier that operates at frequencies up to 1000 MHz. The device can be used in a wide variety of wired and wireless devices, including cellular, broadband, CATV, and LMDS/MMDS applications.

The ADL5530 provides a gain of 16.5 dB, which is stable over frequency, temperature, power supply, and from device to device. It achieves an OIP3 of 37 dBm with an output compression point of 21.8 dB and a noise figure of 3 dB.

This amplifier is single-ended and internally matched to 50 Ω with an input return loss of 11 dB. Only input/output ac-coupling capacitors, a power supply decoupling capacitor, and an external inductor are required for operation.

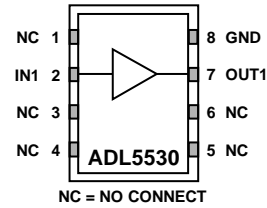
FUNCTIONAL BLOCK DIAGRAM


Figure 1.

05534-001

The ADL5530 operates with supply voltages of 3 V or 5 V with a supply current of 110 mA.

The ADL5530 is fabricated on a GaAs pHEMPT process. The device is packaged in a 3 mm \times 2 mm LFCSP that uses an exposed paddle for excellent thermal impedance. It operates from -40°C to $+85^{\circ}\text{C}$. A fully populated evaluation board is also available.

Rev. 0

Information furnished by Analog Devices is believed to be accurate and reliable. However, no responsibility is assumed by Analog Devices for its use, nor for any infringements of patents or other rights of third parties that may result from its use. Specifications subject to change without notice. No license is granted by implication or otherwise under any patent or patent rights of Analog Devices. Trademarks and registered trademarks are the property of their respective owners.

TABLE OF CONTENTS

Features	1	Typical Performance Characteristics	7
Applications.....	1	Theory of Operation	10
Functional Block Diagram	1	Soldering Information and Recommended PCB Land Pattern.....	10
General Description	1	Evaluation Board	11
Revision History	2	Outline Dimensions	12
Specifications.....	3	Ordering Guide	12
Typical Scattering Parameters.....	4		
Absolute Maximum Ratings.....	5		
ESD Caution.....	5		
Pin Configuration and Function Descriptions.....	6		

REVISION HISTORY

7/06—Revision 0: Initial Version

SPECIFICATIONS

VPOS = 5 V and $T_A = 25^\circ\text{C}$, unless otherwise noted.

Table 1.

Parameter	Conditions	Min	Typ	Max	Unit
OVERALL FUNCTION (See Table 2)					
Frequency Range ¹		10		1000	MHz
Gain (S21)			16.5		dB
Input Return Loss (S11)			-11		dB
Output Return Loss (S22)			-20		dB
Reverse Isolation (S12)			-21.5		dB
FREQUENCY = 70 MHz					
Gain		15	16.7	18	dB
vs. Temperature	$-40^\circ\text{C} \leq T_A \leq +85^\circ\text{C}$		± 0.1		dB
vs. Supply	4.75 V to 5.25 V		± 0.02		dB
Output 1 dB Compression Point			21.7		dBm
Output Third-Order Intercept	$\Delta f = 10 \text{ MHz}$, Output Power (P_{OUT}) = 10 dBm per tone		37		dBm
Noise Figure			5		dB
	VPOS = 3 V		3.2		dB
FREQUENCY = 190 MHz					
Gain		15	16.8	18.5	dB
vs. Frequency	$\pm 50 \text{ MHz}$		± 0.1		dB
vs. Temperature	$-40^\circ\text{C} \leq T_A \leq +85^\circ\text{C}$		± 0.2		dB
vs. Supply	4.75 V to 5.25 V		± 0.02		dB
Output 1 dB Compression Point			21.8		dBm
Output Third-Order Intercept	$\Delta f = 10 \text{ MHz}$, $P_{\text{OUT}} = 10 \text{ dBm}$ per tone		37		dBm
Noise Figure			3	4.5	dB
	VPOS = 3 V		2.3		dB
FREQUENCY = 380 MHz					
Gain		14.8	16	17.3	dB
vs. Frequency	$\pm 50 \text{ MHz}$		± 0.1		dB
vs. Temperature	$-40^\circ\text{C} \leq T_A \leq +85^\circ\text{C}$		± 0.3	± 0.8	dB
vs. Supply	4.75 V to 5.25 V		± 0.02		dB
Output 1 dB Compression Point		19.5	21.6		dBm
Output Third-Order Intercept	$\Delta f = 10 \text{ MHz}$, $P_{\text{OUT}} = 10 \text{ dBm}$ per tone		36		dBm
Noise Figure			2.5	3.5	dB
	VPOS = 3 V		2		dB
FREQUENCY = 900 MHz					
Gain		13	14.5	16	dB
vs. Frequency	$\pm 50 \text{ MHz}$		± 0.2		dB
vs. Temperature	$-40^\circ\text{C} \leq T_A \leq +85^\circ\text{C}$		± 0.5	± 1	dB
vs. Supply	4.75 V to 5.25 V		± 0.02		dB
Output 1 dB Compression Point			21.4		dBm
Output Third-Order Intercept	$\Delta f = 10 \text{ MHz}$, $P_{\text{OUT}} = 10 \text{ dBm}$ per tone		37		dBm
Noise Figure			2.7	3.5	dB
	VPOS = 3 V		2.3		dB
POWER INTERFACE	Pin VPOS				
Supply Voltage (VPOS)		3	5	5.5	V
Supply Current			110	135	mA
vs. Temperature	$-40^\circ\text{C} \leq T_A \leq +85^\circ\text{C}$		± 5		mA
Power Dissipation	VPOS = 5 V		0.55		W
	VPOS = 3 V		0.33		W

¹ For operation at lower frequencies, see the Theory of Operation section.

ADL5530

TYPICAL SCATTERING PARAMETERS

VPOS = 5 V and T_A = 25°C.

Table 2.

Freq. (MHz)	S11			S21			S12			S22			K Factor
	dB	Magnitude	Angle	dB	Magnitude	Angle	dB	Magnitude	Angle	dB	Magnitude	Angle	
10	-7.1	0.44	-34	17.2	7.23	172	-22.5	0.08	22	-17.7	0.13	-69	0.94
20	-9.7	0.33	-26	16.7	6.81	174	-21.9	0.08	12	-24.4	0.06	-73	1.07
50	-11.2	0.28	-16	16.6	6.73	174	-21.7	0.08	4	-31.4	0.03	-42	1.10
100	-11.5	0.27	-13	16.5	6.70	171	-21.6	0.08	1	-30.4	0.03	-23	1.10
150	-11.4	0.27	-14	16.5	6.67	167	-21.6	0.08	-1	-29.3	0.03	-24	1.10
200	-11.5	0.27	-16	16.4	6.59	162	-21.6	0.08	-3	-27.7	0.04	-25	1.11
250	-11.4	0.27	-19	16.3	6.52	157	-21.6	0.08	-4	-26.6	0.05	-25	1.11
300	-11.4	0.27	-23	16.2	6.45	153	-21.6	0.08	-5	-25.1	0.06	-27	1.12
350	-11.3	0.27	-26	16.1	6.36	149	-21.6	0.08	-6	-23.7	0.07	-29	1.12
400	-11.2	0.27	-29	16.0	6.29	144	-21.6	0.08	-7	-22.2	0.08	-32	1.12
450	-11.1	0.28	-32	15.9	6.21	140	-21.6	0.08	-8	-20.7	0.09	-33	1.12
500	-11.1	0.28	-36	15.7	6.11	136	-21.6	0.08	-9	-19.6	0.10	-35	1.12
550	-11.0	0.28	-39	15.6	6.02	132	-21.7	0.08	-10	-18.4	0.12	-37	1.13
600	-10.9	0.29	-42	15.5	5.94	128	-21.7	0.08	-11	-17.3	0.14	-38	1.13
650	-10.8	0.29	-45	15.3	5.84	124	-21.6	0.08	-12	-16.4	0.15	-40	1.12
700	-10.7	0.29	-49	15.2	5.73	119	-21.6	0.08	-13	-15.5	0.17	-41	1.13
750	-10.6	0.29	-52	15.0	5.62	115	-21.6	0.08	-13	-14.6	0.19	-44	1.13
800	-10.6	0.30	-55	14.8	5.51	111	-21.6	0.08	-14	-13.8	0.20	-45	1.12
850	-10.4	0.30	-58	14.6	5.39	107	-21.6	0.08	-15	-13.1	0.22	-47	1.12
900	-10.3	0.30	-61	14.4	5.28	104	-21.6	0.08	-16	-12.4	0.24	-49	1.12
950	-10.2	0.31	-64	14.3	5.17	100	-21.6	0.08	-17	-11.7	0.26	-51	1.12
1000	-10.1	0.31	-66	14.1	5.06	96	-21.6	0.08	-18	-11.2	0.28	-52	1.11

ABSOLUTE MAXIMUM RATINGS

Table 3.

Parameter	Rating
Supply Voltage, VPOS	6 V
Input Power (re: 50 Ω)	10 dBm
Internal Power Dissipation (Paddle Soldered)	600 mW
θ_{JC} (Junction to Paddle)	154 $^{\circ}\text{C}/\text{W}$
Maximum Junction Temperature	180 $^{\circ}\text{C}$
Operating Temperature Range	-40 $^{\circ}\text{C}$ to +85 $^{\circ}\text{C}$
Storage Temperature Range	-65 $^{\circ}\text{C}$ to +150 $^{\circ}\text{C}$

Stresses above those listed under Absolute Maximum Ratings may cause permanent damage to the device. This is a stress rating only; functional operation of the device at these or any other conditions above those indicated in the operational section of this specification is not implied. Exposure to absolute maximum rating conditions for extended periods may affect device reliability.

ESD CAUTION

ESD (electrostatic discharge) sensitive device. Electrostatic charges as high as 4000 V readily accumulates on the human body and test equipment and can discharge without detection. Although this product features proprietary ESD protection circuitry, permanent damage may occur on devices subjected to high-energy electrostatic discharges. Therefore, proper ESD precautions are recommended to avoid performance degradation or loss of functionality.



ADL5530

PIN CONFIGURATION AND FUNCTION DESCRIPTIONS

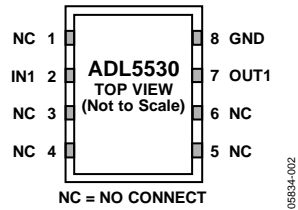


Figure 2. Pin Configuration

Table 4. Pin Function Descriptions

Pin No.	Mnemonic	Description
1, 3, 4, 5, 6	NC	No Connect.
2	IN1	RF Input. Requires a DC blocking capacitor.
7	OUT1/ VPOS	RF Output and VPOS (Supply Voltage). DC bias is provided to this pin through an inductor. RF path requires a DC blocking capacitor.
8	GND	Ground. Connect this pin to a low impedance ground plane.
Exposed Paddle		Internally connected to GND. Solder to a low impedance ground plane.

TYPICAL PERFORMANCE CHARACTERISTICS

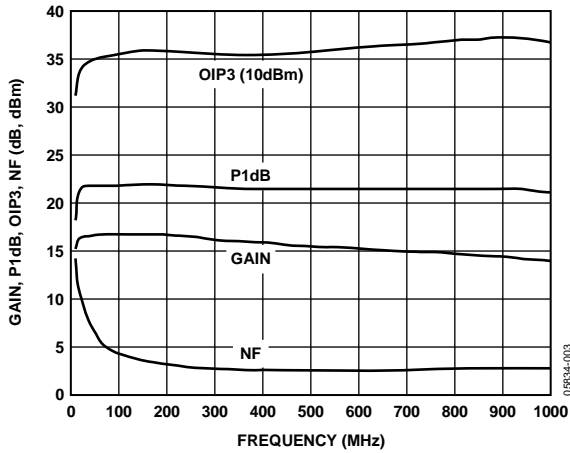


Figure 3. Gain, P1dB, OIP3, and Noise Figure vs. Frequency, VPOS = 5 V

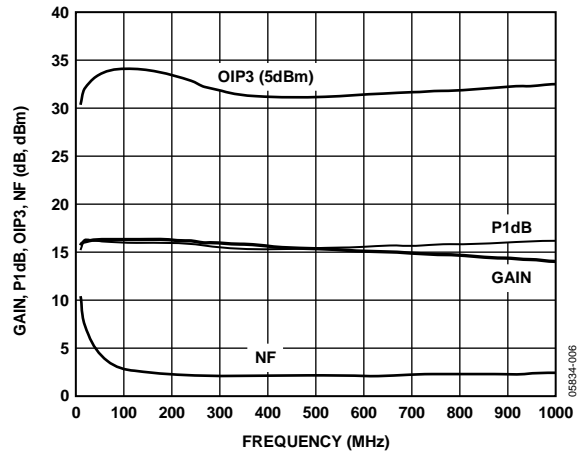


Figure 6. Gain, P1dB, OIP3, and Noise Figure vs. Frequency, VPOS = 3 V

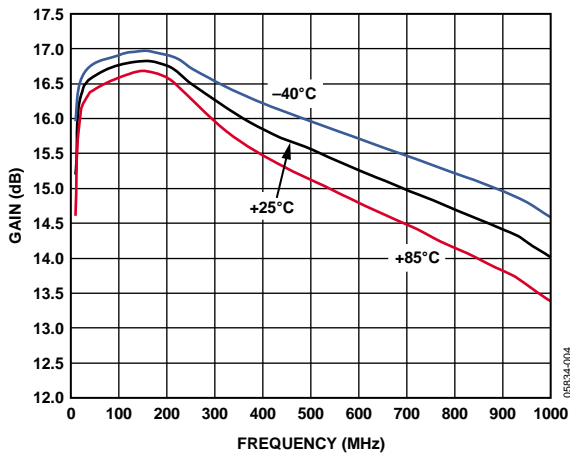


Figure 4. Gain vs. Frequency and Temperature, VPOS = 5 V

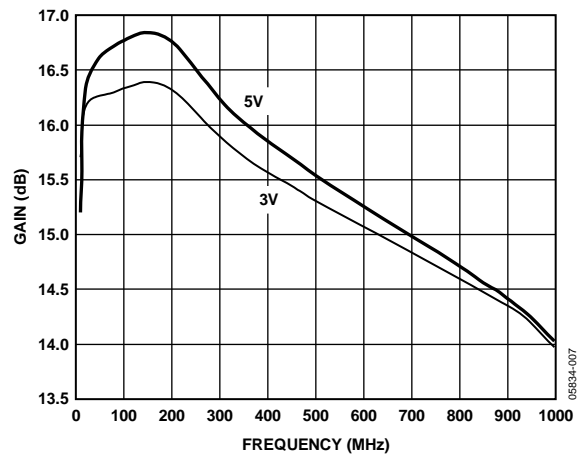


Figure 7. Gain vs. Frequency and Supply, VPOS = 5 V and 3 V

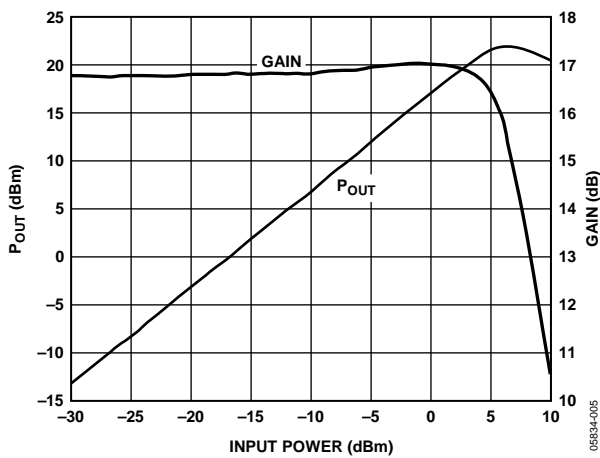


Figure 5. Output Power and Gain vs. Input Power, $f = 190$ MHz, VPOS = 5 V

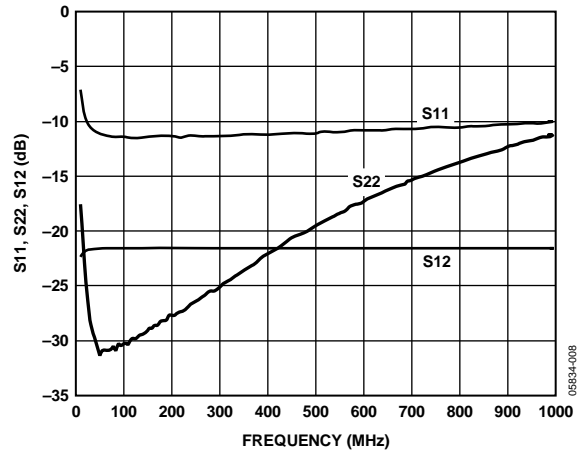


Figure 8. Input Return Loss, Output Return Loss, and Reverse Isolation vs. Frequency, VPOS = 5 V

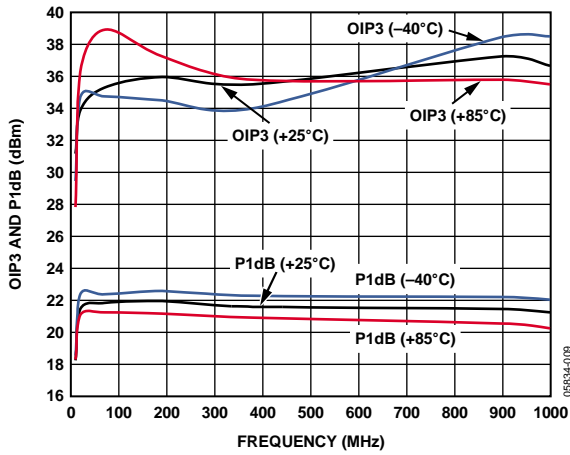


Figure 9. OIP3 and P1dB vs. Frequency and Temperature, VPOS = 5 V

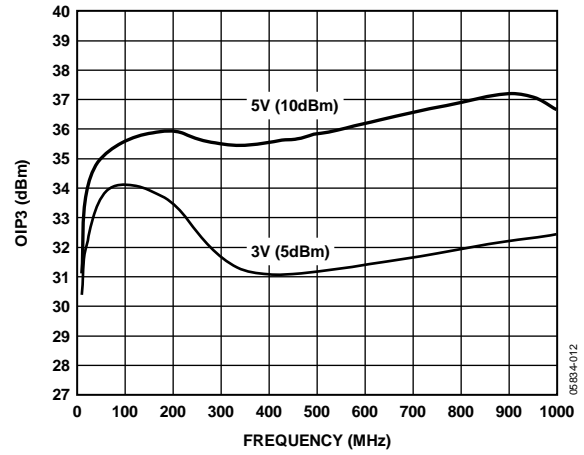


Figure 12. OIP3 vs. Frequency and Supply, VPOS = 5 V and 3 V

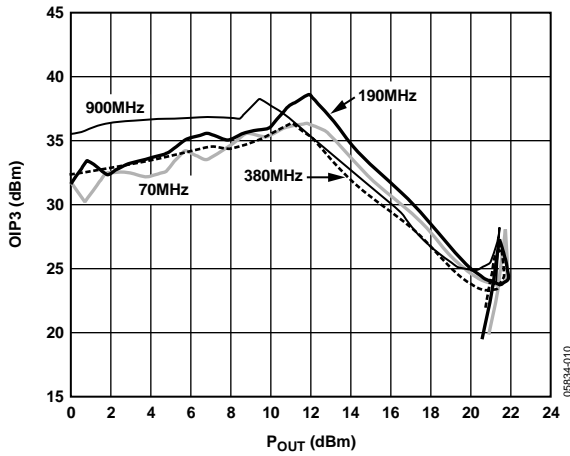


Figure 10. OIP3 vs. Output Power and Frequency, VPOS = 5 V

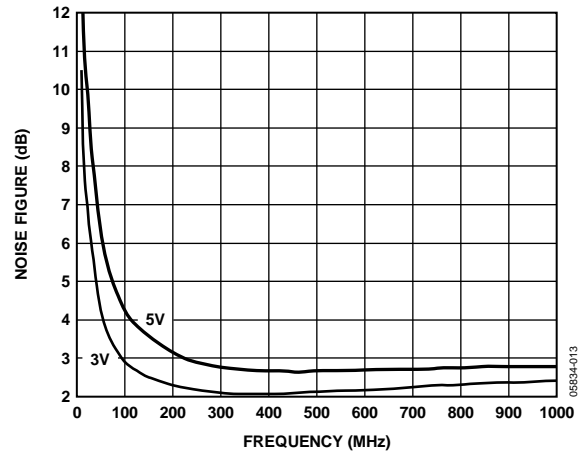


Figure 13. Noise Figure vs. Frequency and Supply, VPOS = 5 V and 3 V

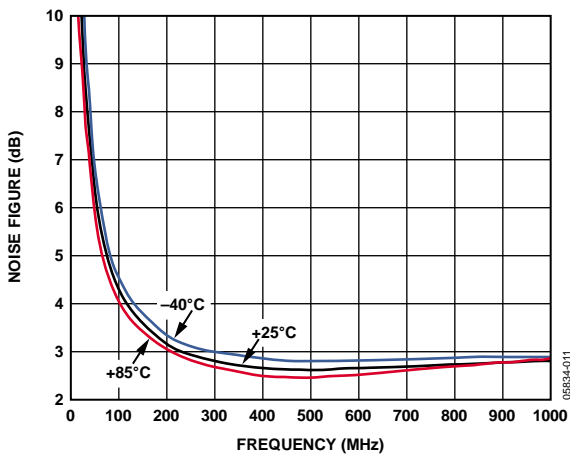


Figure 11. Noise Figure vs. Frequency and Temperature, VPOS = 5 V

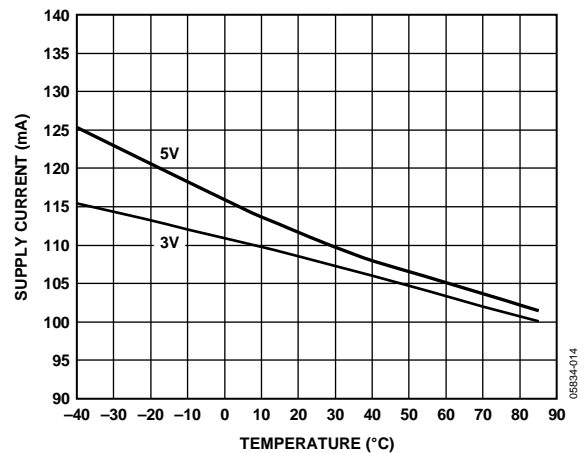


Figure 14. Supply Current vs. Temperature and Supply, VPOS = 5 V and 3 V

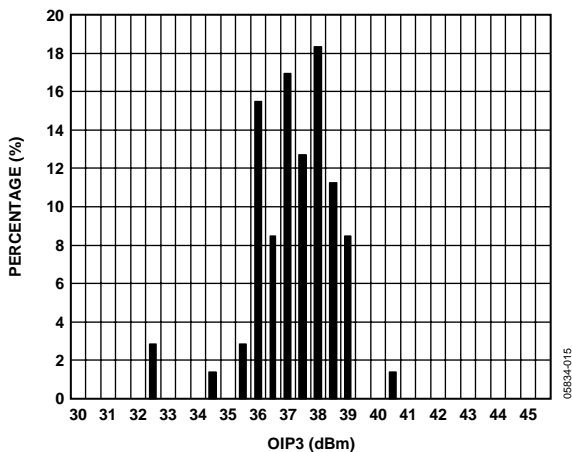


Figure 15. OIP3 Distribution at 190 MHz, 5 V

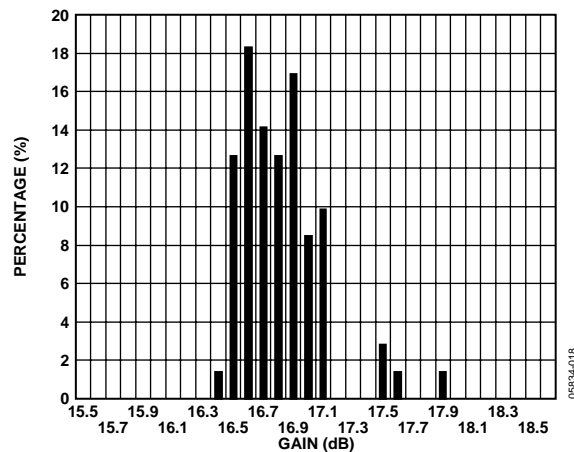


Figure 18. Gain Distribution at 190 MHz, VPOS = 5 V

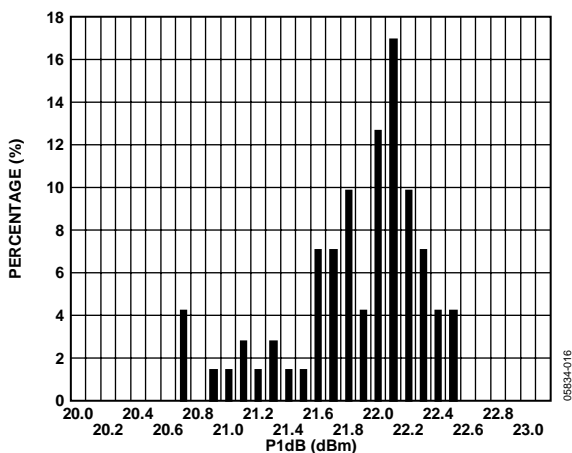


Figure 16. P1dB Distribution at 190 MHz, VPOS = 5 V

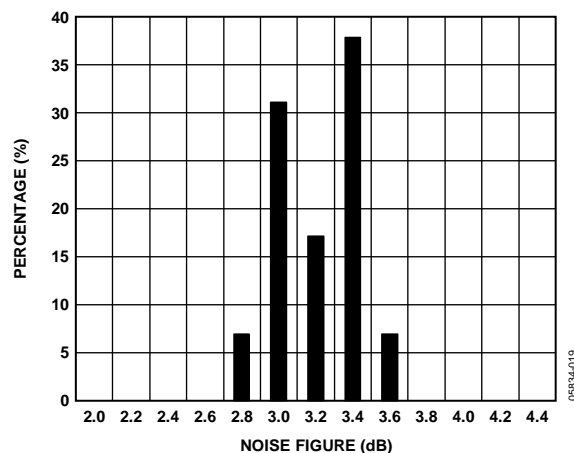


Figure 19. Noise Figure Distribution at 190 MHz, VPOS = 5 V

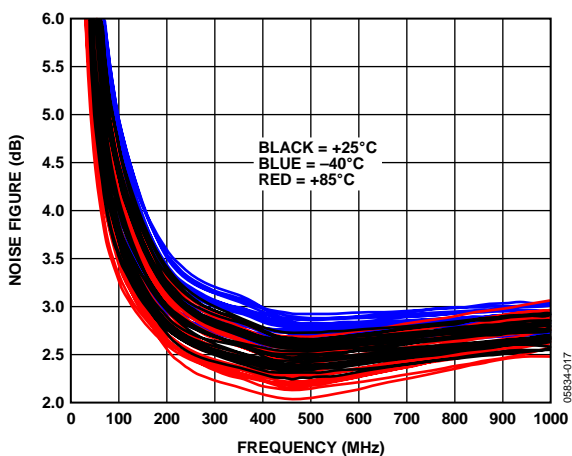


Figure 17. Noise Figure Temperature Distribution, VPOS = 5 V

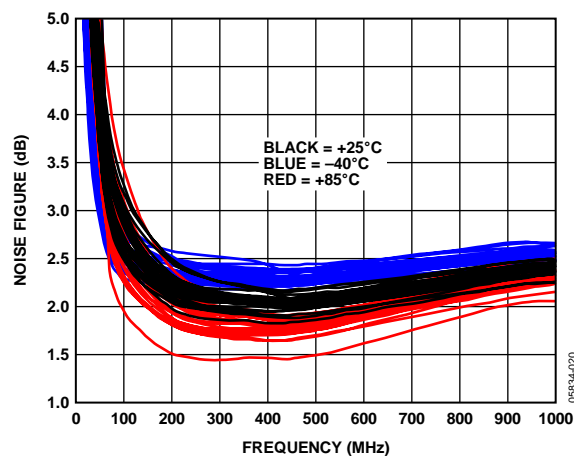
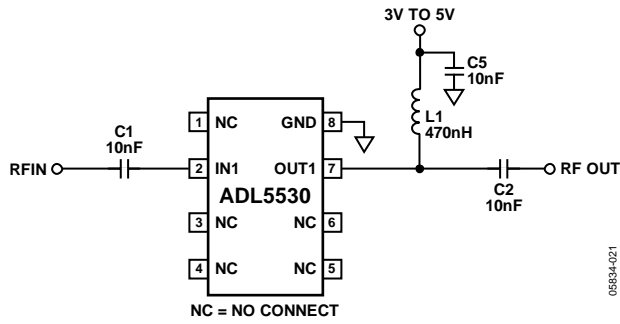


Figure 20. Noise Figure Temperature Distribution, VPOS = 3 V

THEORY OF OPERATION

The basic connections for operating the ADL5530 are shown in Figure 21. Recommended components are listed in Table 5. The inputs and outputs should be ac coupled with appropriately sized capacitors (device characterization was performed with 10 nF capacitors). DC bias is provided to the amplifier via an inductor connected to the RF output pin. The bias voltage should be decoupled using a 10 nF capacitor.

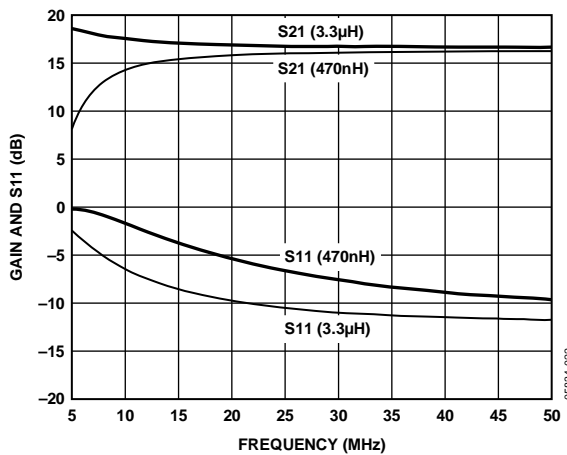
A bias voltage of 5 V is recommended. However, the device is specified to operate down to 3 V with a slightly reduced compression point and a reduced noise figure.



For operation down to 10 MHz, a larger biasing choke is recommended (see Table 5) along with larger ac-coupling capacitors. Figure 22 shows a plot of input return loss and gain with the recommended components.

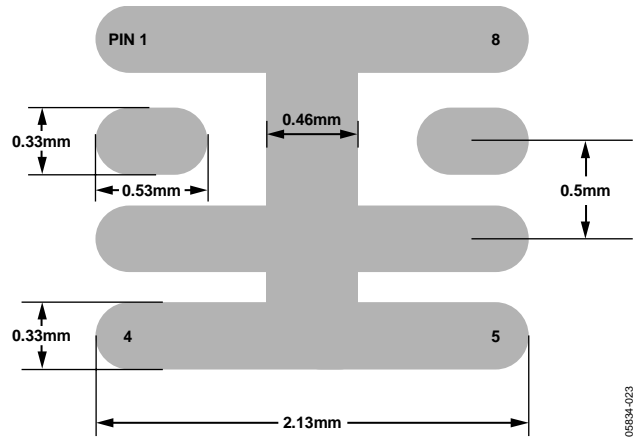
Table 5. Recommended Components for Basic Connections

Frequency	C1	C2	L1	C5
10 MHz to 50 MHz	0.1 μ F	0.1 μ F	3.3 μ H	0.1 μ F
50 MHz to 1000 MHz	10 nF	10 nF	470 nH	10 nF



SOLDERING INFORMATION AND RECOMMENDED PCB LAND PATTERN

Figure 23 shows the recommended land pattern for ADL5530. To minimize thermal impedance, the exposed paddle on the package underside should be soldered down to a ground plane along with Pin 8. If multiple ground layers exist, they should be stitched together using vias. Pin 1, Pin 3, Pin 4, Pin 5 and Pin 6 can be left unconnected, or can be connected to ground. Connecting these pins to ground slightly enhances thermal impedance.



OUTLINE DIMENSIONS

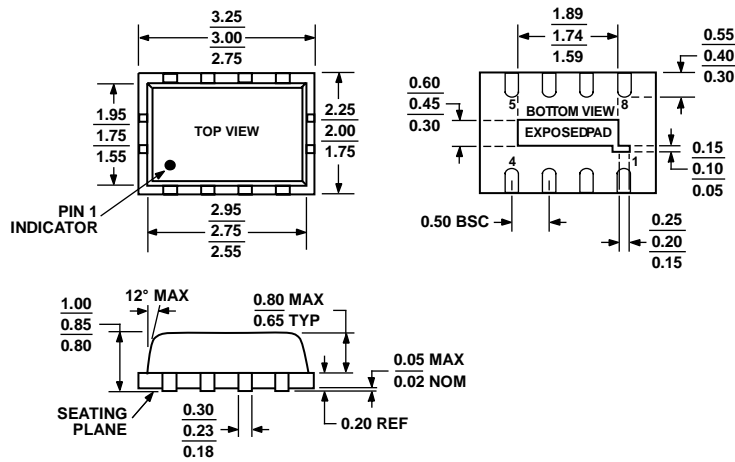


Figure 26. 8-Lead Lead Frame Chip Scale Package [LFCSP_VD]
 2 mm × 3 mm Body, Very Thin, Dual Lead
 CP-8-1
 Dimensions shown in millimeters

ORDERING GUIDE

Model	Temperature Range	Package Description	Package Option	Branding	Ordering Quantity
ADL5530ACPZ-R7 ¹	-40°C to +85°C	8-Lead LFCSP_VD, 7" Tape and Reel	CP-8-1	OT	1500
ADL5530ACPZ-WP ¹	-40°C to +85°C	8-Lead LFCSP_VD, Waffle Pack	CP-8-1	OT	50
ADL5530-EVAL		Evaluation Board			1

¹ Z = Pb-free part.

[Restart](#) [Retrieve](#)

Configuration Summary

Please see your system summary below.

Academic Pricing available! Add to cart or get a quote to view Academic Discounts.
 Note: All academic discounts are subject to final verification and approval by National Instruments

[Controller](#) [Modules](#) [Chassis](#) [Software](#) **[Summary](#)**

[Close X](#)



You may drag and drop modules to rearrange their positions in the chassis.

[« Back](#)

Configuration ID: PX598649

Modules and Options

Part Number	Model	Description	Quantity	Price
779772-03	NI PXI-5152/512MB	NI PXI-5152, 2 GS/s(1-Ch)/1 GS/s(2-Ch) Digitizer w/ 512 MB Memory	2	\$ 9,999.00 \$ 8,999.10
778827-01	SMB 112	SMB112, Double Shielded SMB to BNC Male Coax Cable, 50 Ohm, 1m	2	\$ 79.00 \$ 71.10
Subtotal: \$ 18,140.40				You Save: \$ 2,015.60 (10%)

Chassis and Options

Part Number	Model	Description	Quantity	Price
779758-01	NI PXI-1033 Chassis with ExpressCard MXI Controller and (3m) Cable	NI PXI-1033 Integrated MXIe, 5 Periph Slots, ExpressCard, 3m Cable	1	\$ 1,099.00 \$ 989.10
778949-01	PXI-103x Side handle and rubber feet kit	PXI-103x Side handle and rubber feet kit	1	\$ 50.00 \$ 45.00
763000-01	United States 120VAC	Power Cord, AC, U.S., 120 VAC	1	\$ 5.00 \$ 4.50
960597-04	PXI 4-Slot Factory Installation Service	PXI 4 & 6-Slot Factory Installation Service and Extended Warranty	1	\$ 545.00
Subtotal: \$ 1,583.60				You Save: \$ 115.40 (7%)

Software

Part Number	Model	Description	Quantity	Price
776670-09	NI LabVIEW Full Development System for Windows	LabVIEW Full Development System, Windows, Includes 1 Year SSP	1	\$ 2,499.00 \$ 624.75
Subtotal: \$ 624.75				You Save: \$ 1,874.25 (75%)

Total Price: \$ 20,348.75

You Save: \$ 4,005.25 (16%)

Guarantee your price for 30 days with an NI Instant Quote ([learn more](#)) [Instant Quote](#)

* Price does not include local taxes (GST) or delivery charges.

My Configuration

Configuration ID **PX598649**

Total Price: \$ 20,348.75

You Save: \$ 4,005.25 (16.0%)

Next Steps

- Instant Quote**
Guarantee your price for 30 days!
- Add to Cart**
- Add to My Parts List**
- Print Summary**
- Download to Excel**
- Save Configuration**
- Email and Share**



Click image to view system

Controller

[PXI-1033 Chassis with ExpressCard MXI Controller](#) [edit](#)

Modules

[NI PXI-5152/512MB SMB 112](#) [edit](#)

[NI PXI-5152/512MB SMB 112](#) [edit](#)

Subtotal: \$ 18,140.40

You Save: \$ 2,015.60 (10.0%)

Chassis

[NI PXI-1033 Chassis with ExpressCard MXI Controller and \(3m\) Cable](#) [edit](#)
[PXI-103x Side handle and rubber feet kit](#)
[United States 120VAC](#)
[PXI 4-Slot Factory Installation Service](#)

Subtotal: \$ 1,583.60

You Save: \$ 115.40 (7.0%)

Software

[NI LabVIEW Full Development System for Windows](#) [edit](#)

Subtotal: \$ 624.75

>>TDJ-1800SP10 Grid Parabolic Antenna



- **Model:** TDJ-1800SP10
- **Product Type:** Repeater Antennas
- **Place of origin:** China
- **Price Terms:** FOB, CIF
- **Payment Terms:** L/C, D/P, T/T
- **Minimum Order:**
- **Brand Name:** Kenbotong/KBT

Products Information

Applications

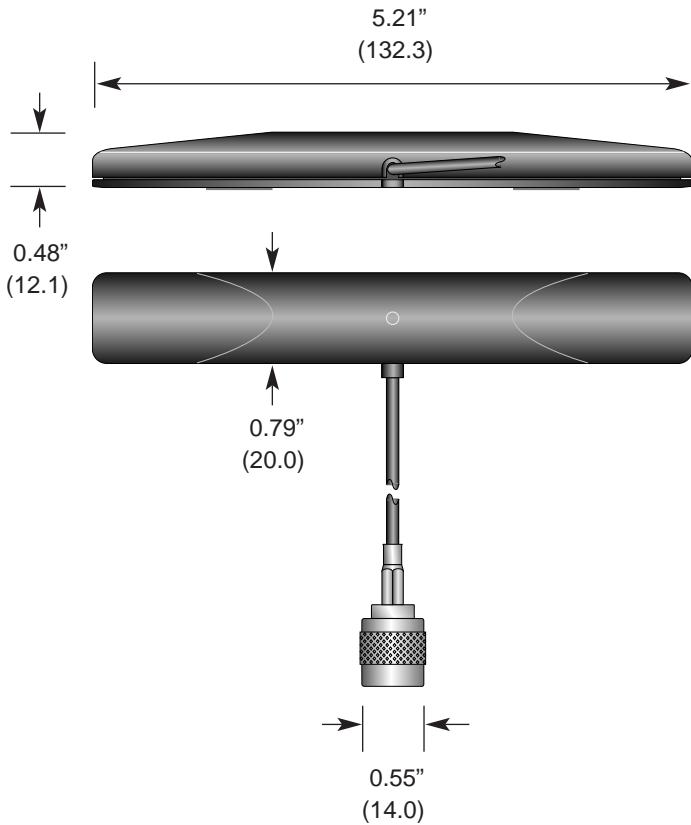
- * 1800MHz Communications Band
- * Long-distance Communications
- * Point to Point/ Point to Multipoint System
- * Wireless Bridges

Features

- * High Gain, High F/B Ratio
- * Aluminum Die Cast Grid Parabolic
- * Low Wind Loading
- * UV Stable Coat Finish
- * Vertical or Horizontal Polarization

Specifications	
Model	TDJ-1800SP10
Frequency Range-MHz	1710-1880
Bandwidth-MHz	170
Gain-dBi	22
Vertical Beamwidth-°	14
Horizontal Beamwidth-°	10
F/B Ratio-dB	≥25
VSWR	≤1.5
Impedance-Ω	50
Polarization	Vertical or Horizontal
Maximum Power-W	100
Connector	N Female or Customized
Dimensions-m	0.6×0.9
Weight-Kg	3.5
Rated Wind Velocity-m/s	60
Mounting Mast Diameter-mm	Φ40 to 50

Product Dimensions



Description



The HDP Series is a compact, center-fed antenna that achieves efficient operation at either or both of two frequency bands. Its durable, unobtrusive housing attaches permanently with integral adhesive to flat, non-conductive surfaces such as windows, drywall, ceiling tiles, plastic, etc. The antenna is supplied with 9.8 feet (3m) of RG-174 cable and can be terminated in an FCC Part 15 compliant RP-SMA connector or a TNC connector.

Features

- Dual-band (860-960MHz and 1.77-1.88GHz)
- Compact & center-fed
- Surface-mount
- Low VSWR
- Excellent performance
- Omni-directional pattern
- Fully weatherized
- Durable & unobtrusive
- RP-SMA or TNC connector

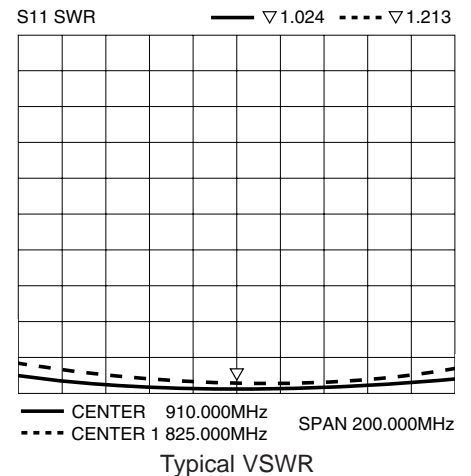
Electrical Specifications

- Freq. Bands Band 1 860-960MHz
Band 2 1.77-1.88GHz
- Bandwidth 200MHz
- Wavelength 1/4-wave
- VSWR <1.5 typ. at center
- Impedance 50 ohms
- Connector RP-SMA or TNC
- Cable 9.8' RG-174 coax

Ordering Information

- ANT-DB1-HDP-RPS (with RP-SMA connector)
- ANT-DB1-HDP-TNC (with TNC connector)

Plots





[Enlarge image](#)

1.8 GHz (0.6 x 0.9 m) Die Cast Grid Antenna

\$64.80

Model No : TDJ-1800SPL10

Product Description :

Frequency : 1710 - 1990 MHz

Frequency : 170 MHz

Bandwidth

Gain : ≥ 22 dBi

VSWR : ≤ 1.5

F/B Ratio : ≥ 30 dB

Horizontal Beamwidth : 12°

Vertical Beamwidth : 18°

Polarization : Vertical or Horizontal

Electrical Downtilt :

Nominal Impedence : 50 ohm

Maximum Power : ≥ 100 W

Connector Type : N Female or Customized

Rated Wind Velocity :

Mounting Type :

Dimensions (Metric) : 0.6 x 0.9 m

Dimensions (Inch) :

Net Weight (Kg) : 3.5 Kg

Net Weight (lb) : 7.7 lb

Additional Information :

Appendix II - Matlab Code

```

% makeWave.m
% Subroutine to generate the in-phase and quadrature chirp waveforms.
% Written by Adam Luchies - June 2007.
% Modified by Matt Casper - Spring 2010.

% Variable definitions
f1 = 10E6; % Start frequency (Hz)
f2 = 245E6; % End frequency (Hz)
k = (f2 - f1)/1E-6; % Chirp rate (Hz/s)
%mid_time = 0:0.5E-8:99.995E-6; % time vector (s)
mid_time = linspace(0,1e-6,1000);
pre_time = -50E-9:1E-9:-1E-9; % Amplitude-ramp-up time vector (s)
post_time = 1001E-9:1E-9:1050E-9; % Amplitude-ramp-down time vector (s)
time = [pre_time,mid_time,post_time]; % assembled time vector (s)

% Amplitude percentage ramp - pre/post wave
amp_ramp = 0:.02:.98;

% Scaling factor to account for AWG-DAC sin(x)/x.
% Only scale the main body of the waveform.
% amp_ro = sinc(1/(.8E-6)*(mid_time-.5E-6));
% Bandwidth includes unity
amp_ro = sinc(1/(1.86E-6)*(mid_time)); % 10MHz - 50MHz
amp_ro = sinc(1/(1.55E-6)*(mid_time)); % 10MHz - 60MHz
amp_ro = sinc(1/(1.35E-6)*(mid_time)); % 10MHz - 70MHz
amp_ro = sinc(1/(1.27E-6)*(mid_time)); % 10MHz - 80MHz
amp_ro = sinc(1/(1.23E-6)*(mid_time)); % 10MHz - 90MHz
amp_ro = sinc(1/(1.19E-6)*(mid_time)); % 10MHz - 100MHz
amp_ro = sinc(1/(1.15E-6)*(mid_time)); % 10MHz - 100MHz

% Create the pre-wave (constant start frequency, increasing amplitude).
wave_IP_pre = amp_ramp.*cos(2*pi*f1*pre_time);
wave_PQ_pre = amp_ramp.*sin(2*pi*f1*pre_time);

% Create the post-wave (constant end frequency, decreasing amplitude).
wave_IP_post = 5*sort(amp_ramp,'descend').*cos(2*pi*(f2)*post_time);%/amp_ro(end);
wave_PQ_post = -5*sort(amp_ramp,'descend').*sin(2*pi*(f2)*post_time);%/amp_ro(end);

% Create main body of the waveform [FM chirp, amplitude scaled by sin(x)/x].
wave_IP_mid = cos(2*pi*(f1+k/2*mid_time).*mid_time);%/amp_ro;
wave_PQ_mid = sin(2*pi*(f1+k/2*mid_time).*mid_time);%/amp_ro;

% Predistortion function
% predist=1e12*(mid_time-500e-9).^2+1; %narrow BW
predist=4e12*mid_time.^2+1; %wide BW

% Assemble the waveforms.
wave_IP = [wave_IP_pre, wave_IP_mid.*predist, wave_IP_post];
wave_PQ = [wave_PQ_pre, wave_PQ_mid.*predist, wave_PQ_post];

% Chirp waveforms are scaled to produce vectors in the range of [-1 1].
a=max(wave_IP);
b=min(wave_IP);

```

```

if(abs(a) > abs(b))
    wave_IP = wave_IP/a;
else
    wave_IP = -wave_IP/b;
end

a=max(wave_PQ);
b=min(wave_PQ);
if(abs(a) > abs(b))
    wave_PQ = wave_PQ/a;
else
    wave_PQ = -wave_PQ/b;
end

% figure(1);
% plot(time,wave_IP,'r');title('Total Signal vs. Time');xlabel('Time
[s]');ylabel('S(t) [V]');hold on;
% %figure(2);
% plot(time,wave_PQ,'g');hold off;%title('Quadrature Signal vs.
Time');xlabel('Time [s]');ylabel('Q(t) [V]');
% Lx = 221;
% Fsx = 2E8;
% Tx = 1/Fsx;
% tx = (0:Lx-1)*Tx;
% NFFTx = 2^nextpow2(Lx);
% X = fft(wave_IP,NFFTx)/Lx;
% fx = Fsx/2*linspace(0,1,NFFTx/2);
% %Plot the single-sided amplitude spectrum of chirp signal
% figure(3);
% plot(fx,2*abs(X(1:NFFTx/2)))
% title('Single-Sided Amplitude Spectrum of x(t)')
% xlabel('Frequency (Hz)')
% ylabel('|X(f)|')

% Clear variables
clear f1 f2 k amp_ramp amp_ro a b mid_time pre_time post_time;
clear wave_IP_mid wave_IP_pre wave_IP_post wave_PQ_mid wave_PQ_pre
wave_PQ_post;

```

```

% IQ_wave.m
% Subroutine to program an Agilent 81150A 120 MHz Pulse Function Arbitrary
% Generator to produce in-phase and quadrature waveforms triggered by an
% external source.
% Written by Matt Booth (Oct 2008) using basic programs written by Adam
% Luchies (June 2007) for two Agilent 33250A's. Combines IP_wave and
% PQ_wave into one file for use with Agilent 81150A.

% Create a VISA-USB object.
interfaceIQ = instrfind('Type', 'visa-usb', 'RsrcName',
'USB0::2391::16648::DE47C00377::0::INSTR', 'Tag', '');

% Create the VISA-USB object if it does not exist
% otherwise use the object that was found.
if isempty(interfaceIQ)
    interfaceIQ = visa('ni', 'USB0::2391::16648::DE47C00377::0::INSTR');

%NOTE: The program was not functioning on the radar testbed laptop
%(which has LabVIEW installed on it) when the vendor name was 'agilent'
%so it was changed to 'ni' even though the devices are made by Agilent.

else
    fclose(interfaceIQ);
    interfaceIQ = interfaceIQ(1);
end

% Create a device object.
deviceIQ = icdevice('agilent_81150a.mdd', interfaceIQ);
% Connect device object to hardware.
connect(deviceIQ);

% In-phase and phase-quadrature waveforms pre-defined by subroutine
'makeWave.m'
% Load the arbitrary waveform onto the device.
% Sample load command:
% fprintf(interface, cmd_str_PQ);

% Build string of data points used by AWG to construct IP waveform
% Waveform will be loaded into "Volatile" memory
cmd_str_IP = ':DATA1 VOLATILE';
[m n] = size(wave_IP);
for i = 1:n
    cmd_str_IP = [cmd_str_IP, ',' num2str(wave_IP(i),8)];
end

% Build string of data points used by AWG to construct PQ waveform
% Waveform will be loaded into "Volatile" memory
cmd_str_PQ = ':DATA2 VOLATILE';
[m n] = size(wave_PQ);
for i = 1:n
    cmd_str_PQ = [cmd_str_PQ, ',' num2str(wave_PQ(i),8)];
    pause
end

% Send command to AWG to load waveforms

```

```

fprintf(interfaceIQ,cmd_str_IP);
fprintf(interfaceIQ,cmd_str_PQ);

% Set the device to arbitrary waveform mode
fprintf(interfaceIQ,'FUNC1 USER');
fprintf(interfaceIQ,'FUNC2 USER');
% Set the device to produce the waveform in "Volatile" memory
fprintf(interfaceIQ,'FUNC1:USER VOLATILE');
fprintf(interfaceIQ,'FUNC2:USER VOLATILE');
% Set the waveform frequency, amplitude and offset
fprintf(interfaceIQ,'APPL1:USER 1000000, 1.0, 0.0');
fprintf(interfaceIQ,'APPL2:USER 1000000, 1.0, 0.0');
% Set the device to burst mode
fprintf(interfaceIQ,'BURS1:STAT ON');
fprintf(interfaceIQ,'BURS2:STAT ON');
% Set the burst mode to N-Cycle triggered
fprintf(interfaceIQ,'BURS1:MODE TRIG');
fprintf(interfaceIQ,'BURS2:MODE TRIG');

fprintf(interfaceIQ,'TRIG1:COUN 1');
fprintf(interfaceIQ,'TRIG2:COUN 1');

fprintf(interfaceIQ,'TRAC:CHAN1 ON');
fprintf(interfaceIQ,'TRAC:CHAN2 ON');

% % Set the number of cycles (one)
fprintf(interfaceIQ,'BURS1:NCYC 1');
fprintf(interfaceIQ,'BURS2:NCYC 1');

% Set the burst trigger source
fprintf(interfaceIQ,'ARM:SOUR1 EXT');
fprintf(interfaceIQ,'ARM:SOUR2 EXT');
% Set the burst mode to trigger on positive edges
fprintf(interfaceIQ,'ARM:SLOP1 POS');
fprintf(interfaceIQ,'ARM:SLOP2 POS');
% Set triggering threshold to 0.5V
fprintf(interfaceIQ,'ARM:LEV 0.4V');
fprintf(interfaceIQ,'ARM:LEV 0.4V');
% Activate the AWG output
fprintf(interfaceIQ,'OUTP1 ON');
fprintf(interfaceIQ,'OUTP2 ON');
% Turn off output complement
% fprintf(interfaceIQ,'OUTP1:COMP OFF');
% fprintf(interfaceIQ,'OUTP2:COMP OFF');

% Disconnect and delete device and interface
disconnect(deviceIQ);
delete([deviceIQ interfaceIQ]);
clear deviceIQ;
clear interfaceIQ;

% Cleanup variables
clear cmd_str_IP m n i;
clear cmd_str_PQ m n i;

```

This page intentionally left blank

```

% PRF_wave.m
% Subroutine to program an Agilent 33220A 20MHz Function Generator to
% control the pulse-repetition frequency (PRF) of the radar testbed.
% Written by Adam Luchies (June 2007) and modified by Matt Booth (Oct 2008).

% Create a VISA-USB object.
interfacePRF = instrfind('Type', 'visa-usb', 'RsrcName',
'USB0::2391::1031::MY44022711::0::INSTR', 'Tag', '');

% Create the VISA-USB object if it does not exist
% otherwise use the object that was found.
if isempty(interfacePRF)
    interfacePRF = visa('ni', 'USB0::2391::1031::MY44022711::0::INSTR');

%NOTE: The program was not functioning on the radar testbed laptop
%(which has LabVIEW installed on it) when the vendor name was 'agilent'
%so it was changed to 'ni' even though the devices are made by Agilent.

else
    fclose(interfacePRF);
    interfacePRF = interfacePRF(1);
end

% Create a device object.
devicePRF = icdevice('agilent_33220a.mdd', interfacePRF);
% Connect device object to hardware.
connect(devicePRF);

% Configure property value(s).
% Set device to produce a square wave.
set(devicePRF, 'Waveform', 'square');
% Set square wave amplitude
set(devicePRF, 'Amplitude', 1);
% Set square wave frequency
set(devicePRF, 'Frequency', 100000);
% Activate the device output
set(devicePRF, 'Output', 'on');

% Disconnect and delete device and interface
disconnect(devicePRF);
delete([devicePRF interfacePRF]);
clear devicePRF;
clear interfacePRF;

```

```

function [delta_t, voltages] = parse_voltage_file(voltage_file_name)

%-----
% FILENAME: parse_voltage_file.m
%
% DESCRIPTION:
% Extracts delta value between voltage measurements from header of provided
% file, as well as extracting and storing all voltage data from the body of
% the file. The delta value and voltages are returned.
%
% INPUTS:
%   voltage_file_name: file name of voltage text file, including extension
%
% OUTPUTS:
%   delta_t: delta value in header, representing delta between measurements
%   voltages: vector of voltages in column form in same order as file
%             (column vector in Matlab)
%-----

%--- Open the voltages file for reading
fid = fopen(voltage_file_name, 'r');

%--- Read header information
% Read waveform line (first line of header) to find # of channels
line = fgetl(fid);
A=sscanf(line, '%s');
if (length(A)==11)
    n=2;    % one channel
elseif (length(A)==14)
    n=3;    % two channels
elseif (length(A)==17)
    n=4;    % three channels
elseif (length(A)==20)
    n=5;    % four channels
end;
% Discard t0 line (second line of header)
line = fgetl(fid);
% Read delta t line and extract delta value
line = fgetl(fid);
if (n==2)
[tmp1,tmp2,delta_t] = sscanf(line, '%s%s%f');
elseif (n==3)
[tmp1,tmp2,tmp3,delta_t] = sscanf(line, '%s%s%f%f');
elseif (n==4)
[tmp1,tmp2,tmp3,tmp4,delta_t] = sscanf(line, '%s%s%f%f%f');
elseif (n==5)
[tmp1,tmp2,tmp3,tmp4,tmp5,delta_t] = sscanf(line, '%s%s%f%f%f%f');
end
clear tmp*;
% Skip empty line separating header from voltage data
line = fgetl(fid);

%--- Read voltage data
% Read labels for following voltage data
line = fgetl(fid);
% Read remainder of file in and extract voltages as we go until EOF

```

```
voltages = [];  
while(~feof(fid))  
    vals = str2num(fgetl(fid));  
  
% depending on number of channels used, values we want are 4th-7th in vals  
    if (n==2)  
        voltages = [voltages; vals(n)];  
    elseif (n==3)  
        voltages = [voltages; vals(n-1) vals(n)];  
    elseif (n==4)  
        voltages = [voltages; vals(n-2) vals(n-1) vals(n)];  
    elseif (n==5)  
        voltages = [voltages; vals(n-3) vals(n-2) vals(n-1) vals(n)];  
    end  
end  
  
%--- Close the voltages file  
fclose(fid);
```

Appendix III

Testbed Operation

There are some nuances to operating the testbed that make it non-trivial to operate. When turning on equipment, the digitizer must be turned on before the laptop which the processing is run on. This allows for the laptop to identify an active instrument. If it is not on, that laptop port will not read anything because upon startup there was nothing to be read. Otherwise all other equipment may be turned on in whatever order necessary.

Files are uploaded to the function generator and arbitrary waveform generator (AWG) via Matlab. The files that do this are named "IQ_wave" and "PRF_wave." Both of these files are found in C:Research\Matlab Code\New Equipment. In order to run these files a waveform reference needs to be created. The file named "makewave" establishes the waveform to be uploaded to the testbed via the aforementioned programs. Also in this folder is the "parse_voltage_file" script that takes the generated text files based on received data and stores it in a variable named "voltages."

To program the RF signal generators one must select File > Recall. Since the only file that is stored in the RF signal generator is the desired file, a specific file need not be selected. This sets the frequency to 1.8425 GHz, the center of the band of operation. Since slightly different bandwidth requirements are utilized than what was originally programmed, the frequency will need to change. It is desired to have 1.8425 GHz be the center of the operation band, therefore for the 10-85 MHz chirp, the frequency will need to be set to 1.795 GHz. The in-phase and quadrature inputs will also need to be arranged to keep the upper sideband if not already in that configuration. For the 10-245 MHz chirp, the frequency will need to be set to 1.715 GHz. This is further adaptable based on bandwidth requirements of specific tests.

Once the equipment is setup up, data is taken through a national instruments labview interface. To do this, open up labview. The first item in the list of previously used programs is called "research." Select this program to proceed to the data collection setup. This program allows the user to change the settings of the digitizer and specify where the data is to be stored. The main categories that will need to be manipulated are "number of samples", "sampling rate", and "destination". The sampling rate has been verified up to 1 GSPS, and one can basically record as many points as necessary. One note of caution, when uploading files much longer than 50000 samples into Matlab, the processing time becomes exponentially longer. The "destination" field is used to specify where the generated text file (needs the .txt extension at the end of the name" is to be stored.